

AD-A255 256



2

WL-TR-92-1028



RADAR SIGNAL PROCESSING FOR
OVER RESOLVED TARGETS

Ajit K. Choudhury
Mifang Ruan
Department of Electrical Engineering
School of Engineering
Howard University
Washington, DC 20059

DTIC
ELECTE
SEP 17 1992
S C D

May 1992

Final Report for Period (07/90-12/91)

Approved for public release; distribution is unlimited.

92 9 16 043

Avionics Directorate
Wright Laboratory
AIR FORCE SYSTEMS COMMAND
WRIGHT-PATTERSON AIR FORCE BASE, OHIO 45433

414048

92-25336




9898

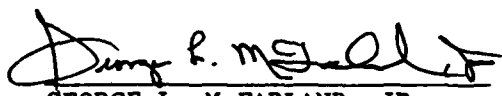
NOTICE

WHEN GOVERNMENT DRAWINGS, SPECIFICATIONS, OR OTHER DATA ARE USED FOR ANY PURPOSE OTHER THAN IN CONNECTION WITH A DEFINITELY GOVERNMENT-RELATED PROCUREMENT, THE UNITED STATES GOVERNMENT INCURS NO RESPONSIBILITY OR ANY OBLIGATION WHATSOEVER. THE FACT THAT THE GOVERNMENT MAY HAVE FORMULATED OR IN ANY WAY SUPPLIED THE SAID DRAWINGS, SPECIFICATIONS, OR OTHER DATA, IS NOT TO BE REGARDED BY IMPLICATION, OR OTHERWISE IN ANY MANNER CONSTRUED, AS LICENSING THE HOLDER, OR ANY OTHER PERSON OR CORPORATION; OR AS CONVEYING ANY RIGHTS OR PERMISSION TO MANUFACTURE, USE, OR SELL ANY PATENTED INVENTION THAT MAY IN ANY WAY BE RELATED THERETO.

THIS TECHNICAL REPORT HAS BEEN REVIEWED AND IS APPROVED FOR PUBLICATION.


MARK C. HEATON, CAPT
PROJECT ENGINEER


DONALD H. CAMPBELL, CHIEF
TECHNOLOGY DEVELOPMENT GROUP


GEORGE L. MCFARLAND, JR.
ACTG DIRECTOR
MISSION AVIONICS DIVISION
AVIONICS DIRECTORATE

IF YOUR ADDRESS HAS CHANGED, IF YOU WISH TO BE REMOVED FROM OUR MAILING LIST, OR IF THE ADDRESSEE IS NO LONGER EMPLOYED BY YOUR ORGANIZATION, PLEASE NOTIFY WL/AARM-1, WRIGHT-PATTERSON AFB OH 45433-6543 TO HELP MAINTAIN A CURRENT MAILING LIST.

COPIES OF THIS REPORT SHOULD NOT BE RETURNED UNLESS RETURN IS REQUIRED BY SECURITY CONSIDERATIONS, CONTRACTUAL OBLIGATIONS, OR NOTICE ON A SPECIFIC DOCUMENT.

REPORT DOCUMENTATION PAGE			Form Approved OMB No. 0704-0188	
Public reporting burden for this collection of information is estimated to average 1 hour per response, including the time for reviewing instructions, searching existing data sources, gathering and maintaining the data needed, and completing and reviewing the collection of information. Send comments regarding this burden estimate or any other aspect of this collection of information, including suggestions for reducing this burden, to Washington Headquarters Services, Directorate for Information Operations and Reports, 1215 Jefferson Davis Highway, Suite 1204, Arlington, VA 22202-4302, and to the Office of Management and Budget, Paperwork Reduction Project (0704-0188), Washington, DC 20503.				
1. AGENCY USE ONLY (Leave blank)	2. REPORT DATE May 92	3. REPORT TYPE AND DATES COVERED Final: (07/90-12/91)		
4. TITLE AND SUBTITLE Radar Signal Processing for Over Resolved Targets		5. FUNDING NUMBERS C-F33615-90-C-1443 PE-62204F PR-2003 TA-12 WU-07		
6. AUTHOR(S) Ajit K. Choudhury Mifang Ruan				
7. PERFORMING ORGANIZATION NAME(S) AND ADDRESS(ES) Dept. of Electrical Engineering School of Engineering Howard University Washington, DC 20059		8. PERFORMING ORGANIZATION REPORT NUMBER		
9. SPONSORING/MONITORING AGENCY NAME(S) AND ADDRESS(ES) Mark Heaton (513-255-6427) Avionics Directorate (WL/AARM) Wright-Patterson AFB OH 45433-6543		10. SPONSORING/MONITORING AGENCY REPORT NUMBER WL-TR-92-1028		
11. SUPPLEMENTARY NOTES				
12a. DISTRIBUTION / AVAILABILITY STATEMENT Approved for public release, distribution is unlimited.		12b. DISTRIBUTION CODE		
13. ABSTRACT (Maximum 200 words) Many formulas involved in the computation of radar detection performance, such as incomplete Toronto function and modified Bessel function, have very bad numerical behaviors. This fact leads to errors of the computed results. We developed and presented in this report the numerical methods which greatly improve the accuracy of the results. Another major work in this report is to investigate the effects of the energy distribution on the radar detection performance. In contrast to ordinary assumption of uniformly distributed energy, we allow the resolution cells to have different energy. Many results are obtained based on the new energy distribution model. And the relationship between uniformly and non-uniformly distributed energy is discussed.				
14. SUBJECT TERMS Radar, Resolution, Probability of Detection			15. NUMBER OF PAGES 83	
			16. PRICE CODE	
17. SECURITY CLASSIFICATION OF REPORT Unclassified	18. SECURITY CLASSIFICATION OF THIS PAGE Unclassified	19. SECURITY CLASSIFICATION OF ABSTRACT Unclassified	20. LIMITATION OF ABSTRACT UL	

SUMMARY

In this report, we presented two major parts of our research in radar detection performance of over resolved targets.

In the first part of this report, we investigate the numerical problems in computation of radar detection performance. We found that a significant difficulty in the computation of radar detection performance is that many involved formulas, such as incomplete Toronto functions and modified Bessel functions, have very bad numerical behaviors. This fact leads to errors of the results. We developed numerical methods to overcome this difficulty and thus obtained much more accurate results.

In the second part of this report we investigated the effects of energy distribution on the radar detection performance. In the calculation of radar detection performance, it is generally assumed that the energy is uniformly distributed over the resolution cells. However, in practice the cells may have different energy. In these cases, modifications are necessary in computing the detection performance. We developed a realistic model of energy distribution, and found that the probability of detection generally tends to increase when the energy is not uniformly distributed. The phenomena are interpreted by the shape of the curves corresponding to uniformly-distributed energy.

DTIC QUALITY INSPECTED 3

Accession For	
NTIS GRA&I	<input checked="" type="checkbox"/>
DTIC TAB	<input type="checkbox"/>
Unannounced	<input type="checkbox"/>
Justification	
by	
Distribution/	
Availability Codes	
Dist	Avail and/or Special
A-1	

Table of Contents

List of Figures	v
 PART I: Numerical Methods in Computation of Radar Detection Performance	 1
Introduction	2
The Involved Formula	3
The Numerical Difficulties	6
The Numerical Methods	7
The Results	9
Summary	9
Figures	10
 PART II: The Effects of Non-Uniformly Distributed Energy on Radar Detection Performance	 37
Introduction	38
Formulation	39
Results	42
Discussion	45
Summary	47
Figures	49
 REFERENCES	 83

Figures

<u>Figure Number</u>	<u>Caption</u>	<u>Page Number</u>
1.1a	The reproduced figure for single-pulse constant amplitude scatterers when $P_{fa} = 1.E-2$	10
1.1b	The figure from Ref. [1] for single-pulse constant amplitude scatterers when $P_{fa} = 1.E-2$	10
1.2a	The reproduced figure for single-pulse constant amplitude scatterers when $P_{fa} = 1.E-5$	11
1.2b	The figure from Ref. [1] for single-pulse constant amplitude scatterers when $P_{fa} = 1.E-5$	11
1.3a	The reproduced figure for single-pulse constant amplitude scatterers when $P_{fa} = 1.E-8$	12
1.3b	The figure from Ref. [1] for single-pulse constant amplitude scatterers when $P_{fa} = 1.E-8$	12
1.4a	The reproduced figure for 4-pulse constant amplitude scatterers when $P_{fa} = 1.E-2$	13
1.4b	The figure from Ref. [1] for 4-pulse constant amplitude scatterers when $P_{fa} = 1.E-2$	13
1.5a	The reproduced figure for 4-pulse constant amplitude scatterers when $P_{fa} = 1.E-5$	14
1.5b	The figure from Ref. [1] for 4-pulse constant amplitude scatterers when $P_{fa} = 1.E-5$	14
1.6a	The reproduced figure for 4-pulse constant amplitude scatterers when $P_{fa} = 1.E-8$	15
1.6b	The figure from Ref. [1] for 4-pulse constant amplitude scatterers when $P_{fa} = 1.E-8$	15
1.7a	The reproduced figure for 16-pulse constant amplitude scatterers when $P_{fa} = 1.E-2$	16

1.7b	The figure from Ref. [1] for 16-pulse constant amplitude scatterers when $P_{fa} = 1.E-2$	16
1.8a	The reproduced figure for 16-pulse constant amplitude scatterers when $P_{fa} = 1.E-5$	17
1.8b	The figure from Ref. [1] for 16-pulse constant amplitude scatterers when $P_{fa} = 1.E-5$	17
1.9a	The reproduced figure for 16-pulse constant amplitude scatterers when $P_{fa} = 1.E-8$	18
1.9b	The figure from Ref. [1] for 16-pulse constant amplitude scatterers when $P_{fa} = 1.E-8$	18
1.10a	The reproduced figure for 16-pulse slow-fluctuating Rayleigh scatterers when $P_{fa} = 1.E-8$	19
1.10b	The figure from Ref. [1] for 16-pulse slow-fluctuating Rayleigh scatterers when $P_{fa} = 1.E-8$	19
1.11a	The reproduced figure for 16-pulse fast-fluctuating Rayleigh scatterers when $P_{fa} = 1.E-8$	20
1.11b	The figure from Ref. [1] for 16-pulse fast-fluctuating Rayleigh scatterers when $P_{fa} = 1.E-8$	20
1.12a	The reproduced figure for 16-pulse slow-fluctuating dominant plus Rayleigh scatterers when $P_{fa} = 1.E-2$	21
1.12b	The figure from Ref. [1] for 16-pulse slow-fluctuating dominant plus Rayleigh scatterers when $P_{fa} = 1.E-2$	21
1.13a	The reproduced figure for 16-pulse slow-fluctuating dominant plus Rayleigh scatterers when $P_{fa} = 1.E-8$	22
1.13b	The figure from Ref. [1] for 16-pulse slow-fluctuating dominant plus Rayleigh scatterers when $P_{fa} = 1.E-8$	22
1.14a	The reproduced figure for 16-pulse fast-fluctuating dominant plus Rayleigh scatterers when $P_{fa} = 1.E-8$	23
1.14b	The figure from Ref. [1] for 16-pulse fast-fluctuating dominant plus Rayleigh scatterers when $P_{fa} = 1.E-8$	23

1.15	The reproduced figure for single-pulse Rayleigh scatterers when $P_{fa} = 1.E-2$	24
1.16	The reproduced figure for single-pulse Rayleigh scatterers when $P_{fa} = 1.E-5$	24
1.17	The reproduced figure for single-pulse Rayleigh scatterers when $P_{fa} = 1.E-8$	25
1.18	The reproduced figure for single-pulse dominant plus Rayleigh scatterers when $P_{fa} = 1.E-2$	25
1.19	The reproduced figure for single-pulse dominant plus Rayleigh scatterers when $P_{fa} = 1.E-5$	26
1.20	The reproduced figure for single-pulse dominant plus Rayleigh scatterers when $P_{fa} = 1.E-8$	26
1.21	The reproduced figure for 4-pulse slow-fluctuating Rayleigh scatterers when $P_{fa} = 1.E-2$	27
1.22	The reproduced figure for 4-pulse slow-fluctuating Rayleigh scatterers when $P_{fa} = 1.E-5$	27
1.23	The reproduced figure for 4-pulse slow-fluctuating Rayleigh scatterers when $P_{fa} = 1.E-8$	28
1.24	The reproduced figure for 16-pulse slow-fluctuating Rayleigh scatterers when $P_{fa} = 1.E-2$	28
1.25	The reproduced figure for 16-pulse slow-fluctuating Rayleigh scatterers when $P_{fa} = 1.E-5$	29
1.26	The reproduced figure for 4-pulse fast-fluctuating Rayleigh scatterers when $P_{fa} = 1.E-2$	29
1.27	The reproduced figure for 4-pulse fast-fluctuating Rayleigh scatterers when $P_{fa} = 1.E-5$	30
1.28	The reproduced figure for 4-pulse fast-fluctuating Rayleigh scatterers when $P_{fa} = 1.E-8$	30
1.29	The reproduced figure for 16-pulse fast-fluctuating Rayleigh scatterers when $P_{fa} = 1.E-2$	31

1.30	The reproduced figure for 16-pulse fast-fluctuating Rayleigh scatterers when $P_{fa} = 1.E-5$	31
1.31	The reproduced figure for 4-pulse slow-fluctuating dominant plus Rayleigh scatterers when $P_{fa} = 1.E-2$	32
1.32	The reproduced figure for 4-pulse slow-fluctuating dominant plus Rayleigh scatterers when $P_{fa} = 1.E-5$	32
1.33	The reproduced figure for 4-pulse slow-fluctuating dominant plus Rayleigh scatterers when $P_{fa} = 1.E-8$	33
1.34	The reproduced figure for 16-pulse slow-fluctuating dominant plus Rayleigh scatterers when $P_{fa} = 1.E-5$	33
1.35	The reproduced figure for 4-pulse fast-fluctuating dominant plus Rayleigh scatterers when $P_{fa} = 1.E-2$	34
1.36	The reproduced figure for 4-pulse fast-fluctuating dominant plus Rayleigh scatterers when $P_{fa} = 1.E-5$	34
1.37	The reproduced figure for 4-pulse fast-fluctuating dominant plus Rayleigh scatterers when $P_{fa} = 1.E-8$	35
1.38	The reproduced figure for 16-pulse fast-fluctuating dominant plus Rayleigh scatterers when $P_{fa} = 1.E-2$	35
1.39	The reproduced figure for 16-pulse fast-fluctuating dominant plus Rayleigh scatterers when $P_{fa} = 1.E-5$	36
2.0	An Example of Cell Distribution over Eight Energy Levels	49
2.1a	Comparison between Uniformly Distributed Energy and Non-Uniformly Distributed Energy for Single-Pulse Constant Amplitude Scatterers when $M = 2$ and $P_{fa} = 1.E-2$	49
2.1b	Comparison between Uniformly Distributed Energy and Non-Uniformly Distributed Energy for Single-Pulse Constant Amplitude Scatterers when $M = 2$ and $P_{fa} = 1.E-8$	50
2.1c	Comparison between Different Values of σ for Single-Pulse Constant Amplitude Scatterers when $N_I = 8$, $M = 10$, $\tilde{E} = 5$ and $P_{fa} = 1.E-2$	50

2.1d	Comparison between Different Values of σ for Single-Pulse Constant Amplitude Scatterers when $N_I = 8$, $M = 10$, $\tilde{E} = 5$ and $P_{fa} = 1.E-8$	51
2.1e	Comparison between Different Values of \tilde{E} for Single-Pulse Constant Amplitude Scatterers when $N_I = 8$, $M = 10$, $\sigma = 0.5$ and $P_{fa} = 1.E-2$	51
2.1f	Comparison between Different Values of \tilde{E} for Single-Pulse Constant Amplitude Scatterers when $N_I = 8$, $M = 10$, $\sigma = 3.0$ and $P_{fa} = 1.E-2$	52
2.1g	Comparison between Different Values of \tilde{E} for Single-Pulse Constant Amplitude Scatterers when $N_I = 8$, $M = 10$, $\sigma = 2.0$ and $P_{fa} = 1.E-8$	52
2.2a	Comparison between Uniformly Distributed Energy and Non-Uniformly Distributed Energy for Single-Pulse Rayleigh Scatterers when $M = 2$ and $P_{fa} = 1.E-2$	53
2.2b	Comparison between Uniformly Distributed Energy and Non-Uniformly Distributed Energy for Single-Pulse Rayleigh Scatterers when $M = 2$ and $P_{fa} = 1.E-8$	53
2.2c	Comparison between Different Values of σ for Single-Pulse Rayleigh Scatterers when $N_I = 8$, $M = 10$, $\tilde{E} = 5$ and $P_{fa} = 1.E-2$	54
2.2d	Comparison between Different Values of σ for Single-Pulse Rayleigh Scatterers when $N_I = 8$, $M = 10$, $\tilde{E} = 5$ and $P_{fa} = 1.E-8$	54
2.2e	Comparison between Different Values of \tilde{E} for Single-Pulse Rayleigh Scatterers when $N_I = 8$, $M = 10$, $\sigma = 0.5$ and $P_{fa} = 1.E-2$	55
2.2f	Comparison between Different Values of \tilde{E} for Single-Pulse Rayleigh Scatterers when $N_I = 8$, $M = 10$, $\sigma = 3.0$ and $P_{fa} = 1.E-2$	55
2.2g	Comparison between Different Values of \tilde{E} for Single-Pulse Rayleigh Scatterers when $N_I = 8$, $M = 10$, $\sigma = 2.0$ and $P_{fa} = 1.E-8$	56
2.3a	Comparison between Uniformly Distributed Energy and Non-Uniformly Distributed Energy for Single-Pulse Dominant plus Rayleigh Scatterers when $M = 2$ and $P_{fa} = 1.E-2$	57

2.3b	Comparison between Uniformly Distributed Energy and Non-Uniformly Distributed Energy for Single-Pulse Dominant plus Rayleigh Scatterers when $M = 2$ and $P_{fa} = 1.E-8$	57
2.3c	Comparison between Different Values of σ for Single-Pulse Dominant plus Rayleigh Scatterers when $N_I = 8$, $M = 10$, $\tilde{E} = 5$ and $P_{fa} = 1.E-2$	58
2.3d	Comparison between Different Values of σ for Single-Pulse Dominant plus Rayleigh Scatterers when $N_I = 8$, $M = 10$, $\tilde{E} = 5$ and $P_{fa} = 1.E-8$	58
2.3e	Comparison between Different Values of \tilde{E} for Single-Pulse Dominant plus Rayleigh Scatterers when $N_I = 8$, $M = 10$, $\sigma = 0.5$ and $P_{fa} = 1.E-2$	59
2.3f	Comparison between Different Values of \tilde{E} for Single-Pulse Dominant plus Rayleigh Scatterers when $N_I = 8$, $M = 10$, $\sigma = 3.0$ and $P_{fa} = 1.E-2$	59
2.3g	Comparison between Different Values of \tilde{E} for Single-Pulse Dominant plus Rayleigh Scatterers when $N_I = 8$, $M = 10$, $\sigma = 2.0$ and $P_{fa} = 1.E-8$	60
2.4a	Comparison between Uniformly Distributed Energy and Non-Uniformly Distributed Energy for 4-Pulse Constant Amplitude Scatterers when $M = 2$ and $P_{fa} = 1.E-2$	61
2.4b	Comparison between Uniformly Distributed Energy and Non-Uniformly Distributed Energy for 4-Pulse Constant Amplitude Scatterers when $M = 2$ and $P_{fa} = 1.E-8$	61
2.4c	Comparison between Different Values of σ for 4-Pulse Constant Amplitude Scatterers when $N_I = 8$, $M = 10$, $\tilde{E} = 5$ and $P_{fa} = 1.E-2$	62
2.4d	Comparison between Different Values of σ for 4-Pulse Constant Amplitude Scatterers when $N_I = 8$, $M = 10$, $\tilde{E} = 5$ and $P_{fa} = 1.E-8$	62
2.4e	Comparison between Different Values of \tilde{E} for 4-Pulse Constant Amplitude Scatterers when $N_I = 8$, $M = 10$, $\sigma = 0.5$ and $P_{fa} = 1.E-2$	63

2.4f	Comparison between Different Values of \tilde{E} for 4-Pulse Constant Amplitude Scatterers when $N_I = 8$, $M = 10$, $\sigma = 3.0$ and $P_{fa} = 1.E-2$	63
2.4g	Comparison between Different Values of \tilde{E} for 4-Pulse Constant Amplitude Scatterers when $N_I = 8$, $M = 10$, $\sigma = 2.0$ and $P_{fa} = 1.E-8$	64
2.5a	Comparison between Uniformly Distributed Energy and Non-Uniformly Distributed Energy for 4-Pulse Slow-Fluctuating Rayleigh Scatterers when $M = 2$ and $P_{fa} = 1.E-2$	65
2.5b	Comparison between Uniformly Distributed Energy and Non-Uniformly Distributed Energy for 4-Pulse Slow-Fluctuating Rayleigh Scatterers when $M = 2$ and $P_{fa} = 1.E-8$	65
2.5c	Comparison between Different Values of σ for 4-Pulse Slow-Fluctuating Rayleigh Scatterers when $N_I = 8$, $M = 10$, $\tilde{E} = 5$ and $P_{fa} = 1.E-2$	66
2.5d	Comparison between Different Values of σ for 4-Pulse Slow-Fluctuating Rayleigh Scatterers when $N_I = 8$, $M = 10$, $\tilde{E} = 5$ and $P_{fa} = 1.E-8$	66
2.5e	Comparison between Different Values of \tilde{E} for 4-Pulse Slow-Fluctuating Rayleigh Scatterers when $N_I = 8$, $M = 10$, $\sigma = 0.5$ and $P_{fa} = 1.E-2$	67
2.5f	Comparison between Different Values of \tilde{E} for 4-Pulse Slow-Fluctuating Rayleigh Scatterers when $N_I = 8$, $M = 10$, $\sigma = 3.0$ and $P_{fa} = 1.E-2$	67
2.5g	Comparison between Different Values of \tilde{E} for 4-Pulse Slow-Fluctuating Rayleigh Scatterers when $N_I = 8$, $M = 10$, $\sigma = 2.0$ and $P_{fa} = 1.E-8$	68
2.6a	Comparison between Uniformly Distributed Energy and Non-Uniformly Distributed Energy for 4-Pulse Fast-Fluctuating Rayleigh Scatterers when $M = 2$ and $P_{fa} = 1.E-2$	69
2.6b	Comparison between Uniformly Distributed Energy and Non-Uniformly Distributed Energy for 4-Pulse Fast-Fluctuating Rayleigh Scatterers when $M = 2$ and $P_{fa} = 1.E-8$	69

2.6c	Comparison between Different Values of σ for 4-Pulse Fast-Fluctuating Rayleigh Scatterers when $N_I = 8$, $M = 10$, $\tilde{E} = 5$ and $P_{fa} = 1.E-2$	70
2.6d	Comparison between Different Values of σ for 4-Pulse Fast-Fluctuating Rayleigh Scatterers when $N_I = 8$, $M = 10$, $\tilde{E} = 5$ and $P_{fa} = 1.E-8$	70
2.6e	Comparison between Different Values of \tilde{E} for 4-Pulse Fast-Fluctuating Rayleigh Scatterers when $N_I = 8$, $M = 10$, $\sigma = 0.5$ and $P_{fa} = 1.E-2$	71
2.6f	Comparison between Different Values of \tilde{E} for 4-Pulse Fast-Fluctuating Rayleigh Scatterers when $N_I = 8$, $M = 10$, $\sigma = 3.0$ and $P_{fa} = 1.E-2$	71
2.6g	Comparison between Different Values of \tilde{E} for 4-Pulse Fast-Fluctuating Rayleigh Scatterers when $N_I = 8$, $M = 10$, $\sigma = 2.0$ and $P_{fa} = 1.E-8$	72
2.7a	Comparison between Uniformly Distributed Energy and Non-Uniformly Distributed Energy for 4-Pulse Slow-Fluctuating Dominant plus Rayleigh Scatterers when $M = 2$ and $P_{fa} = 1.E-2$	73
2.7b	Comparison between Uniformly Distributed Energy and Non-Uniformly Distributed Energy for 4-Pulse Slow-Fluctuating Dominant plus Rayleigh Scatterers when $M = 2$ and $P_{fa} = 1.E-8$	73
2.7c	Comparison between Different Values of σ for 4-Pulse Slow-Fluctuating Dominant plus Rayleigh Scatterers when $N_I = 8$, $M = 10$, $\tilde{E} = 5$ and $P_{fa} = 1.E-2$	74
2.7d	Comparison between Different Values of σ for 4-Pulse Slow-Fluctuating Dominant plus Rayleigh Scatterers when $N_I = 8$, $M = 10$, $\tilde{E} = 5$ and $P_{fa} = 1.E-8$	74
2.7g	Comparison between Different Values of \tilde{E} for 4-Pulse Slow-Fluctuating Dominant plus Rayleigh Scatterers when $N_I = 8$, $M = 10$, $\sigma = 2.0$ and $P_{fa} = 1.E-8$	75

2.8a	Comparison between Uniformly Distributed Energy and Non-Uniformly Distributed Energy for 4-Pulse Fast-Fluctuating Dominant plus Rayleigh Scatterers when $M = 2$ and $P_{fa} = 1.E-2$	76
2.8b	Comparison between Uniformly Distributed Energy and Non-Uniformly Distributed Energy for 4-Pulse Fast-Fluctuating Dominant plus Rayleigh Scatterers when $M = 2$ and $P_{fa} = 1.E-8$	76
2.8c	Comparison between Different Values of σ for 4-Pulse Fast-Fluctuating Dominant plus Rayleigh Scatterers when $N_I = 8$, $M = 10$, $\tilde{E} = 5$ and $P_{fa} = 1.E-2$	77
2.8d	Comparison between Different Values of σ for 4-Pulse Fast-Fluctuating Dominant plus Rayleigh Scatterers when $N_I = 8$, $M = 10$, $\tilde{E} = 5$ and $P_{fa} = 1.E-8$	77
2.8e	Comparison between Different Values of \tilde{E} for 4-Pulse Fast-Fluctuating Dominant plus Rayleigh Scatterers when $N_I = 8$, $M = 10$, $\sigma = 0.5$ and $P_{fa} = 1.E-2$	78
2.8f	Comparison between Different Values of \tilde{E} for 4-Pulse Fast-Fluctuating Dominant plus Rayleigh Scatterers when $N_I = 8$, $M = 10$, $\sigma = 3.0$ and $P_{fa} = 1.E-2$	78
2.8g	Comparison between Different Values of \tilde{E} for 4-Pulse Fast-Fluctuating Dominant plus Rayleigh Scatterers when $N_I = 8$, $M = 10$, $\sigma = 2.0$ and $P_{fa} = 1.E-8$	79
2.9	Distribution of 10 Cells over 8 Energy Levels for Different Values of \tilde{E} when $\sigma=0.5$	80
2.10	Distribution of 10 Cells over 8 Energy Levels for Different Values of \tilde{E} when $\sigma=1.0$	80
2.11	Distribution of 10 Cells over 8 Energy Levels for Different Values of \tilde{E} when $\sigma=2.0$	81
2.12	Distribution of 10 Cells over 8 Energy Levels for Different Values of \tilde{E} when $\sigma=3.0$	81
2.13	Cell Probability of Detection in Linear Scales for Single-Pulse	82

Part I

NUMERICAL METHODS IN COMPUTATION OF RADAR DETECTION PERFORMANCE

INTRODUCTION

The formulas to compute radar detection performance can be found in many literatures, such as [1]–[9]. Ref. [1] uses those formulas to plot a large amount of figures which show the probability of detection vs. signal-to-noise ratio for various target models, pulse numbers, and cell numbers. These figures are very important in design and development of radar systems, as well as in radar signal processing. The target models studied in Ref. [1] include

- 1) Single pulse, constant amplitude scatterers,
- 2) Single pulse, Rayleigh scatterers,
- 3) Single pulse, dominant plus Rayleigh scatterers,
- 4) Multi-pulses, constant amplitude scatterers,
- 5) Multi-pulses, slow fluctuating targets, Rayleigh scatterers,
- 6) Multi-pulses, fast fluctuating targets, Rayleigh scatterers,
- 7) Multi-pulses, slow fluctuating targets, dominant plus Rayleigh scatterers,
- 8) Multi-pulses, fast fluctuating targets, dominant plus Rayleigh scatterers.

A serious difficulty existing in radar detection performance calculation is that many formulas involved have very bad numerical behaviors, and thus lead to significant errors of the results. Typical numerical error sources are truncation of numbers, subtraction of nearly equal numbers, truncation of series, numerical integration, overflow, underflow, and open-range integration. The overflows and underflows are mainly caused by two involved special functions—incomplete Toronto functions and modified Bessel functions.

Most computers can handle overflows and underflows automatically. The computers assign a maximum representable value to the variable which generates overflow, and assign zero to the valuable which generates underflow. In most cases, overflow will lead to significant error of the results. And in some cases, underflow will lead to significant errors. We can identify the underflow cases which will lead to error and the cases which will not. To ensure the accuracy of the results, we must eliminate all the overflow cases and the underflow cases

which will lead to error.

In this report, we will analyze the causes of the numerical difficulties, and develop the methods to overcome these difficulties. The methods are used to compute the probability of detection for various target models, pulse numbers, and cell numbers. Many of the figures in this report are plotted to show the probability of detection against the signal-to-noise ratio. The figures in this report are compared with those from [1]. Many of the figures show significant difference from those of [1]. One of the purposes of the work in this part of the report is to use the numerical methods in Part II of this report, which investigates the effects of energy distribution on the radar detection performance. The methods developed here can also be applied to the problems other than radar detection.

THE INVOLVED FORMULA

The formula involved in computation of radar detection performance can be found in various literatures. The formulas listed below are obtained from Ref. [1]. It is assumed that the energy is uniformly distributed over the resolution cells.

The relationship between false alarm probability, P_{fa} , and threshold, Y_b , is given by

$$P_{fa} = 1 - \left(1 - \exp(-Y_b)\right)^M \quad \text{for single pulse cases} \quad (1.1a)$$

and

$$P_{fa} = 1 - \left[I\left(\frac{Y_b}{\sqrt{N}}, N-1\right) \right]^M \quad \text{for multi-pulse cases} \quad (1.1b)$$

where M is the total number of resolution cells; N is the number of pulses. $I(u, s)$ is the incomplete Gamma function expressed by

$$I(u, s) = \int_0^u \frac{t^{s-1} e^{-t}}{s!} dt \quad (1.2)$$

The probability of detection, P_d , is given by

$$P_d = 1 - (1 - P_{dm})^M \quad (1.3)$$

where P_{dm} is the probability of a single cell to accross the threshold, and has different expressions for different target models, as shown below.

1) For single-pulse constant amplitude scatterers, P_{dm} is given by

$$P_{dm} = 1 - T_{\sqrt{Y_b}} [1, 0, \sqrt{\bar{E}/(MN_0)}] \quad (1.4)$$

where \bar{E} is the total signal energy, N_0 is the total noise, and $T_B[m,n,r]$ is the incomplete Toronto function which has the following expression:

$$T_B(m,n,r) = 2 r^{n-m+1} \bar{e}^{-r^2} \int_0^1 t^{m-n} \bar{e}^{-t^2} B_n(2rt) dt \quad (1.5)$$

and $B_n(z)$ is the n th order modified Bessel function expressed by either

$$B_n(z) = \sum_{k=0}^{\infty} \frac{1}{k! (k+n)!} (z/2)^{n+2k} \quad (1.6a)$$

or

$$B_n(z) = \frac{(z/2)^n}{\Gamma(n+1/2) \Gamma(1/2)} \int_{-1}^1 (1-t^2)^{n-1/2} e^{-zt} dt \quad (1.6b)$$

where $\Gamma(n)$ is the Gamma function.

2) For single-pulse Rayleigh scatterers, P_{dm} is given by

$$P_{dm} = \exp \left(- \frac{Y_b}{1 + \bar{E}/(2MN_0)} \right) \quad (1.7)$$

3) For single-pulse dominant plus Rayleigh scatterers, P_{dm} is given by

$$P_{dm} = \frac{1}{1 + 4MN_0/\bar{E}} \left(1 + \frac{4MN_0}{\bar{E}} + \frac{Y_b}{1 + \bar{E}/(4MN_0)} \right) \cdot \exp \left(- \frac{Y_b}{1 + \bar{E}/(4MN_0)} \right) \quad (1.8)$$

4) For multi-pulse constant amplitude scatterers, P_{dm} is given by

$$P_{dm} = 1 - T_{\sqrt{Y_b}} [2N-1, N-1, \sqrt{N\bar{E}}/(MN_0)] \quad (1.9)$$

where N is the number of the pulses.

5) For multi-pulse slow-fluctuating-target Rayleigh scatterers, P_{dm} is given by

$$P_{dm} = 1 - I\left(\frac{Y_b}{\sqrt{N-1}}, N-2\right) + \left(1 + \frac{1}{N\bar{E}/(2MN_0)}\right)^{N-1} \cdot \exp\left(-\frac{Y_b}{1 + N\bar{E}/(2MN_0)}\right) \cdot I\left(\frac{Y_b}{\sqrt{N-1}(1 + 2MN_0/(N\bar{E}))}, N-2\right) \quad (1.10)$$

6) For multi-pulse fast-fluctuating-target Rayleigh scatterers, P_{dm} is given by

$$P_{dm} = 1 - I\left(\frac{Y_b}{\sqrt{N}(1 + \bar{E}/(2MN_0))}, N-1\right) \quad (1.11)$$

7) For multi-pulse slow-fluctuating-target dominant plus Rayleigh scatterers, P_{dm} is given by

$$P_{dm} = \int_{Y_b}^{\infty} P(Y) dY \quad (1.12a)$$

where

$$P(Y) = \frac{Y\left(1 + \frac{1}{N\bar{E}/(4MN_0)}\right)^{N-2}}{(1 + N\bar{E}/(4MN_0))^2} \cdot K \cdot \exp\left(\frac{-Y}{(1 + N\bar{E}/(4MN_0))}\right) - \frac{(N-2)\left(1 + \frac{1}{N\bar{E}/(4MN_0)}\right)^{N-1}}{(1 + N\bar{E}/(4MN_0))^2} \cdot K \cdot \exp\left(\frac{-Y}{(1 + N\bar{E}/(4MN_0))}\right) + \frac{Y^{N-1} \exp(-Y)}{(N-2)! (1 + N\bar{E}/(4MN_0))^2} \quad (1.12b)$$

and

$$K = I\left(\frac{Y}{\sqrt{N-1} (1 + 4MN_0/(N\bar{E}))}, N-2\right) \quad (1.12c)$$

8) For multi-pulse fast-fluctuating-target dominant plus Rayleigh scatterers, P_{dm} is given by

$$P_{dm} = 1 - \frac{N!}{(1 + \bar{E}/(4MN_0))^N} \cdot \sum_{k=0}^N \frac{1}{k! (N-k)!} \left(\frac{\bar{E}}{4MN_0}\right)^k \cdot I\left(\frac{Y_b}{\sqrt{N+K} (1 + \bar{E}/(4MN_0))}, N+k-1\right) \quad (1.13)$$

THE NUMERICAL DIFFICULTIES

The formulas involved in computation of radar detection are given in the above section. Most numerical difficulties are caused by the incomplete Toronto function, modified Bessel function and the open-range integral.

The incomplete Toronto function and the Bessel function will generate many overflows and underflows. For the open-range integral in Eq. (1.12a), the function $P(Y)$ may decay slowly with Y . Therefore, in order to obtain accurate results, we must take a large upper limit of the integral. However, when the variable Y becomes large, underflows and overflows may occur in computing $P(Y)$. Also large integral range will result in large computational time.

In the incomplete Toronto function (see Eq. (1.5)), the following problems may appear:

1. The factor r^{n-m+1} may underflow when r is large and m is much greater than n .
2. The factor $\exp(-r^2)$ may underflow when r is large.
3. In the case where m is much larger than n , the factor t^{m-n} may underflow or overflow when t is small or large, respectively.
4. The factor $\exp(-t^2)$ may underflow when t is large.

In the modified Bessel function, if the series form (Eq. (1.6a)) is used and z is not small, we must sum up many terms in order to obtain accurate results. Then, the factors $(z/2)^{n+2k}$, $k!$, and $(k+n)!$ may overflow. If the integral form (Eq. (1.6b)) is used and n is zero, there are singular points at $t = -1$ and $t = 1$. These singular points will seriously degrade the accuracy of the results.

In Eq. (1.12b), when Y is large, the factor Y^{N-1} may overflow, the exponential factors may underflow. Also large value of Y may lead to problems in incomplete Gamma function (Eq. 1.2)). In the incomplete Gamma function, the factor e^{-t} may underflow and the factor t^s may overflow.

The other numerical error sources include truncation of series, truncation of numbers, and numerical integration. Some series, such as the modified Bessel function, may decay slowly with the index. Then if the series are truncated too early, the results are not accurate; while if the series are not truncated early, overflows or underflows may occur.

THE NUMERICAL METHODS

It is relatively easy to reduce the error caused by truncation of numbers and numerical integral. We can reduce the errors caused by truncation of numbers by using double precision variables which are generally sufficient. And we can reduce the errors caused by numerical integration by dividing the integration intervals finely. Also if double precision variables are used, we find that the errors caused by subtraction of numbers are not serious.

To improve the behaviors of the modified Bessel function, we use the integral form when n is not zero and use the series form when n is zero. This method can reduce large numbers of overflows and underflows and to avoid the singular problems.

The remaining difficulties are overflows and underflows. To handle these problems, we classify the overflows into the following patterns:

1. $S \cdot t^{-n}$ when t and S are small and n is large. In this case the factor t^{-n} overflows.

Generally, when a factor overflows, there should be another factor which is small, otherwise the problem can not be solved. In this pattern we can solve the problem by using an equivalent form of $t^{-n + \ln S / \ln t}$.

2. $S \cdot r^n$ when r and n are large, S is small. In this case, the factor r^n overflows. We can solve the problem by using an equivalent form of $r^{n + \ln S / \ln r}$.

3. $S \cdot \Sigma t_i$ when some of t_i overflows and S is small. In this case, we can solve the problem by using an equivalent form of $\Sigma(S \cdot t_i)$.

Similarly, we can classify underflows into the following patterns:

1. $B \cdot \exp(-t)$ when B and t are large. In this case, the factor $\exp(-t)$ underflows. Generally computer will assign zero to the underflowed variables. This method will not introduce errors if no factor is large. Therefore, we only need to take care the cases with a large factor, B . In this pattern, we can solve the problem by using an equivalent form of $\exp(-t + \ln B)$. If the original form is used, the value of the expression is zero, but the equivalent form may give non-zero values.

2. $B \cdot t^n$ when t is small, B and n are large. In this case, the factor t^n underflows. We can solve the problem by using an equivalent form of $t^{n + \ln B / \ln t}$.

3. $B \cdot r^{-n}$ when r , n , and B are all large. In this case, the factor r^{-n} underflows, and we can solve the problem by using an equivalent form of $r^{-n + \ln B / \ln r}$.

4. $B \cdot \Sigma t_i$ when some of t_i underflows and the sum is small. We can solve the problem by using an equivalent form of $\Sigma(B \cdot t_i)$. If the sum is not small, the underflowed term can be neglected without introducing errors.

By using these method, we can significantly improve the accuracy of the results. The methods can eliminate all the overflows. Although some underflows still exist, they will not introduce errors; e.g., all the factors are small, or a term in a series is neglectable compared with other terms in the series.

THE RESULTS

There are 39 independent figures for various target models and pulse numbers in [1]. The figures show the probability of detection vs. the signal to noise ratio for different cell numbers. By using the numerical methods developed above, we reproduced all of those figures.

We compared the figures with those in [1], and found that about 36% of our reproduced figures are significantly different from those in [1]. The others are essentially the same.

Figures 1.1–1.14 show the comparison of the figures with significant differences. Figures 1.1a–1.14a are the reproduced ones by using the numerical methods in this report. Figures 1.1b–1.14b are the corresponding figures from [1]. Figures 1.15–1.39 show the figures without significant differences (with good numerical behaviors).

SUMMARY

The formula involved in calculation of the radar detection performance have had numerical behaviors, and thus lead to errors of the results. Our numerical methods developed can overcome those difficulties, and give much more accurate results.

Incomplete Toronto function, modified Bessel function and open-range integration are main sources of numerical problems.

The target models with good numerical behaviors include single-pulse Rayleigh scatterers and single-pulse dominant plus Rayleigh scatterers. The target models with bad numerical behaviors include single-pulse constant amplitude scatterers and multi-pulse constant amplitude scatterers. The target models with some numerical problems, especially when N and Y_b are large, include multi-pulse Rayleigh scatterers (slow fluctuating or fast fluctuating targets) and multi-pulse dominant plus Rayleigh scatterers (slow fluctuating or fast fluctuation targets).

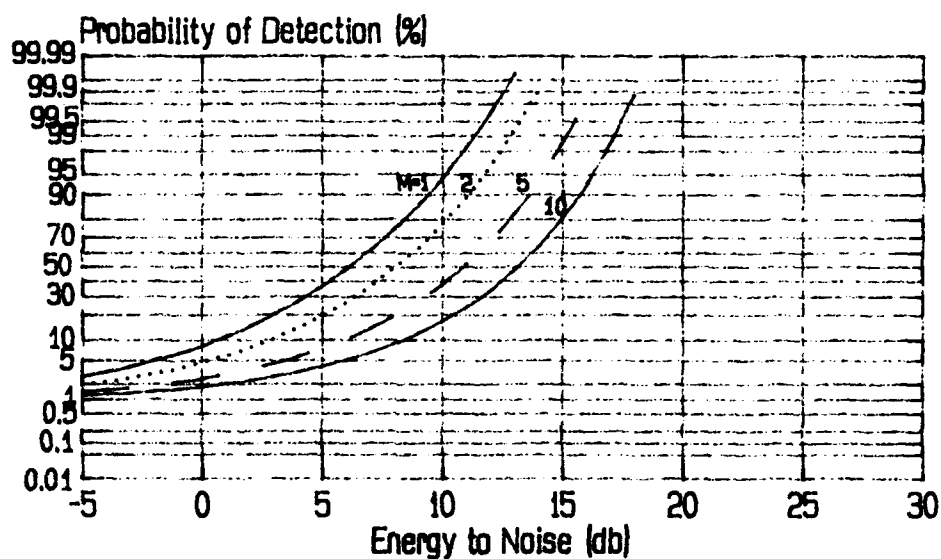


Figure 1.1a The reproduced figure for single-pulse constant amplitude scatterers when $P_{fa} = 1.E-2$

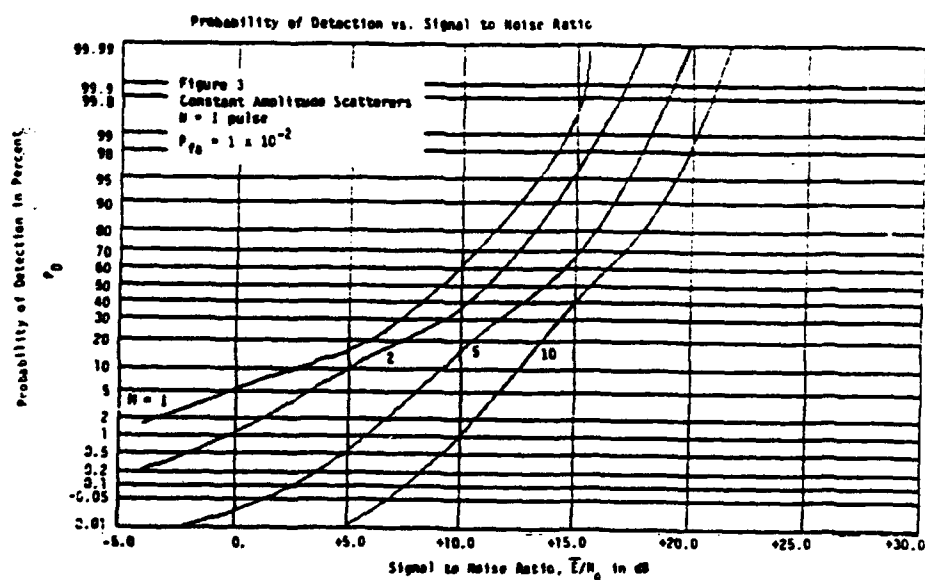


Figure 1.1b The figure from Ref. [1] for single-pulse constant amplitude scatterers when $P_{fa} = 1.E-2$

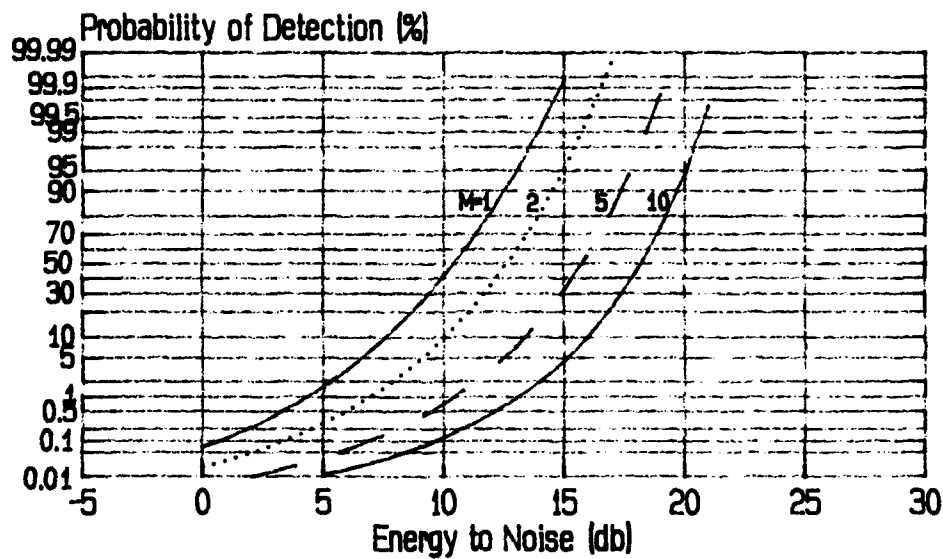


Figure 1.2a The reproduced figure for single-pulse constant amplitude scatterers when $P_{fa} = 1.E-5$

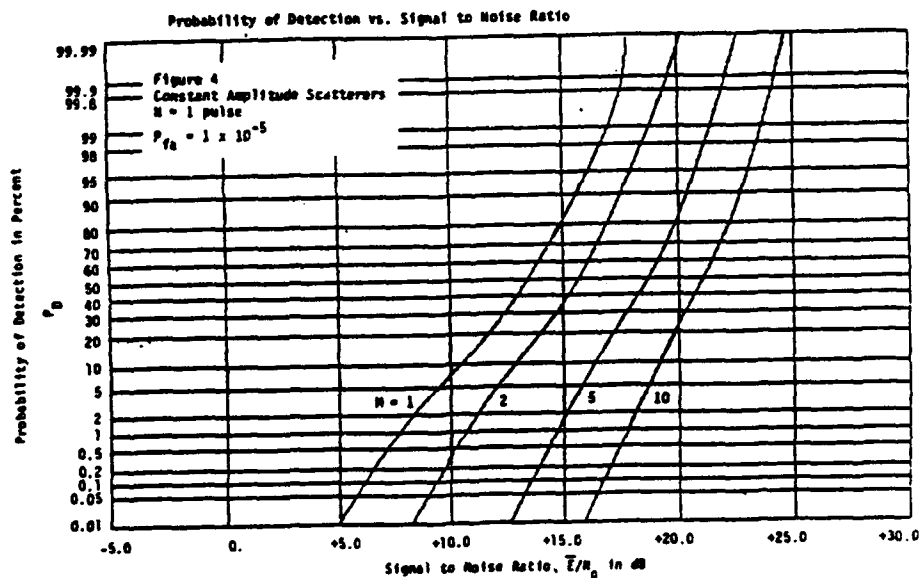


Figure 1.2b The figure from Ref. [1] for single-pulse constant amplitude scatterers when $P_{fa} = 1.E-5$

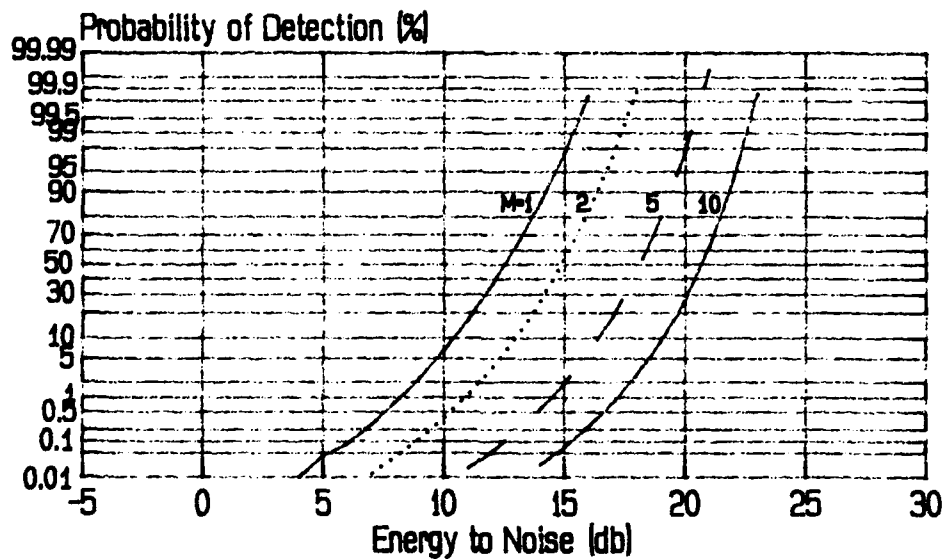


Figure 1.3a The reproduced figure for single-pulse constant amplitude scatterers when $P_{fa} = 1.E-8$

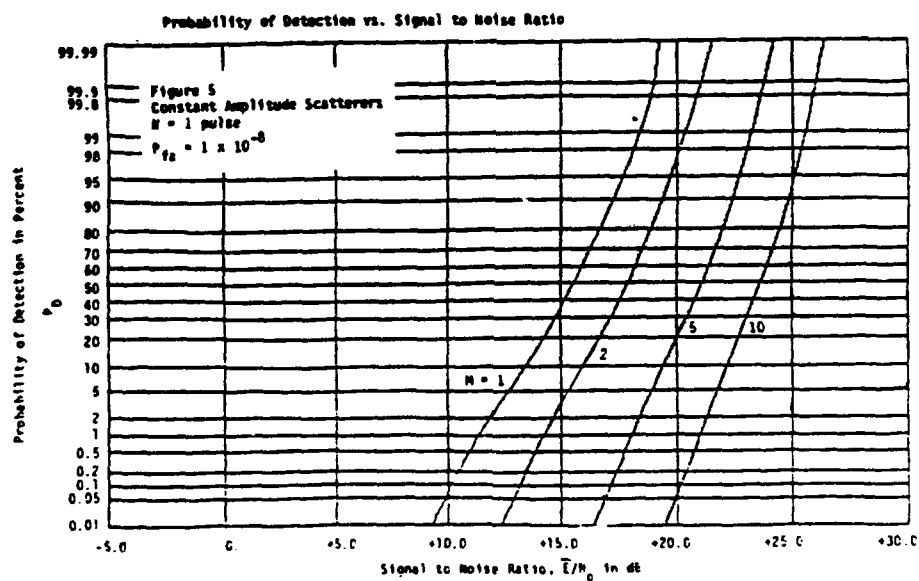


Figure 1.3b The figure from Ref. [1] for single-pulse constant amplitude scatterers when $P_{fa} = 1.E-8$

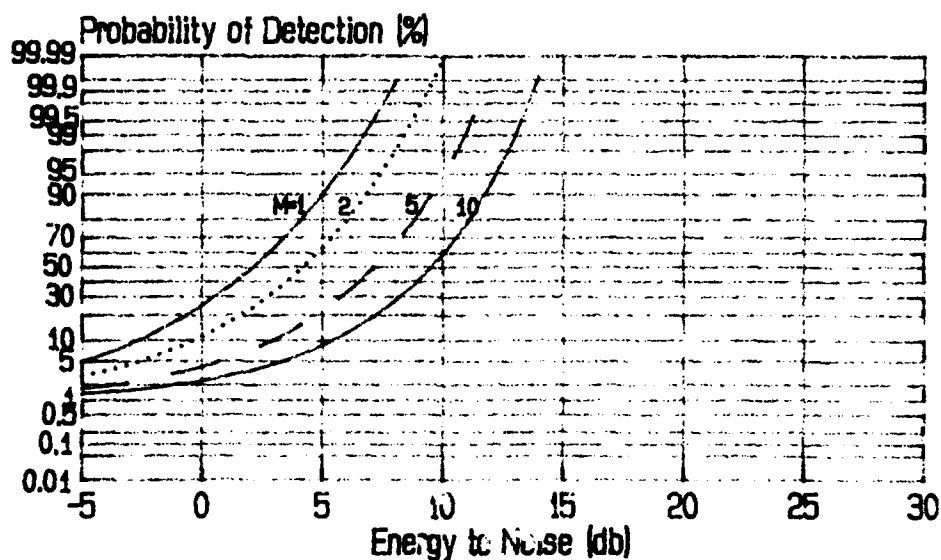


Figure 1.4a The reproduced figure for 4-pulse constant amplitude scatterers when $P_{fa} = 1.E-2$

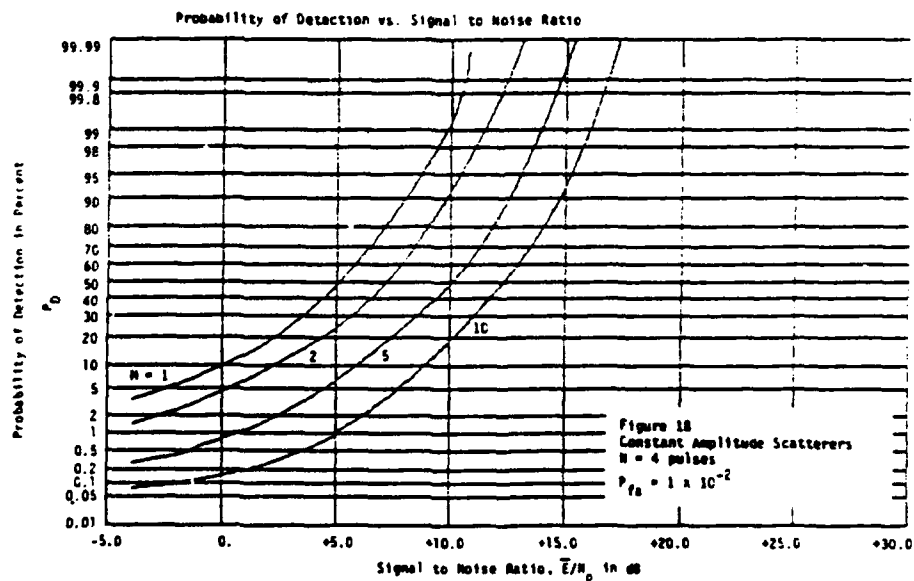


Figure 1.4b The figure from Ref. [1] for 4-pulse constant amplitude scatterers when $P_{fa} = 1.E-2$

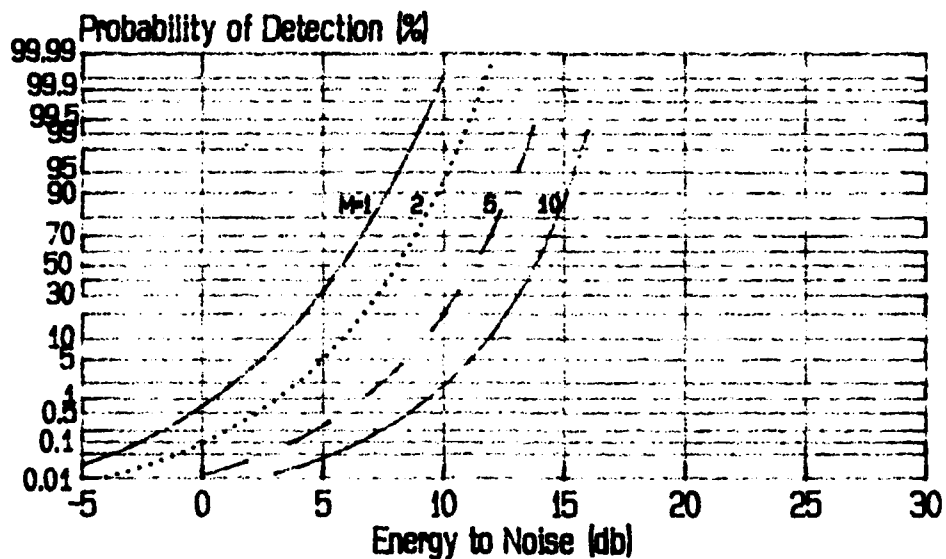


Figure 1.5a The reproduced figure for 4-pulse constant amplitude scatterers when $P_{fa} = 1.E-5$

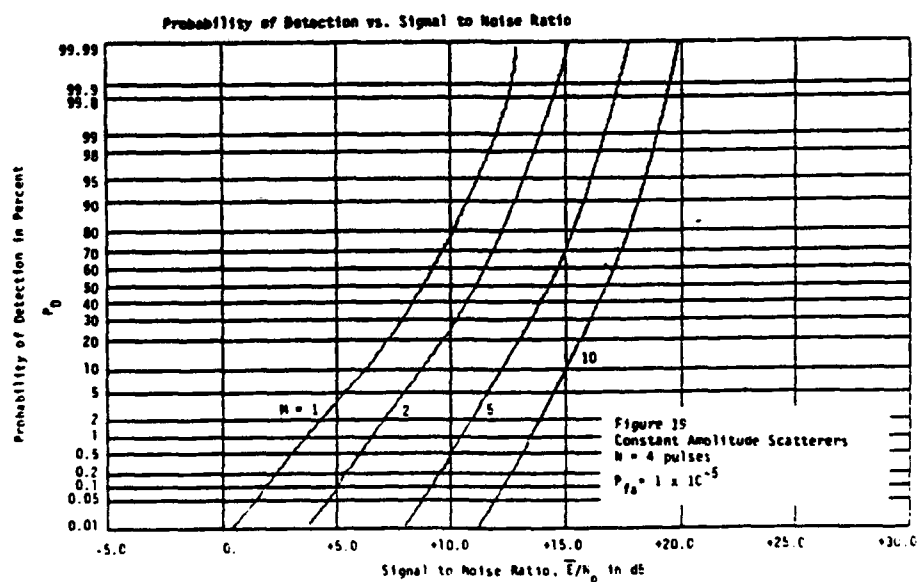


Figure 1.5b The figure from Ref. [1] for 4-pulse constant amplitude scatterers when $P_{fa} = 1.E-5$

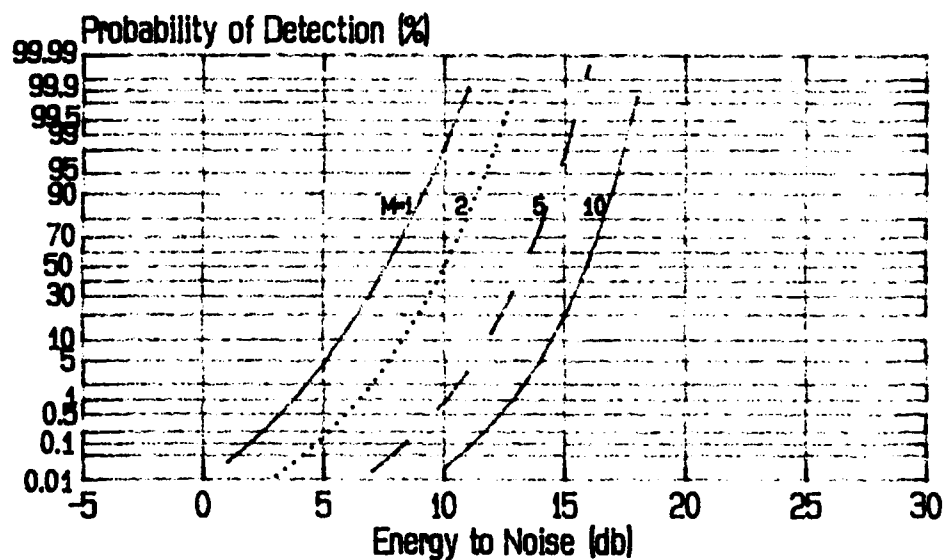


Figure 1.6a The reproduced figure for 4-pulse constant amplitude scatterers when $P_{fa} = 1.E-8$

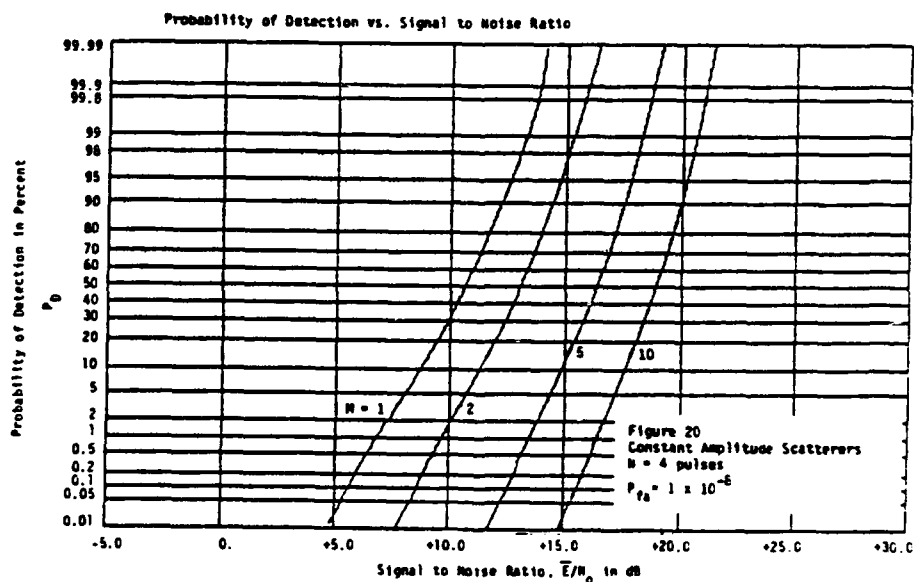


Figure 1.6b The figure from Ref. [1] for 4-pulse constant amplitude scatterers when $P_{fa} = 1.E-8$

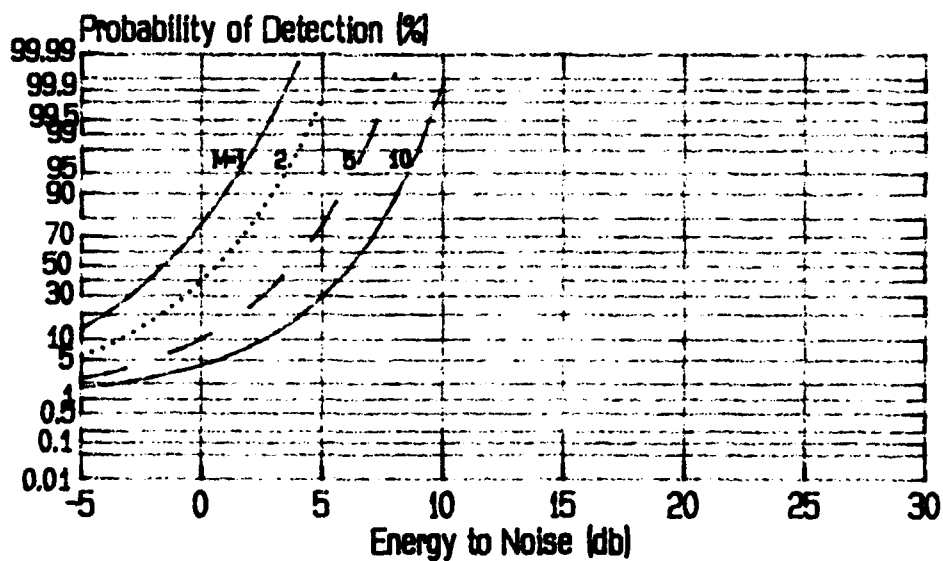


Figure 1.7a The reproduced figure for 16-pulse constant amplitude scatterers when $P_{fa} = 1.E-2$

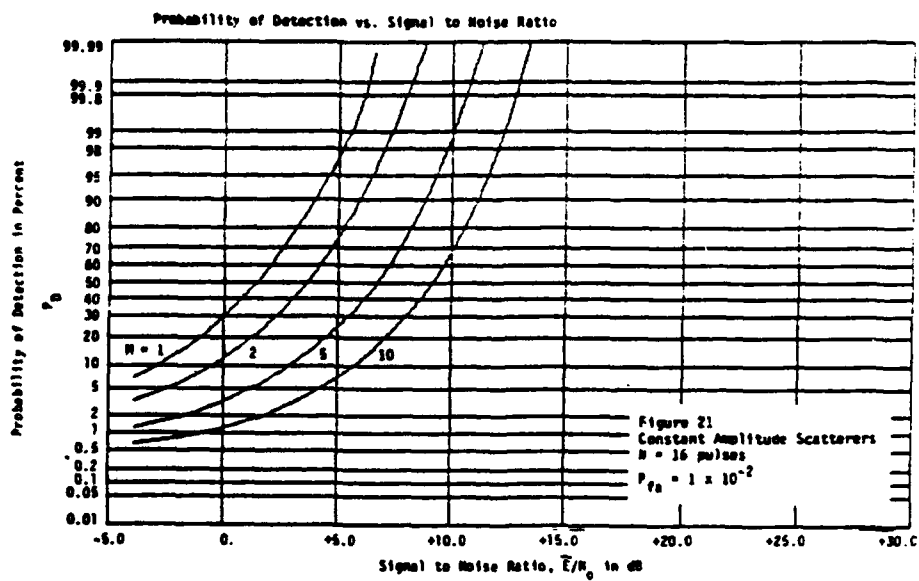


Figure 1.7b The figure from Ref. [1] for 16-pulse constant amplitude scatterers when $P_{fa} = 1.E-2$

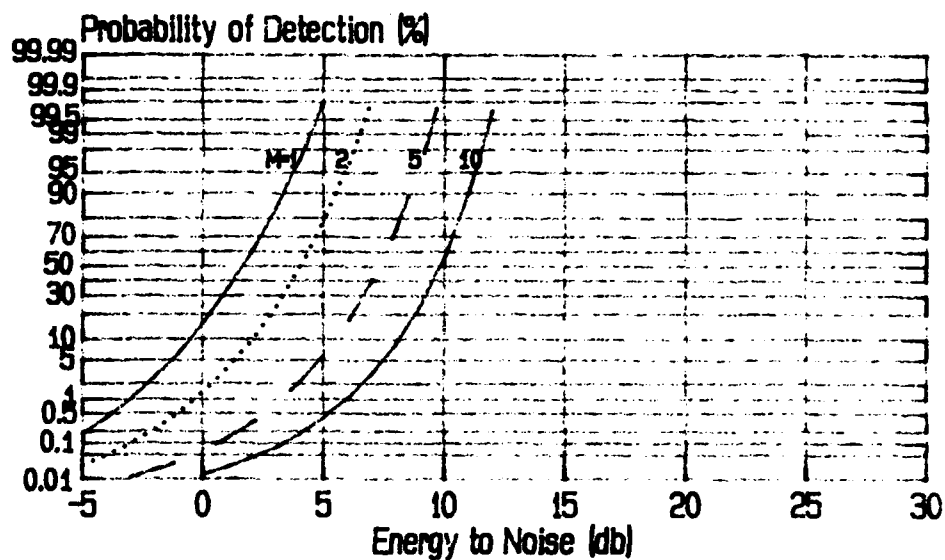


Figure 1.8a The reproduced figure for 16-pulse constant amplitude scatterers when $P_{fa} = 1.E-5$

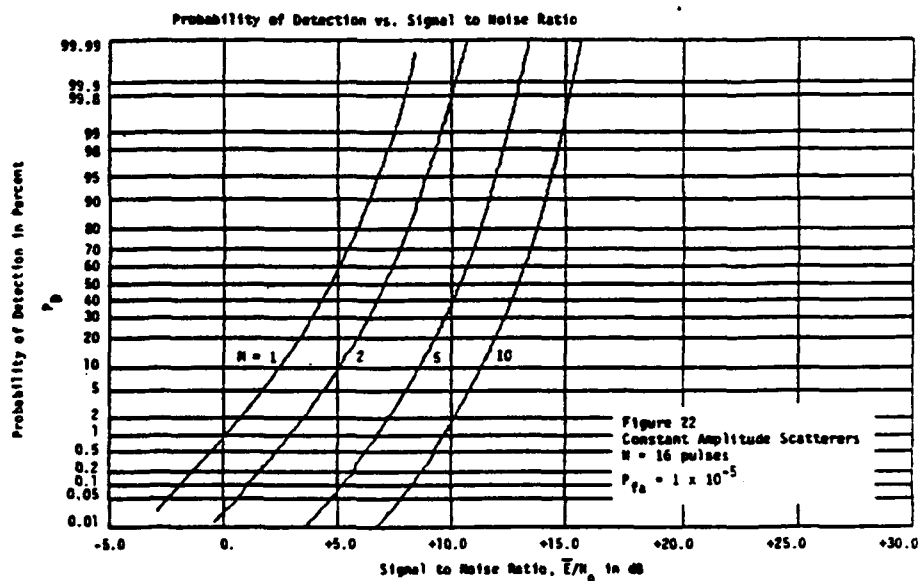


Figure 1.8b The figure from Ref. [1] for 16-pulse constant amplitude scatterers when $P_{fa} = 1.E-5$

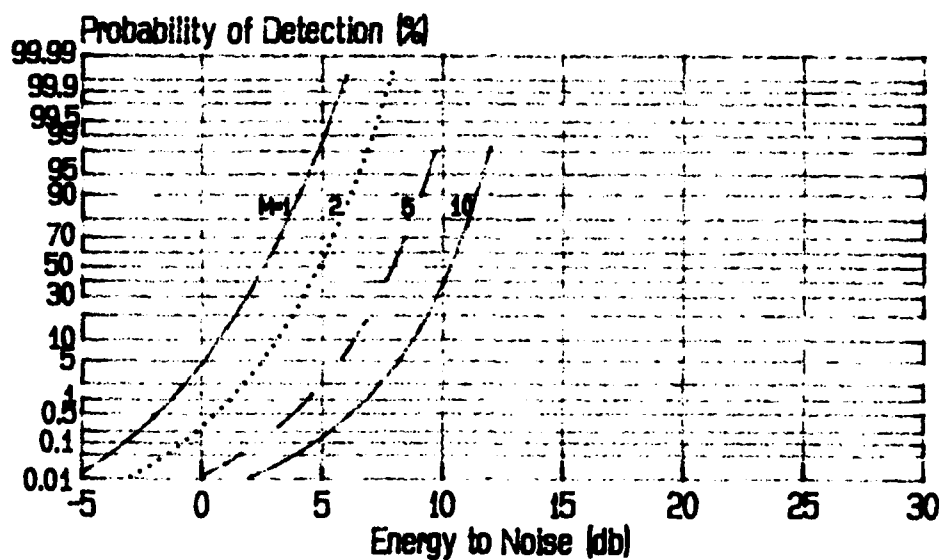


Figure 1.9a The reproduced figure for 16-pulse constant amplitude scatterers when $P_{fa} = 1.E-8$

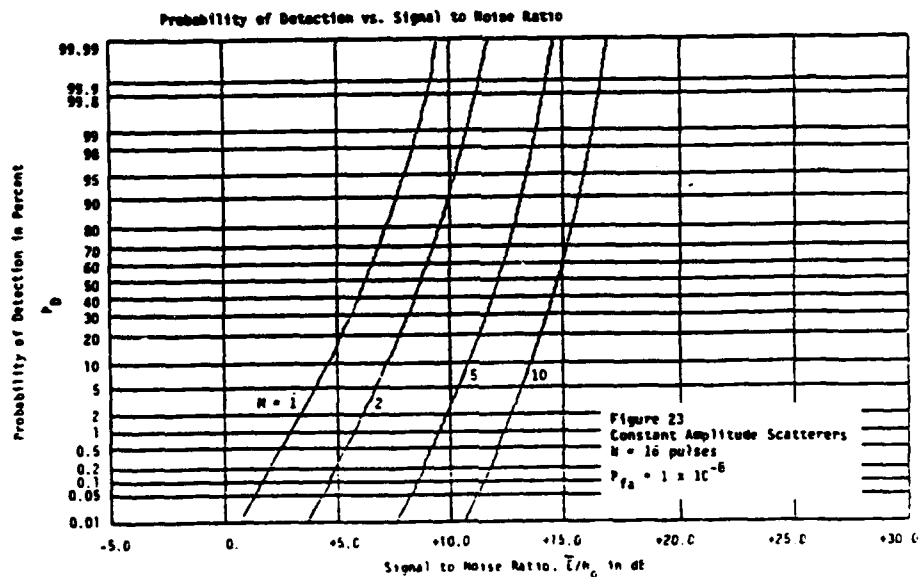


Figure 1.9b The figure from Ref. [1] for 16-pulse constant amplitude scatterers when $P_{fa} = 1.E-8$

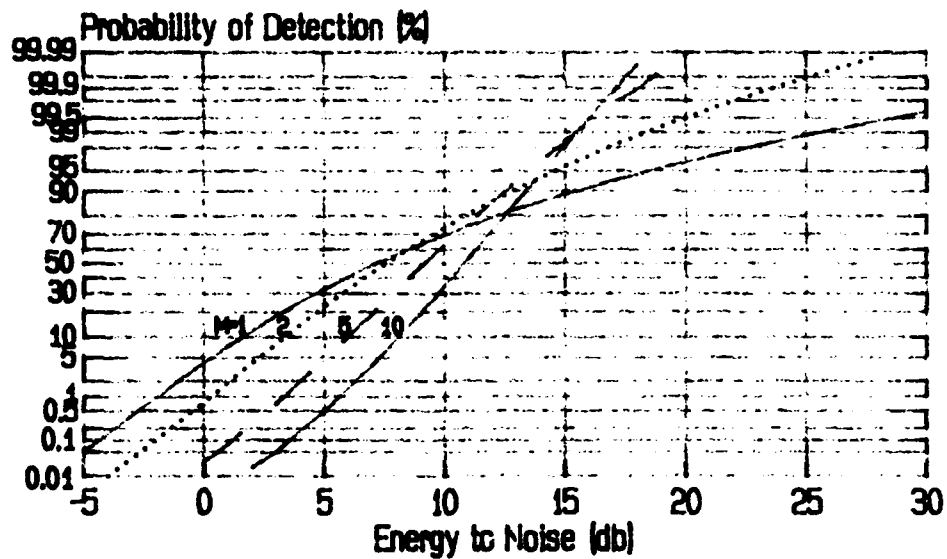


Figure 1.10a The reproduced figure for 16-pulse slow-fluctuating Rayleigh scatterers when $P_{fa} = 1.E-8$

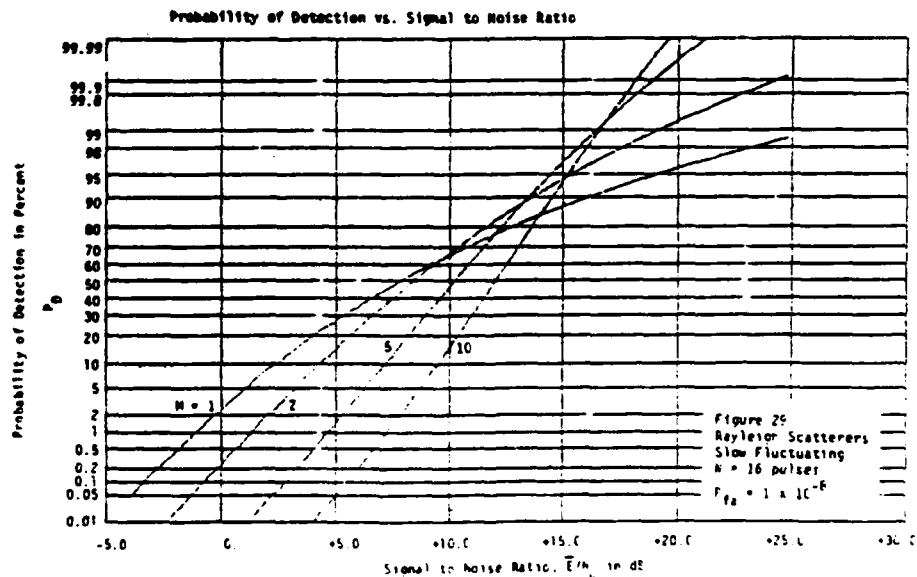


Figure 1.10b The figure from Ref. [1] for 16-pulse slow-fluctuating Rayleigh scatterers when $P_{fa} = 1.E-8$

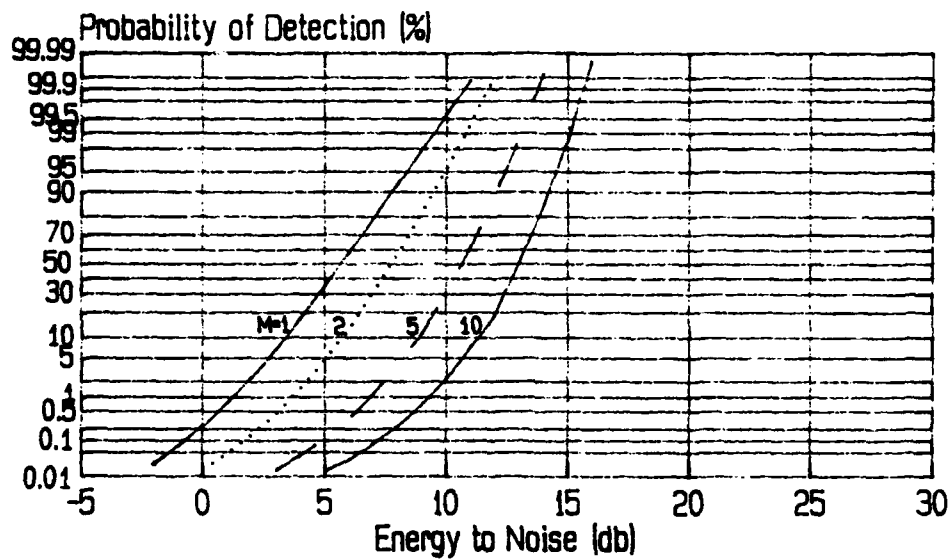


Figure 1.11a The reproduced figure for 16-pulse fast-fluctuating Rayleigh scatterers when $P_{fa} = 1.E-8$

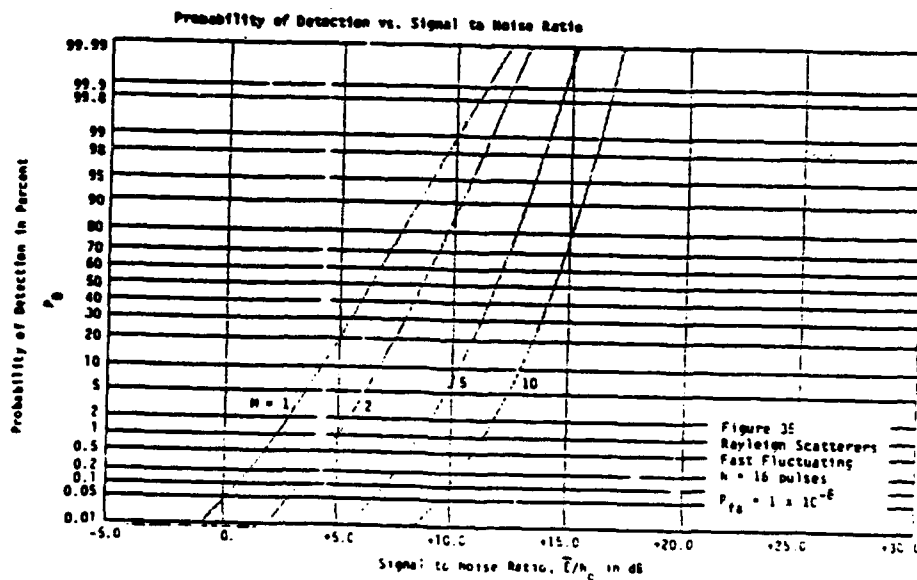


Figure 1.11b The figure from Ref. [1] for 16-pulse fast-fluctuating Rayleigh scatterers when $P_{fa} = 1.E-8$

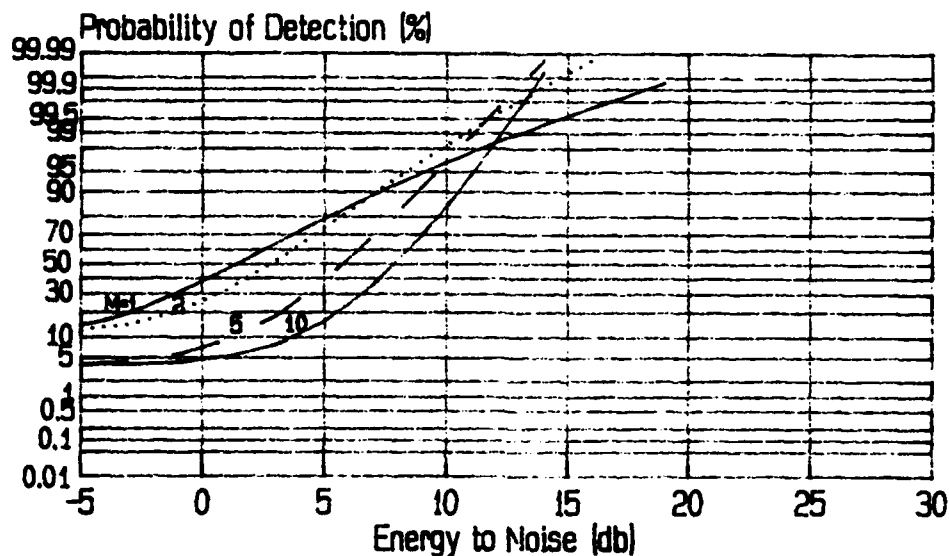


Figure 1.12a The reproduced figure for 16-pulse slow-fluctuating dominant plus Rayleigh scatterers when $P_{fa} = 1.E-2$

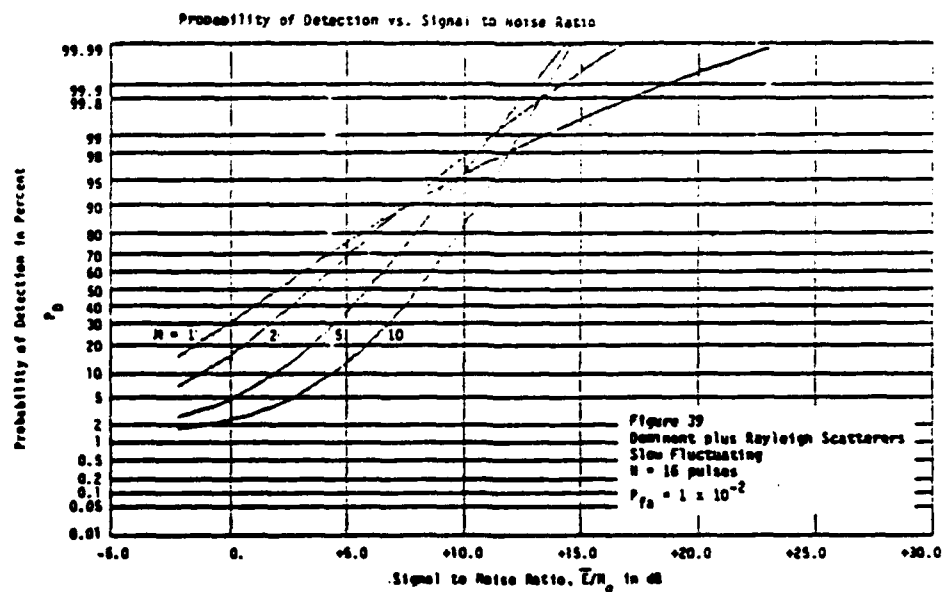


Figure 1.12b The figure from Ref. [1] for 16-pulse slow-fluctuating dominant plus Rayleigh scatterers when $P_{fa} = 1.E-2$

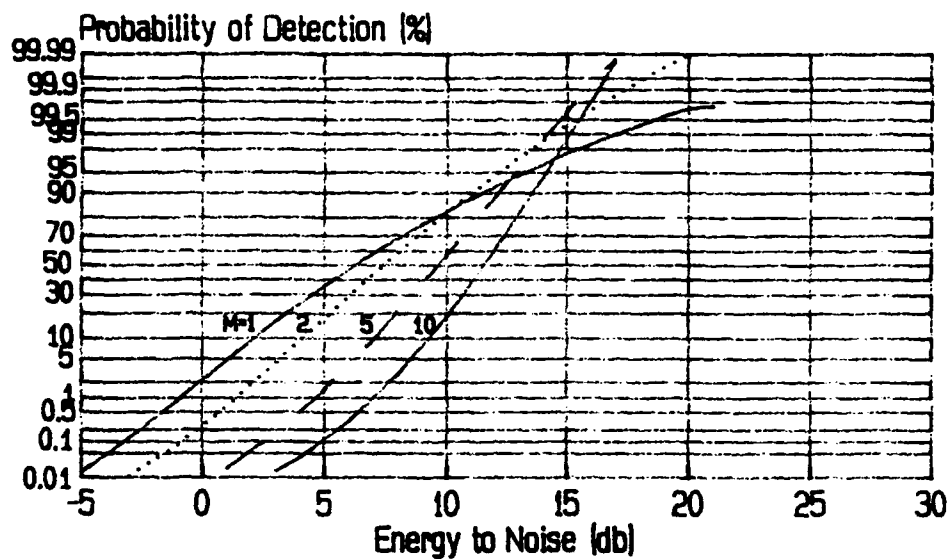


Figure 1.13a The reproduced figure for 16-pulse slow-fluctuating dominant plus Rayleigh scatterers when $P_{fa} = 1.E-8$

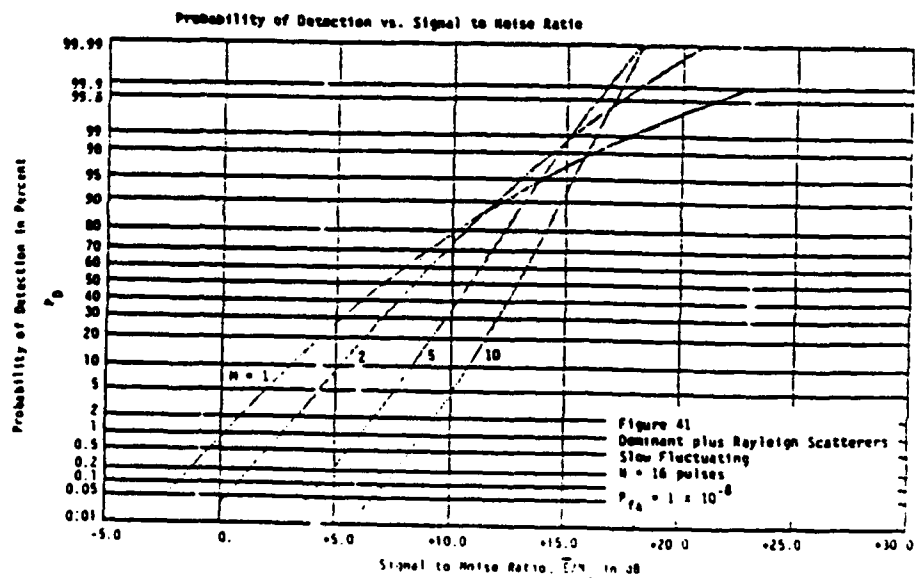


Figure 1.13b The figure from Ref. [1] for 16-pulse slow-fluctuating dominant plus Rayleigh scatterers when $P_{fa} = 1.E-8$

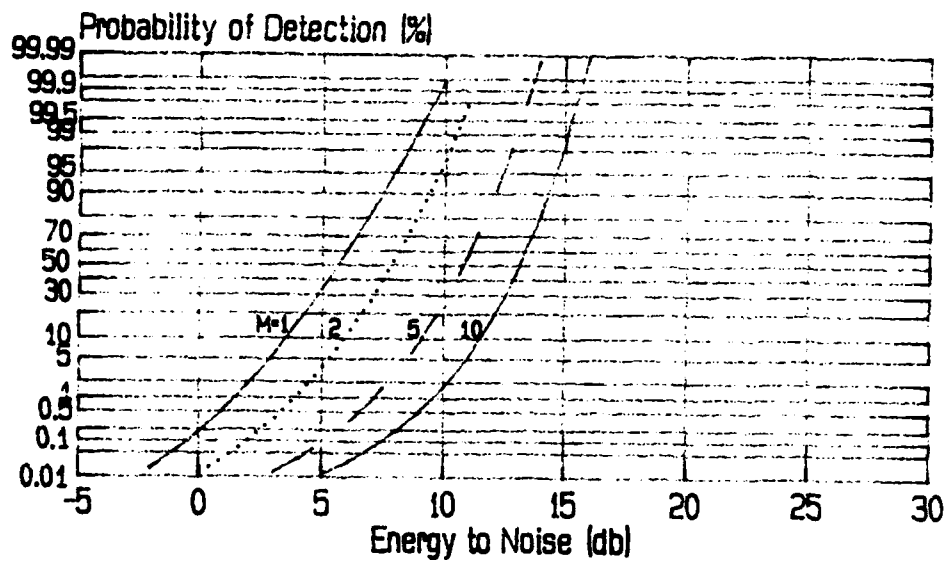


Figure 1.14a The reproduced figure for 16-pulse fast-fluctuating dominant plus Rayleigh scatterers when $P_{fa} = 1.E-8$

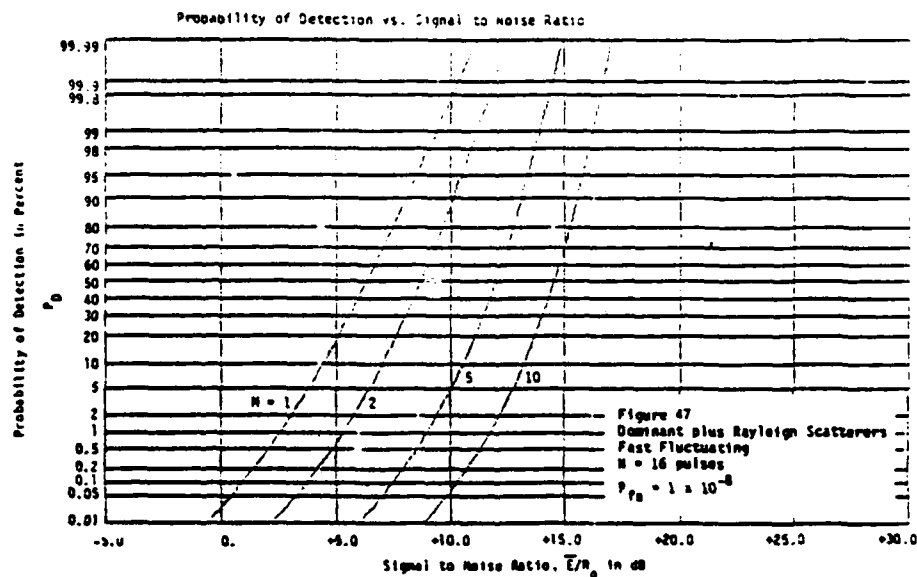


Figure 1.14b The figure from Ref. [1] for 16-pulse fast-fluctuating dominant plus Rayleigh scatterers when $P_{fa} = 1.E-8$

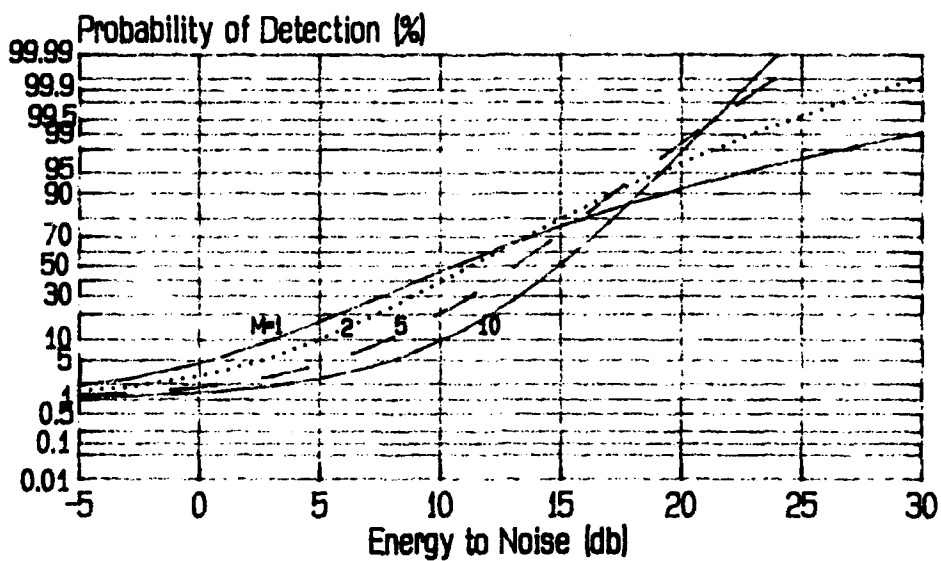


Figure 1.15 The reproduced figure for single-pulse Rayleigh scatterers when $P_{fa} = 1.E-2$

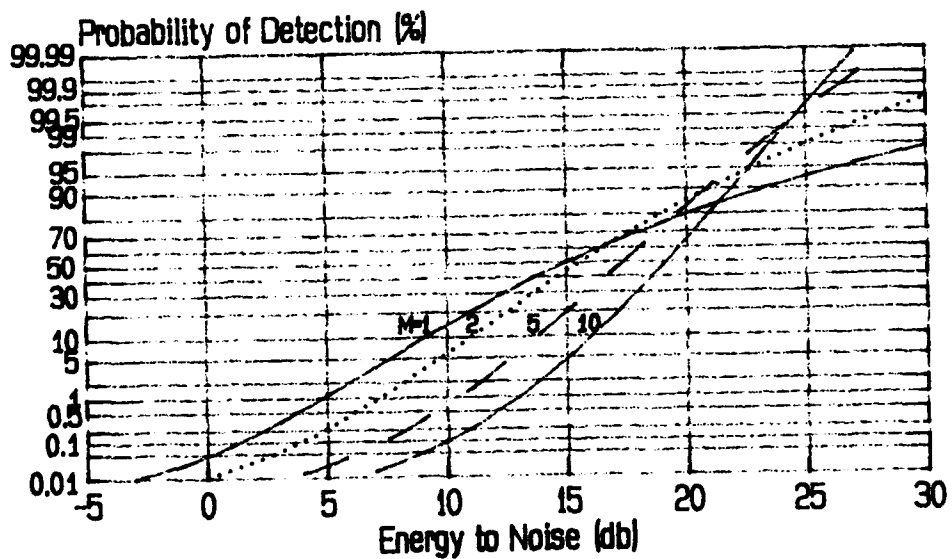


Figure 1.16 The reproduced figure for single-pulse Rayleigh scatterers when $P_{fa} = 1.E-5$

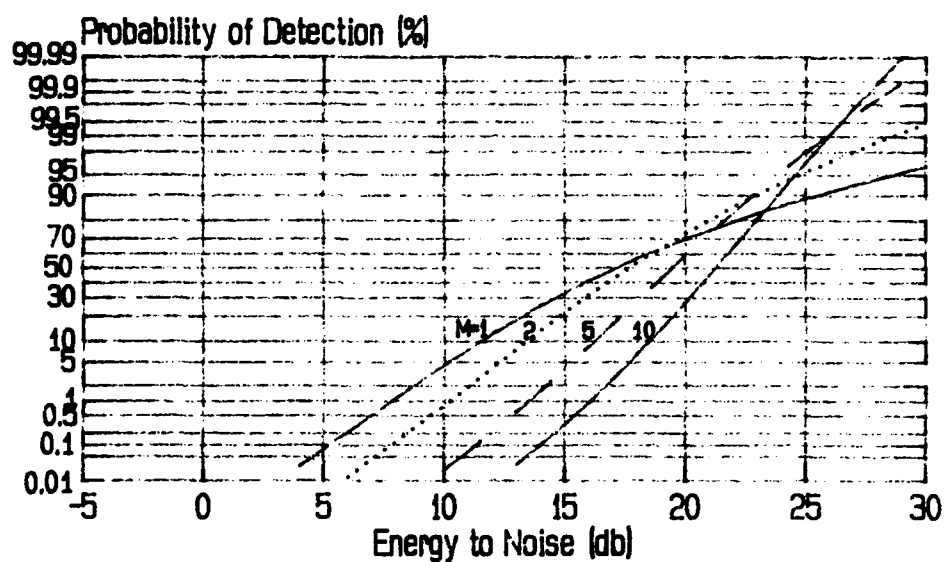


Figure 1.17 The reproduced figure for single-pulse Rayleigh scatterers when $P_{fa} = 1.E-8$

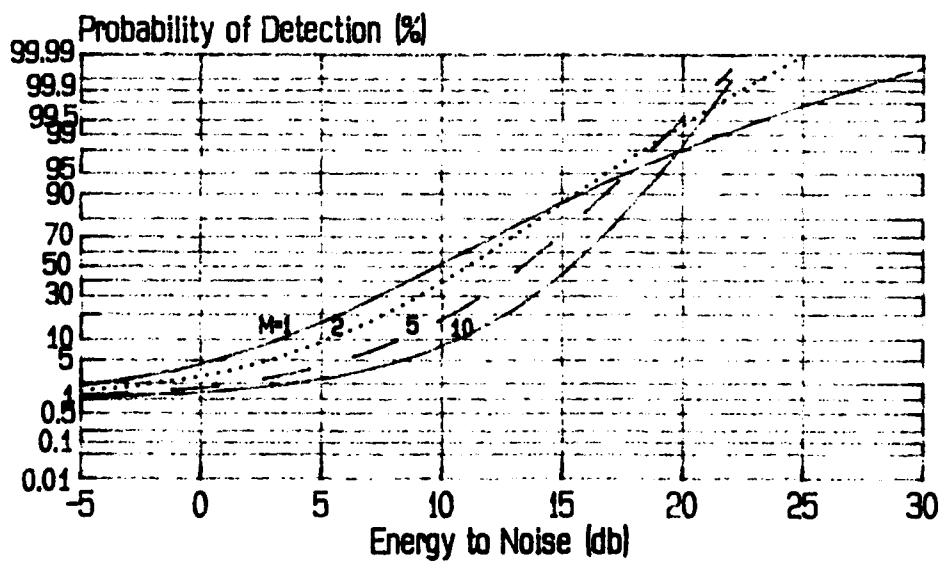


Figure 1.18 The reproduced figure for single-pulse dominant plus Rayleigh scatterers when $P_{fa} = 1.E-2$

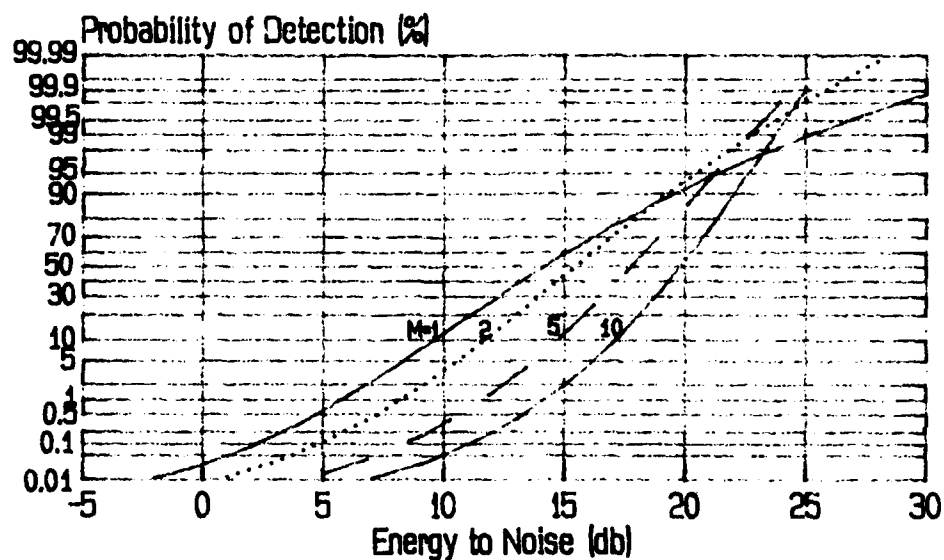


Figure 1.19 The reproduced figure for single-pulse dominant plus Rayleigh scatterers when $P_{fa} = 1.E-5$

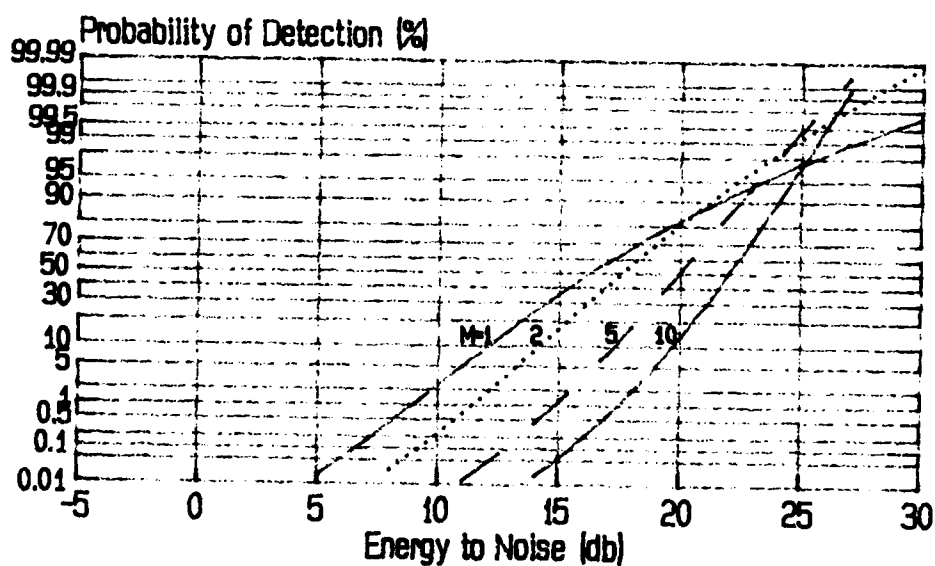


Figure 1.20 The reproduced figure for single-pulse dominant plus Rayleigh scatterers when $P_{fa} = 1.E-8$

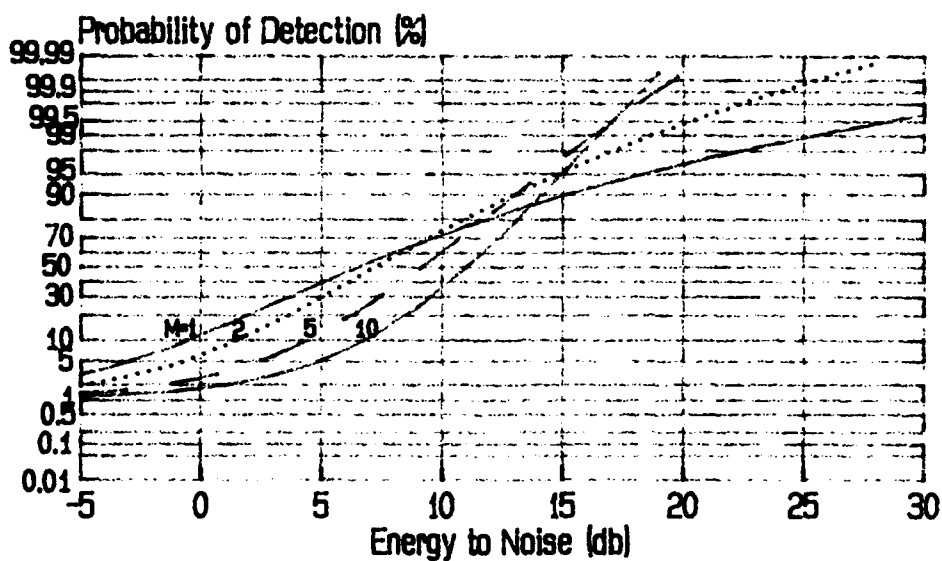


Figure 1.21 The reproduced figure for 4-pulse slow-fluctuating Rayleigh scatterers when $P_{fa} = 1.E-2$

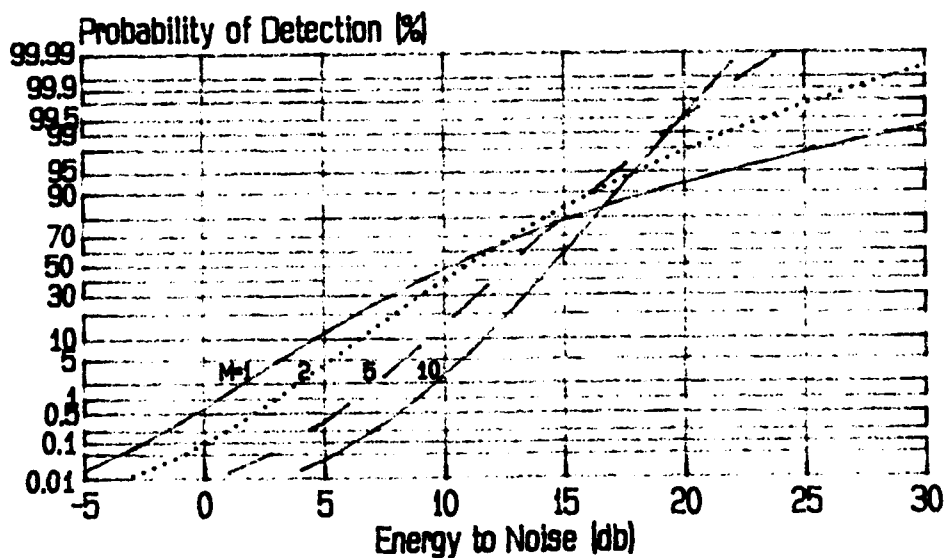


Figure 1.22 The reproduced figure for 4-pulse slow-fluctuating Rayleigh scatterers when $P_{fa} = 1.E-5$

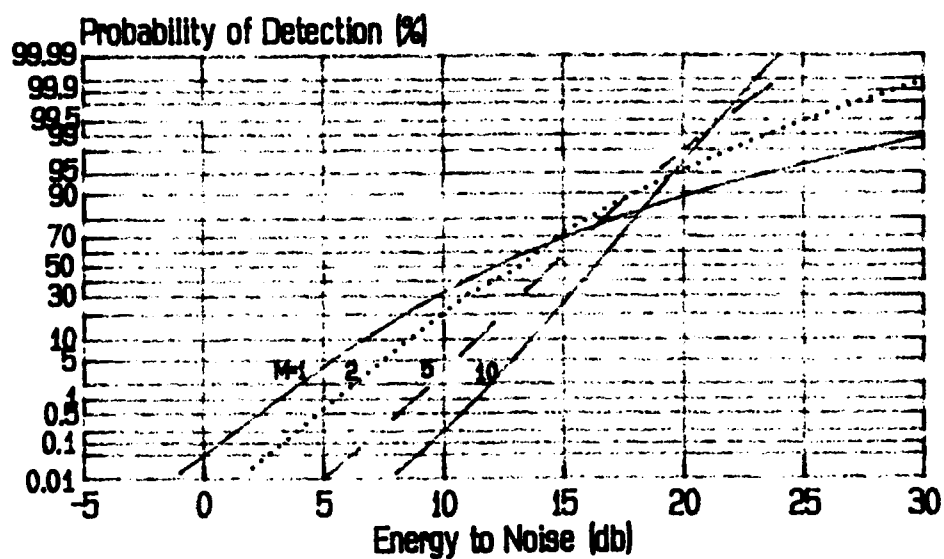


Figure 1.23 The reproduced figure for 4-pulse slow-fluctuating Rayleigh scatterers when $P_{fa} = 1.E-8$

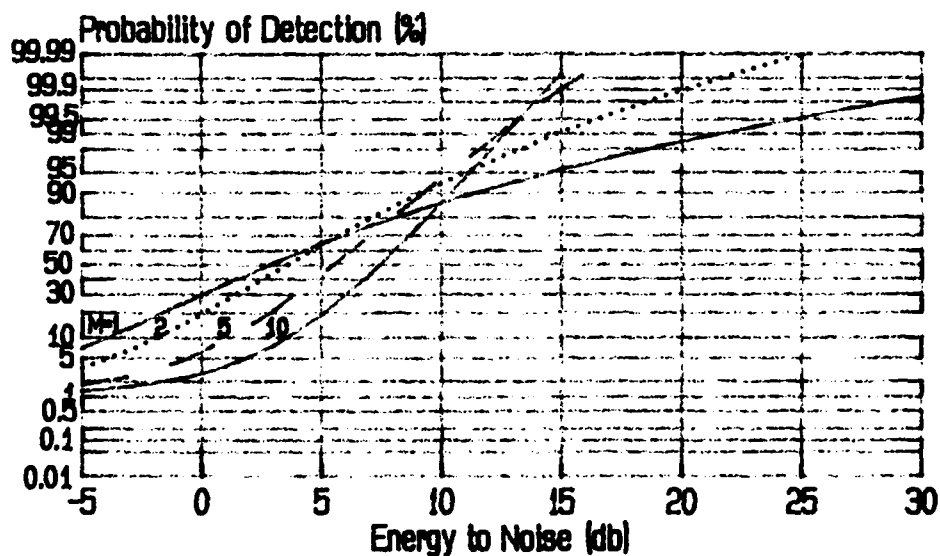


Figure 1.24 The reproduced figure for 16-pulse slow-fluctuating Rayleigh scatterers when $P_{fa} = 1.E-2$

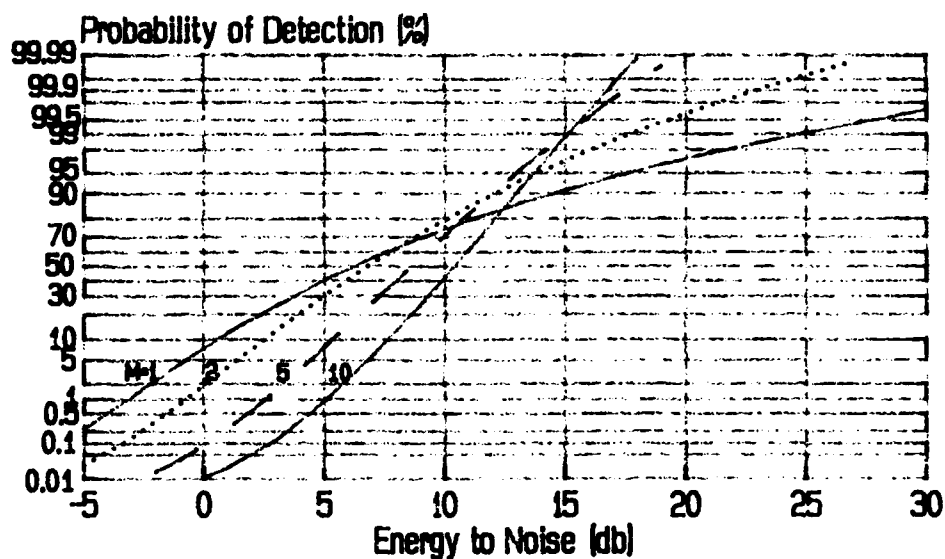


Figure 1.25 The reproduced figure for 16-pulse slow-fluctuating Rayleigh scatterers when $P_{fa} = 1.E-5$

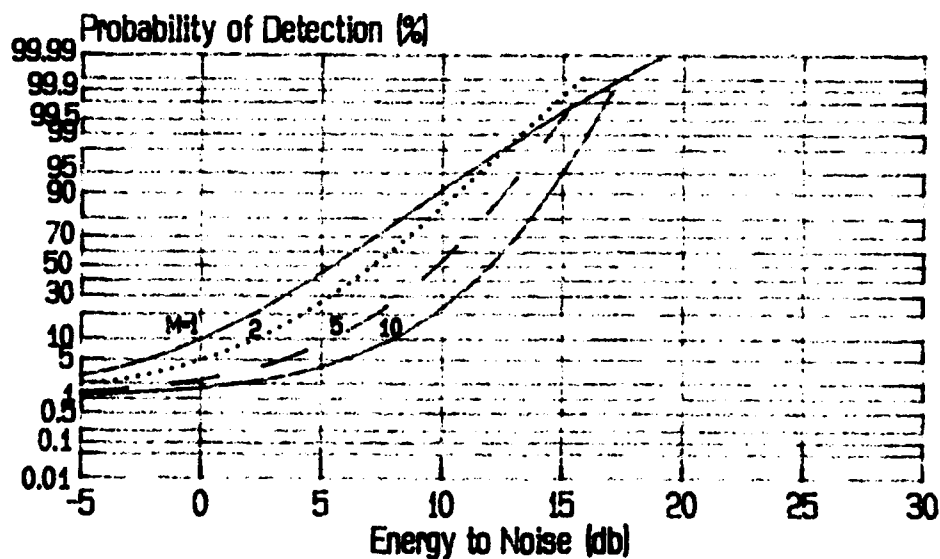


Figure 1.26 The reproduced figure for 4-pulse fast-fluctuating Rayleigh scatterers when $P_{fa} = 1.E-2$

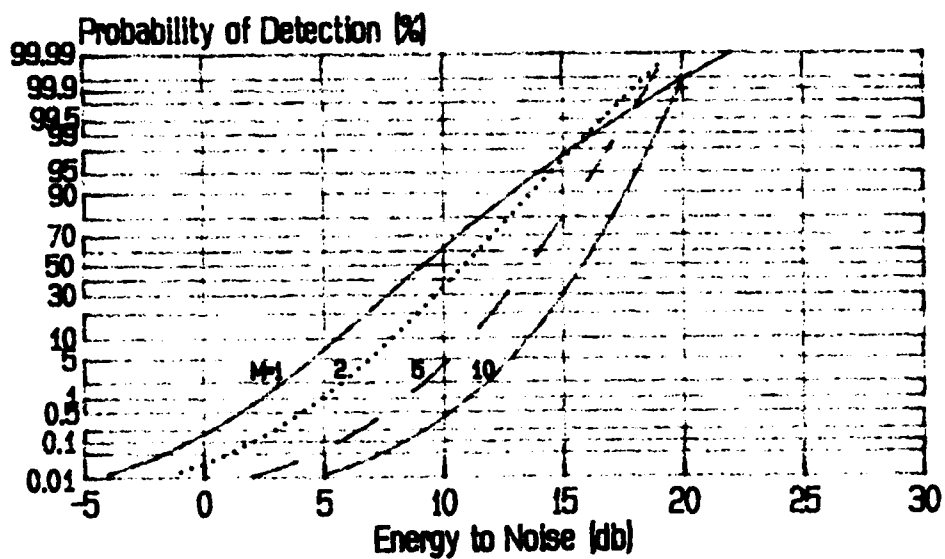


Figure 1.27 The reproduced figure for 4-pulse fast-fluctuating Rayleigh scatterers when $P_{fa} = 1.E-5$

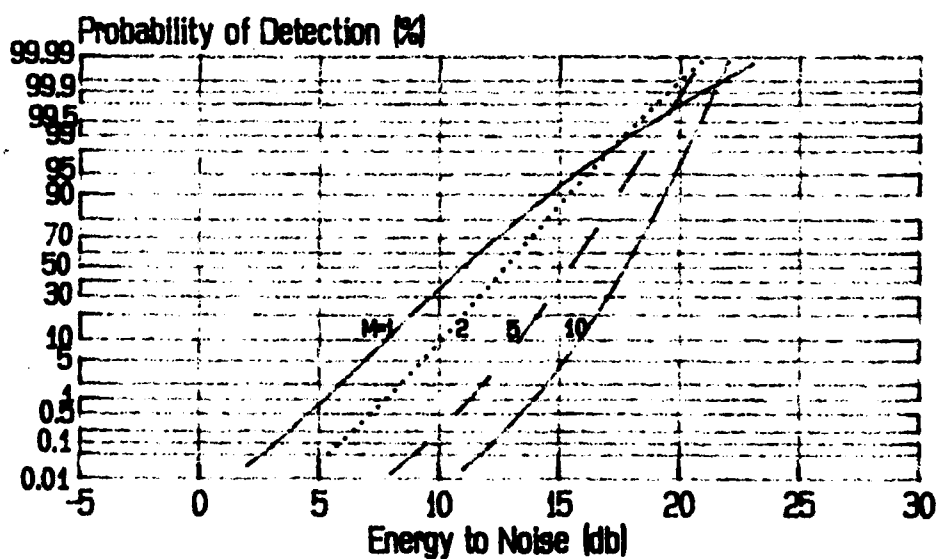


Figure 1.28 The reproduced figure for 4-pulse fast-fluctuating Rayleigh scatterers when $P_{fa} = 1.E-8$

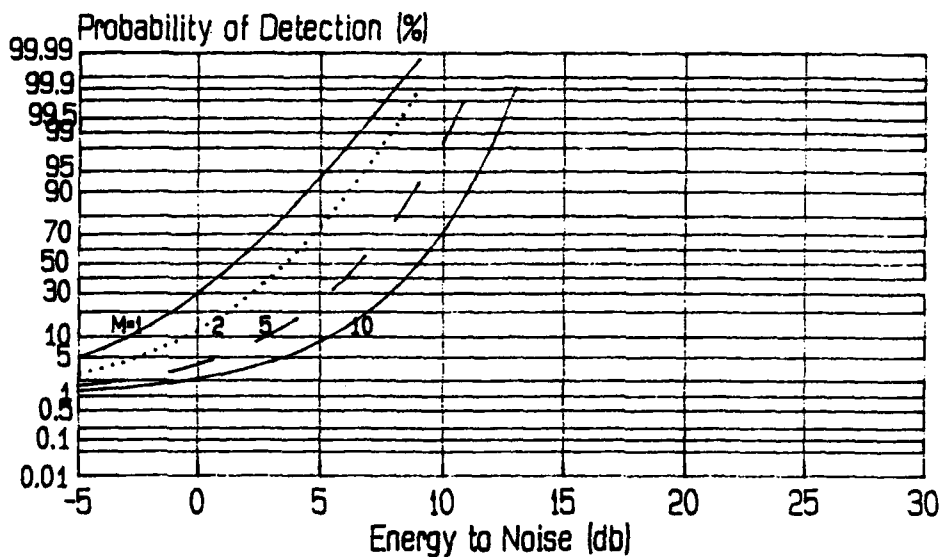


Figure 1.29 The reproduced figure for 16-pulse fast-fluctuating Rayleigh scatterers when $P_{fa} = 1.E-2$

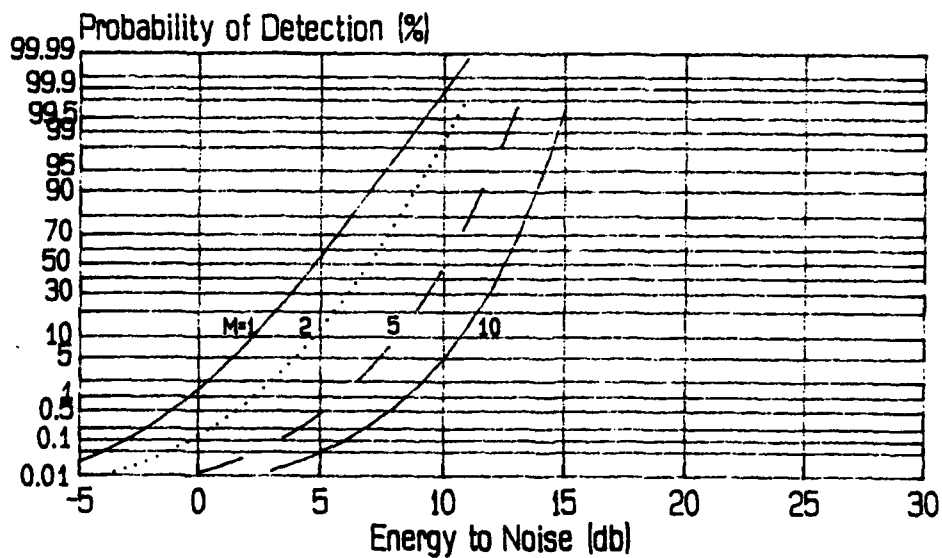


Figure 1.30 The reproduced figure for 16-pulse fast-fluctuating Rayleigh scatterers when $P_{fa} = 1.E-5$

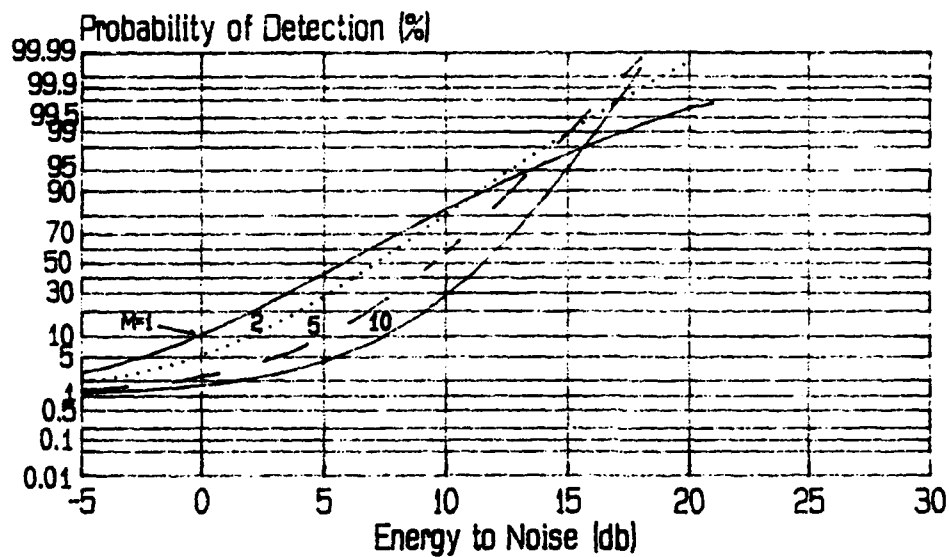


Figure 1.31 The reproduced figure for 4-pulse slow-fluctuating dominant plus Rayleigh scatterers when $P_{fa} = 1.E-2$

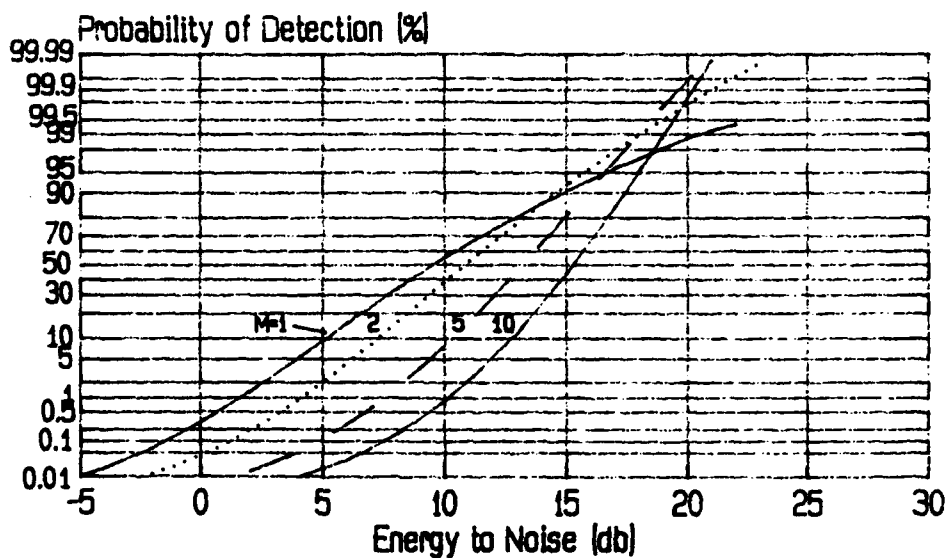


Figure 1.32 The reproduced figure for 4-pulse slow-fluctuating dominant plus Rayleigh scatterers when $P_{fa} = 1.E-5$

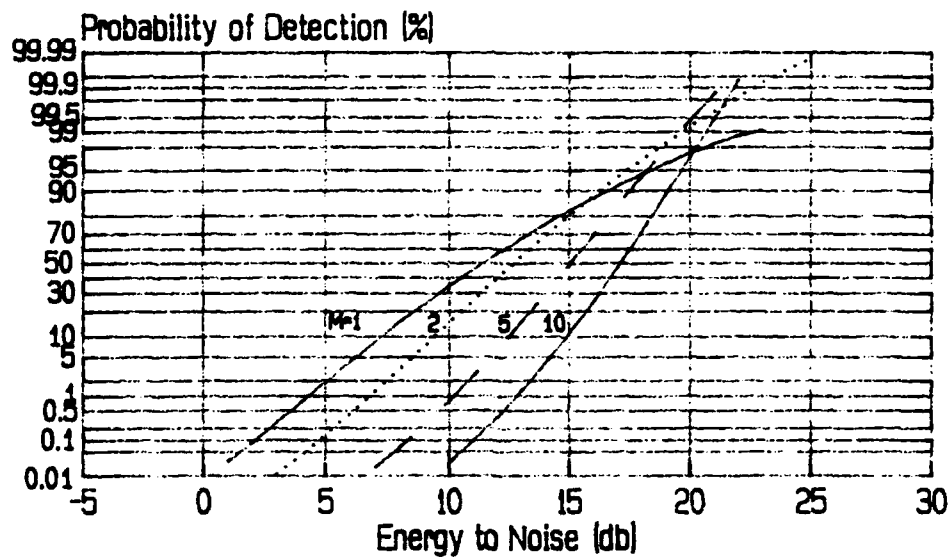


Figure 1.33 The reproduced figure for 4-pulse slow-fluctuating dominant plus Rayleigh scatterers when $P_{fa} = 1.E-8$

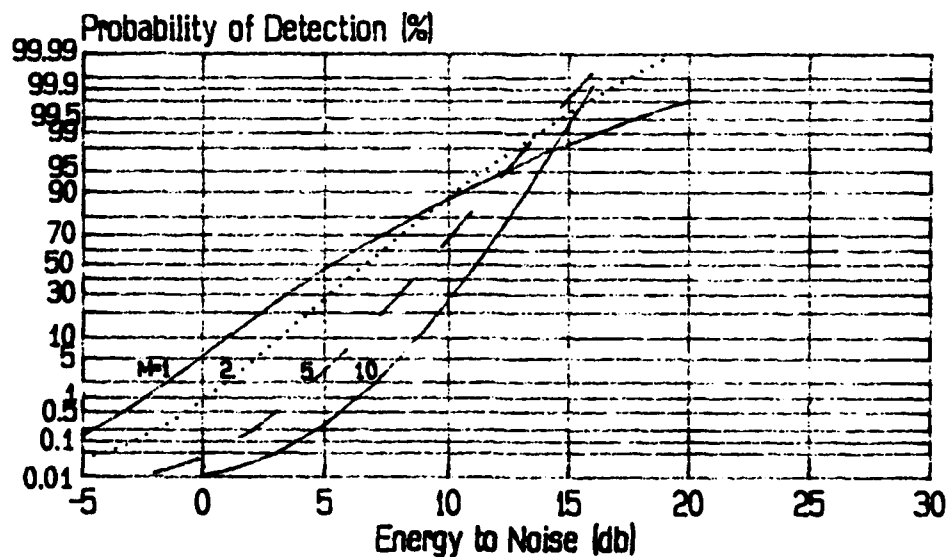


Figure 1.34 The reproduced figure for 16-pulse slow-fluctuating dominant plus Rayleigh scatterers when $P_{fa} = 1.E-5$

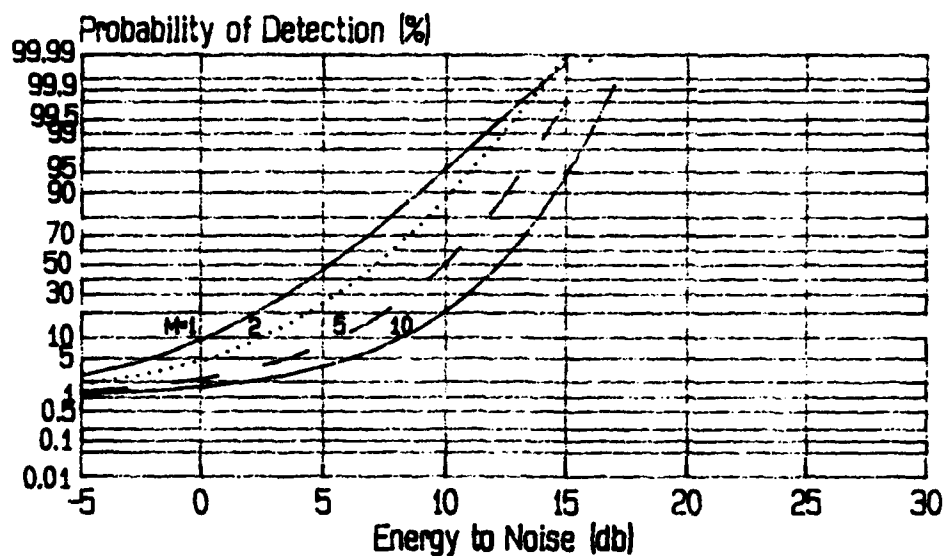


Figure 1.35 The reproduced figure for 4-pulse fast-fluctuating dominant plus Rayleigh scatterers when $P_{fa} = 1.E-2$

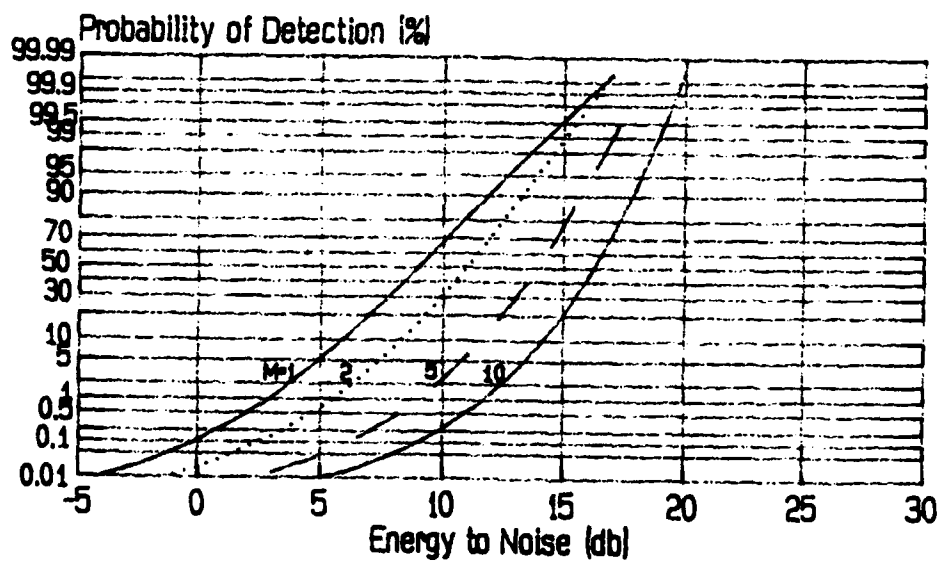


Figure 1.36 The reproduced figure for 4-pulse fast-fluctuating dominant plus Rayleigh scatterers when $P_{fa} = 1.E-5$

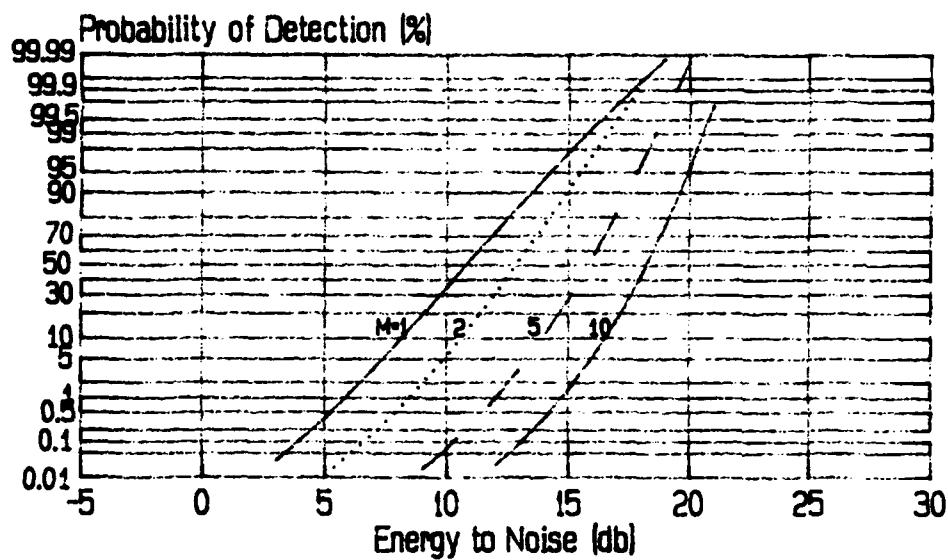


Figure 1.37 The reproduced figure for 4-pulse fast-fluctuating dominant plus Rayleigh scatterers when $P_{fa} = 1.E-8$

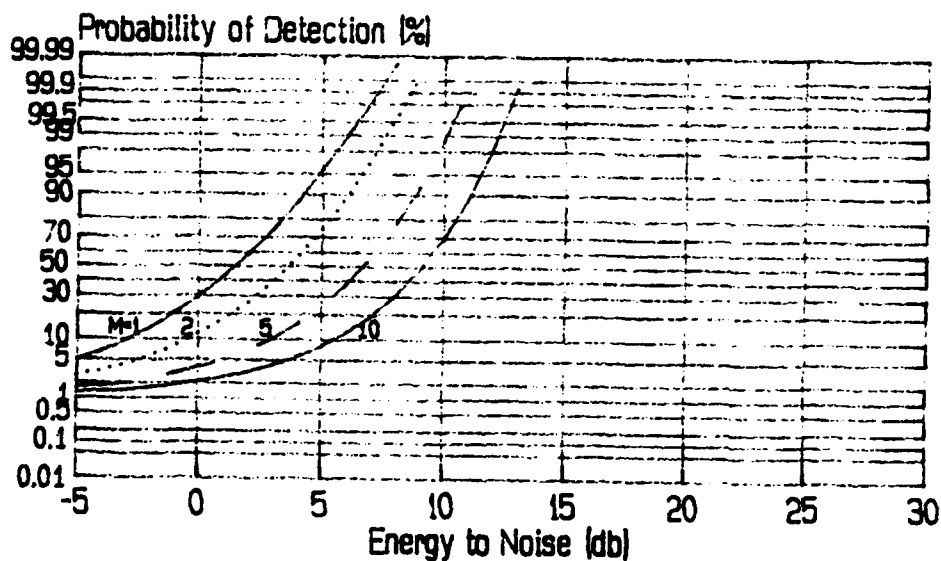


Figure 1.38 The reproduced figure for 16-pulse fast-fluctuating dominant plus Rayleigh scatterers when $P_{fa} = 1.E-2$

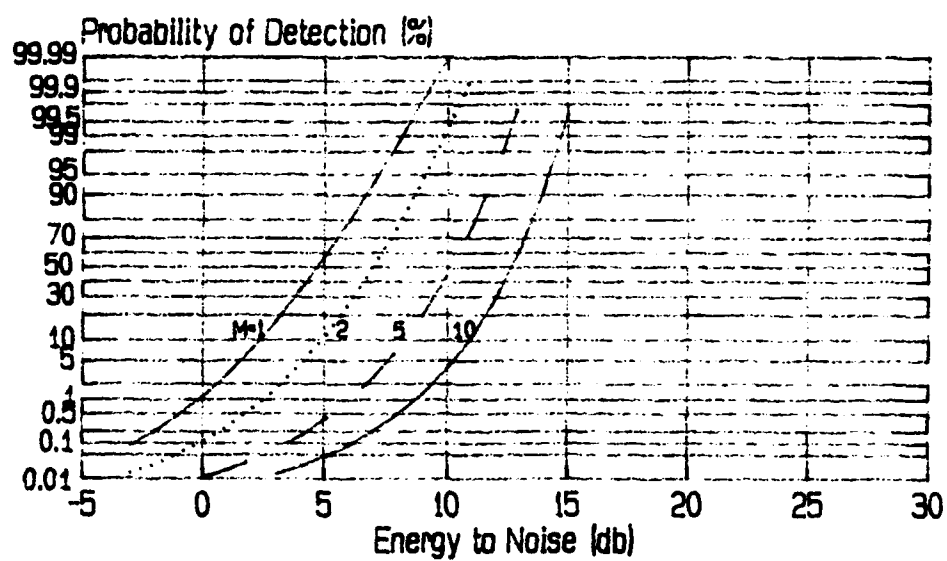


Figure 1.39 The reproduced figure for 16-pulse fast-fluctuating dominant plus Rayleigh scatterers when $P_{fa} \approx 1.E-5$

Part II

THE EFFECTS OF NON-UNIFORMLY DISTRIBUTED ENERGY

ON RADAR DETECTION PERFORMANCE

INTRODUCTION

Radar detection performance has been studied for several decades, e.g. [1]. In the existing works, it is generally assumed that the energy is uniformly distributed over the cells. In [1], the probability of detection was plotted vs. signal-to-noise ratio for different number of cells and different target models under the assumption of uniformly-distributed energy. The target models studied in [1] includes:

- 1) Single pulse, constant amplitude scatterers,
- 2) Single pulse, Rayleigh scatterers,
- 3) Single pulse, dominant plus Rayleigh scatterers,
- 4) Multi-pulses, constant amplitude scatterers,
- 5) Multi-pulses, slow fluctuating targets, Rayleigh scatterers,
- 6) Multi-pulses, fast fluctuating targets, Rayleigh scatterers,
- 7) Multi-pulses, slow fluctuating targets, dominant plus Rayleigh scatterers,
- 8) Multi-pulses, fast fluctuating targets, dominant plus Rayleigh scatterers.

However, in practical applications, the cells may have different energy; i.e., the energy is not uniformly distributed over the cells. In these cases, the actual probability of detection will differ from that with uniformly distributed energy and most of the formula involved in computing the probability must be modified.

A difficulty in studying the effects of energy distribution is caused by too many possible distribution manors of the energy. To overcome this difficulty, we have to develop a simple energy distribution model which can well represent the practical cases.

In this part of the report, we will make all the necessary modifications to the formula involved, develop a simple and realistic model of energy distribution which is described by only two parameters. Then we will compute the probability of detection for different target models, and discuss the change of detection probability caused by the energy distribution. Finally, the change will be interpreted by the results corresponding to uniformly distributed energy.

FORMULATION

To develop the energy distribution model, we assume that the total number of resolution cells, M , is given and the energy of the cells is fallen into a preset number of energy levels. The energy of the second level is twice the energy of the 1st level, the energy of the 3rd level is three times the energy of the 1st level, and so on.

Generally, the energy of more cells is in the middle levels, and energy of only a few cells is in the upper levels and lower levels. Therefore, we assume that the number of the cells with specific energy is normally distributed over energy levels. The number of cells at energy level E_l is given by

$$M_l = S \exp \left(- \frac{(E_l - \tilde{E})^2}{2\sigma^2} \right) \quad (l = 1, 2, \dots, N_l) \quad (2.1)$$

where N_l is the total number of energy levels. Since M_l is generally not an integer at an energy level, it has to be rounded. In Eq. (2.1), \tilde{E} and σ are free parameters to control the shape of the distribution, and S is so selected that the total number of cells equals to the given number, M . Figure 2.0 shows an example with eight energy levels.

Note the difference between energy distribution over cells and the distribution of the number of cells over the energy levels. When σ is small, the number of cells is distributed nearby \tilde{E} ; i.e., the number of cells is unevenly distributed over the energy levels. In this case, all the cells have almost the same energy, \tilde{E} ; i.e., the energy is almost uniformly distributed over the cells.

When the energy is not uniformly distributed over the cells, most of the formula given in Ref. [1] must be modified. The probability of detection is given by

$$P_d = 1 - \prod_{i=1}^{N_l} (1 - P_{dm_i})^{M_i} \quad (2.2)$$

where M_i is the number of cells at the i th energy level. Corresponding to different target

models, the formula to compute P_{dm_i} are given by

(1) Single Pulse, Constant Amplitude Scatterers

$$P_{dm_i} = 1 - T_{\sqrt{Y_b}} [1, 0, \sqrt{\bar{E}_i / M_i N_0}] \quad (2.3)$$

where $T_y[i, j, k]$ is the incomplete Toronto function; N_0 is the total noise energy; \bar{E}_i is the total energy at i th level; Y_b is the threshold. The formula to compute \bar{E}_i and Y_b will be given later.

(2) Single Pulse, Rayleigh Scatterers

$$P_{dm_i} = \exp \left\{ - \frac{Y_b}{1 + \bar{E}_i / 2 M_i N_0} \right\} \quad (2.4)$$

(3) Single Pulse, Dominant plus Rayleigh Scatterers

$$P_{dm_i} = \frac{1}{1 + 4M_i N_0 / \bar{E}_i} \left(1 + \frac{4M_i N_0}{\bar{E}_i} + \frac{Y_b}{1 + \bar{E}_i / 4M_i N_0} \right) \cdot \exp \left(- \frac{Y_b}{1 + \bar{E}_i / 4M_i N_0} \right) \quad (2.5)$$

(4) Multi-Pulses, Constant Amplitude Scatterers

$$P_{dm_i} = 1 - T_{\sqrt{Y_b}} [2N-1, N-1, \sqrt{N\bar{E}_i / M_i N_0}] \quad (2.6)$$

where N is the number of the pulses.

(5) Multi-Pulses, Slow Fluctuating targets, Rayleigh Scatterers

$$P_{dm_i} = 1 - I\left(\frac{Y_b}{\sqrt{N-1}}, N-2\right) + \left(1 + \frac{1}{N\bar{E}_i/2M_iN_0}\right)^{N-1} \cdot \exp\left(-\frac{Y_b}{1 + N\bar{E}_i/2M_iN_0}\right) \cdot I\left(\frac{Y_b}{\sqrt{N-1}(1 + 2M_iN_0/N\bar{E}_i)}, N-2\right) \quad (2.7)$$

where $I(x, j)$ is the incomplete gamma function.

(6) Multi-Pulses, Fast Fluctuating targets, Rayleigh Scatterers

$$P_{dm_i} = 1 - I\left(\frac{Y_b}{\sqrt{N}(1 + \bar{E}_i/2M_iN_0)}, N-1\right) \quad (2.8)$$

(7) Multi-Pulses, Slow Fluctuating targets, Dominant plus Rayleigh Scatterers

$$P_{dm_i} = \int_{Y_b}^{\infty} P(Y) dY \quad (2.9a)$$

where

$$P(Y) = \frac{Y\left(1 + \frac{1}{N\bar{E}_i/4M_iN_0}\right)^{N-2}}{(1 + N\bar{E}_i/4M_iN_0)^2} \cdot K \cdot \exp\left(\frac{-Y}{(1 + N\bar{E}_i/4M_iN_0)}\right) - \frac{(N-2)\left(1 + \frac{1}{N\bar{E}_i/4M_iN_0}\right)^{N-1}}{(1 + N\bar{E}_i/4M_iN_0)^2} \cdot K \cdot \exp\left(\frac{-Y}{(1 + N\bar{E}_i/4M_iN_0)}\right) + \frac{Y^{N-1} \exp(-Y)}{(N-2)! (1 + N\bar{E}_i/4M_iN_0)^2} \quad (2.9b)$$

and

$$K = I\left(\frac{Y}{\sqrt{N-1}(1 + 4M_iN_0/N\bar{E}_i)}, N-2\right) \quad (2.9c)$$

(8) Multi-Pulses, Fast Fluctuating targets, Dominant plus Rayleigh Scatterers.

$$P_{dm_i} = 1 - \frac{N!}{(1 + \bar{E}_i/4M_iN_0)^N} \cdot \sum_{k=0}^N \frac{1}{k! (N-k)!} \left(\frac{\bar{E}_i}{4M_iN_0} \right)^k \cdot I \left(\frac{Y_b}{\sqrt{N+k} (1 + \bar{E}_i/4M_iN_0)}, N+k-1 \right) \quad (2.10)$$

The threshold, Y_b , is related to false alarm probability, P_{fa} , by

$$P_{fa} = 1 - \left(1 - \exp(-Y_b) \right)^M \quad \text{for single pulse cases} \quad (2.11a)$$

and

$$P_{fa} = 1 - \left(I \left(\frac{Y_b}{\sqrt{N}}, N-1 \right) \right)^M \quad \text{for multi-pulse cases} \quad (2.11b)$$

The total signal energy in a given energy level, \bar{E}_i , is related to the total signal energy, \bar{E} , by

$$\bar{E} = \sum_{i=1}^{N_l} \bar{E}_i = \sum_{i=1}^{N_l} i M_i E_b \quad (2.12)$$

where M_i is the number of cells in the i th energy level, E_b is the base energy. Then

$$\bar{E}_i = i M_i E_b = i M_i \bar{E} / \sum_{j=1}^{N_l} j M_j \quad (2.13)$$

RESULTS

Corresponding to different target models, different number of cells, different pulse numbers, and different energy levels, we have plotted a number of figures which show the probability of detection vs. the ratio of total energy to noise. We plotted eight sets of figures corresponding to eight target models. Four pulses are assumed for multi-pulse cases. Each set consists of seven figures, which are described as follows:

- (a) Figures 2.1a–2.8a show the comparison of detection performance between uniformly distributed energy and non-uniformly distributed energy when $M = 2$ and a false alarm probability of 0.01. This false alarm probability corresponds to a Y_b value of 5.296 for single pulse cases and a Y_b value of 10.97 for multi-pulse cases. M is the total number of cells and Y_b is the threshold. When energy is uniformly distributed over the cells, both cells have the same energy; when energy is non-uniformly distributed over the cells, the energy of one of the cells is twice that of the other cell.
- (b) Figures 2.1b–2.8b show the same cases as those in (a) except a false alarm probability of $1.E-8$. This false alarm probability corresponds to a Y_b value of 19.11 for single pulse cases and a Y_b value of 27.35 for multi-pulse cases.
- (c) Figures 2.1c–2.8c show the comparison of detection performance between different values of σ in Eq. (2.1) when $N_l = 8$, $M = 10$, $\tilde{E} = 5$, and a false alarm probability of 0.01. This false alarm probability corresponds to a Y_b value of 6.903 for single pulse cases and a Y_b value of 13.05 for multi-pulse cases. \tilde{E} is the energy level with largest number of cells (see Eq. (2.1)), N_l is the number of energy levels, M is the total number of cells. The energy is more uniformly distributed over the cells when σ is smaller.
- (d) Figures 2.1d–2.8d show the same cases as those in (c) except a false alarm probability of $1.E-8$. This false alarm probability corresponds to a Y_b value of 20.72 for single pulse cases and a Y_b value of 29.15 for multi-pulse cases.
- (e) Figures 2.1e–2.8e show the comparison of detection performance between different values of \tilde{E} when $N_l = 8$, $M = 10$, $\sigma = 0.5$ and a false alarm probability of 0.01. This false alarm probability corresponds to a Y_b value of 6.903 for single pulse cases and a Y_b value of 13.05 for multi-pulse cases.
- (f) Figures 2.1f–2.8f show the same cases as those in (e) except $\sigma = 3.0$.

(g) Figures 2.1g–2.8g show the same cases as those in (e) except $\sigma = 2.0$ and a false alarm probability of $1.E-8$. This false alarm probability corresponds to a Y_b value of 20.72 for single pulse cases and a Y_b value of 29.15 for multi-pulse cases.

In the figures, the horizontal axis denotes the ratio of total signal energy to total noise energy (\bar{E}/N_0) in decibel. The vertical axis denotes the probability of detection in percentage. Y_b is the threshold, M is the total number of cells, “Level” is the total number of energy levels, “Mean” denotes \bar{E} .

The following eight sets of figures describe different target models:

Figures 2.1a–2.1g: single-pulse constant amplitude scatterers;

Figures 2.1a–2.2g: single-pulse Rayleigh scatterers;

Figures 2.3a–2.3g: single-pulse dominant plus Rayleigh scatterers;

Figures 2.4a–2.4g: four-pulses constant amplitude scatterers;

Figures 2.5a–2.5g: four-pulse slow-fluctuating-target Rayleigh scatterers;

Figures 2.6a–2.6g: four-pulse fast-fluctuating-target Rayleigh scatterers;

Figures 2.7a–2.7g: four-pulse slow-fluctuating-target dominant plus Rayleigh scatterers; Figs. 2.7e and 2.7f are omitted to save computational efforts.

Figures 2.8a–2.8g: four-pulse fast-fluctuating-target dominant plus Rayleigh scatterers.

Figs. 2.9–2.12 show the energy distribution of the cells over energy levels for various σ and \bar{E} when the total number of cells is 10 and the total number of energy levels is 8. When σ is small, the cells are distributed over a few energy levels nearby \bar{E} , i.e., the cells have nearly equal energy. This situation is similar as uniformly-distributed energy over the cells. When $\sigma = 0.1$, all the cells are in the energy level \bar{E} ; i.e., the energy is uniformly distributed over the cells.

Table 2.1 shows the distribution of the cells over energy levels for different values of σ when total number of cells is 10 and total number of energy level is 8 and $\bar{E} = 5$.

Table 2.1 Distribution of the 10 Cells over 8 Energy Levels for Different Values of σ when $\bar{E} = 5$.

Energy Level σ	1	2	3	4	5	6	7	8
0.1	0	0	0	0	10	0	0	0
0.5	0	0	0	1	8	1	0	0
1.0	0	0	1	2	4	2	1	0
2.0	0	1	1	2	2	2	1	1
3.0	1	1	1	1	3	1	1	1

DISCUSSION

The figures in this part of the report show the following common phenomenon for every target models:

When Y_b is small, the probability of detection is not significantly affected by energy distribution. When Y_b becomes larger, the effects of energy distribution become more significant. For example, when $Y = 29.15$ and the total number of cells is 10, in the case of 4-pulse constant amplitude scatterers the detection probability is about 20% when $\bar{E}/N_0 = 15$ db and the energy is uniformly distributed over the cells (see Fig. 2.4d, $\sigma = 0.1$). However, when $\sigma = 3.0$ (energy is not uniformly distributed over the cells), the detection probability becomes about 55%.

In addition to this common phenomenon for every target mode. We can also find that the effects of energy distribution are also highly affected by target models. We found that

multi-pulse constant amplitude scatterers are most seriously affected by energy distribution; single pulse constant amplitude scatterers are the second; then it comes in the order of multi-pulse, fast-fluctuating-target dominant plus Rayleigh scatterers, multi-pulse, fast-fluctuating-target Rayleigh scatterers, multi-pulse slow-fluctuating-target dominant plus Rayleigh scatterers, multi-pulse slow-fluctuating-target Rayleigh scatterers, single-pulse dominant plus Rayleigh scatterers, and finally single-pulse Rayleigh scatterers. For constant amplitude scatterers (single-pulse or multi-pulse), the effects of the energy distribution are similar no matter the probability of detection is low or high. However, for other target models (Rayleigh scatterers and dominant plus Rayleigh scatterers), the effects of energy distribution is significant in some of the probability range and less significant in the other ranges. Generally, non-uniformly distributed energy will increase the probability of detection and the effects are more significant in low probability ranges. The reason is that the threshold is hard to across in that range and the non-uniformly distributed energy increase the chance to across the threshold significantly for the cells with higher energy.

Let's define the "cell probability of detection" as P_{dm_i} when the energy is uniformly distributed. Then the effects of the energy distribution can also be explained by the shape of the cell probability of detection. First, it is helpful to consider the problem with only two cells. The probability of detection of the first cell is p_1 , and the probability of detection of the second cell is p_2 . When the energy is uniformly distributed, $p_1 = p_2 = p$ (cell probability of detection). The total probability of detection is given by:

$$P = 1 - (1 - p_1)(1 - p_2) = 2p - p^2 \quad (2.14)$$

Now, let's assume the energy is not uniformly distributed and the first cell has lower energy and the second cell has higher energy. Then p_1 becomes $(p - \delta p_1)$, and p_2 becomes $(p + \delta p_2)$. The total probability of detection becomes

$$P + \delta P = 1 - (1 - p_1)(1 - p_2) \cong P + (1 - p)(\delta p_2 - \delta p_1) \quad (2.15)$$

therefore

$$\delta P \cong (1-p)(\delta p_2 - \delta p_1) \quad (2.16)$$

We can see the trends of δP from the plot of the p vs. signal-to-noise ratio in linear scales. When the curve is concave-up, $\delta p_2 > \delta p_1$, and the non-uniformly distributed energy will increase the probability of detection. When the curve is concave-down, $\delta p_1 > \delta p_2$, and the non-uniformly distributed energy will decrease the probability of detection. The increment or decrement will clearly depend on how large is the curvature of the curve of p , how the energy is distributed and how large p is.

As an example, Figure 2.13 plots the cell probability of detection with different values of Y_b (6.903, 20.72) for single-pulse Rayleigh scatterers when $M = 10$. The figure shows that below 23 db of signal-to-noise ratio the curve is relatively straight when $Y_b = 6.903$; therefore, the probability of detection is not much affected by the energy distribution (see Fig. 2.2c). For $Y_b = 20.72$, Figure 2.13 shows that the curvature of the curve is relatively large in certain ranges of signal-to-noise ratio. The curve changes from concave-up to concave-down at about 24 db. Therefore, the probability of detection is more significantly affected by energy distribution in low probability range and is not much affected by energy distribution nearby 24 db. And when the signal-to-noise ratio is below 24 db, non-uniformly distributed energy increases probability of detection and when the ratio is above 24 db, non-uniformly distributed energy decreases probability of detection (see Fig. 2.2d).

SUMMARY

In realistic radar detection, the cells have different energy. This fact makes modification to the ordinary theory and formula necessary. In this report, we use a realistic model of energy distribution to investigate the probability of detection for various target models.

We have found a common phenomena for every target model: the effect of energy

distribution will become more significant when the threshold, Y_{th} , is increased. However, the effect of energy distribution will also largely depend on the target models. Constant amplitude scatterers are most seriously affected by energy distribution, dominant plus Rayleigh scatterers are the next, and Rayleigh scatterers are least affected by energy distributions. Multi-pulse cases are more seriously affected by energy distribution than single-pulse cases. And fast fluctuating targets are more seriously affected by energy distribution than slow fluctuating targets.

The effect of energy distribution can be interpreted by a plot of so-called "cell probability of detection" vs. signal-to-noise ratio in linear scales. When the curve is concave-up, the non-uniformly distributed energy will increase the probability of detection. When the curve is concave-down, the non-uniformly distributed energy will decrease the probability of detection. The increment and decrement will depend on the curvature of the curve, the energy distribution and the cell probability of detection at the given energy-to-noise ratio. In most cases, non-uniformly distributed energy will increase the probability of detection.

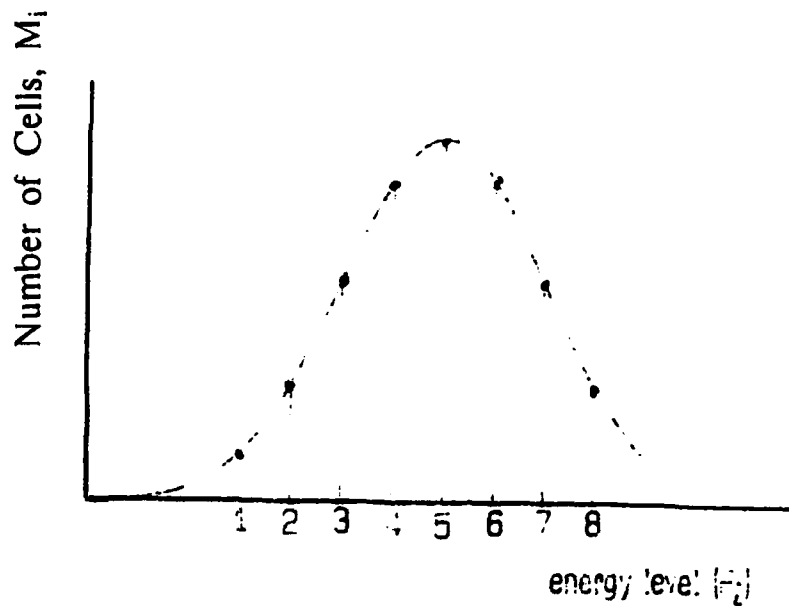


Figure 2.0 An Example of Cell Distribution over Eight Energy Levels

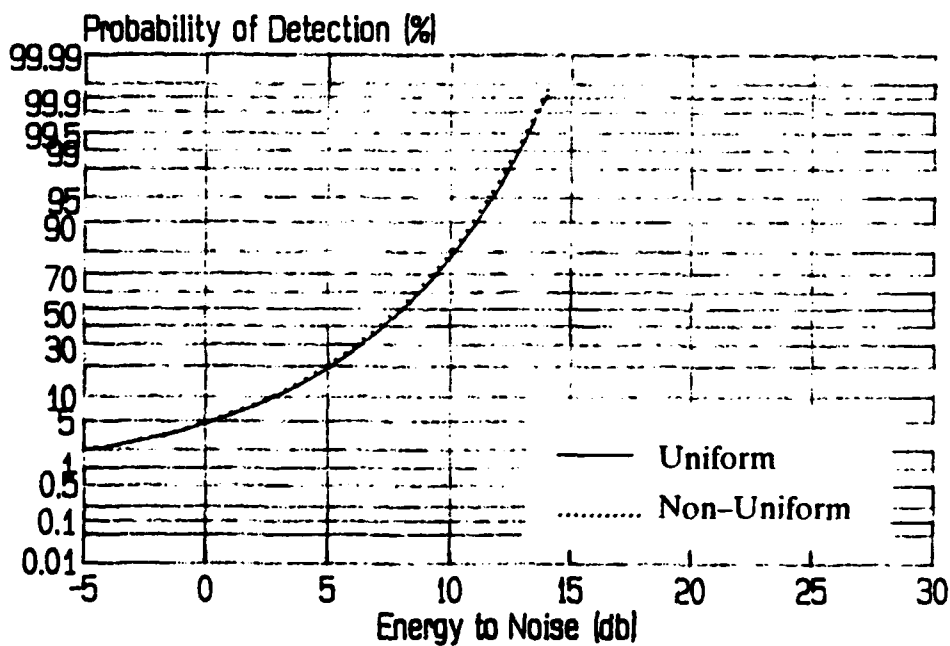


Figure 2.1a Comparison between Uniformly Distributed Energy and Non-Uniformly Distributed Energy for Single-Pulse Constant Amplitude Scatterers when $M = 2$ and $P_{fa} = 1.E-2$

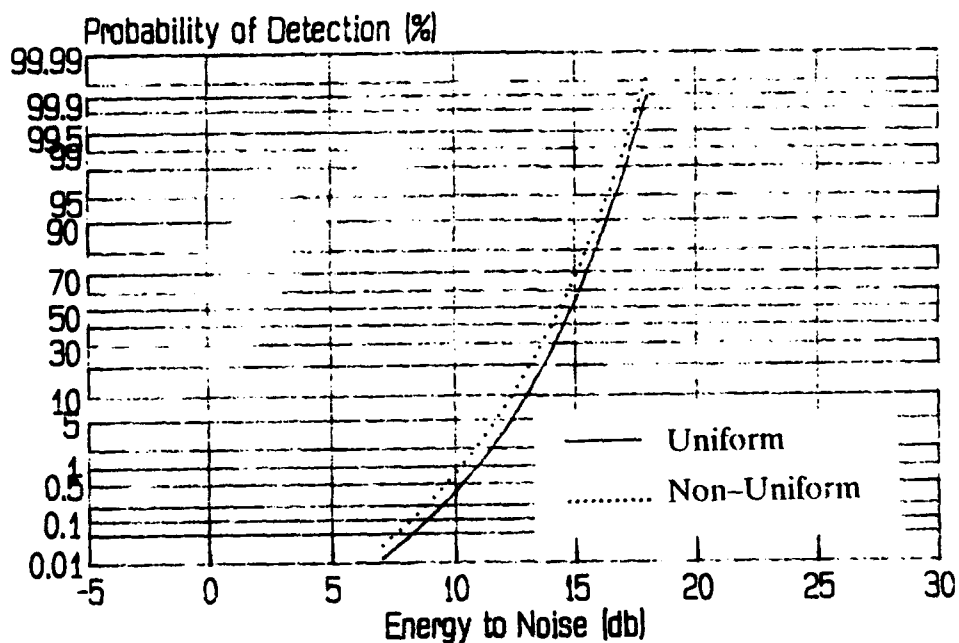


Figure 2.1b Comparison between Uniformly Distributed Energy and Non-Uniformly Distributed Energy for Single-Pulse Constant Amplitude Scatterers when $M = 2$ and $P_{fa} = 1.E-8$

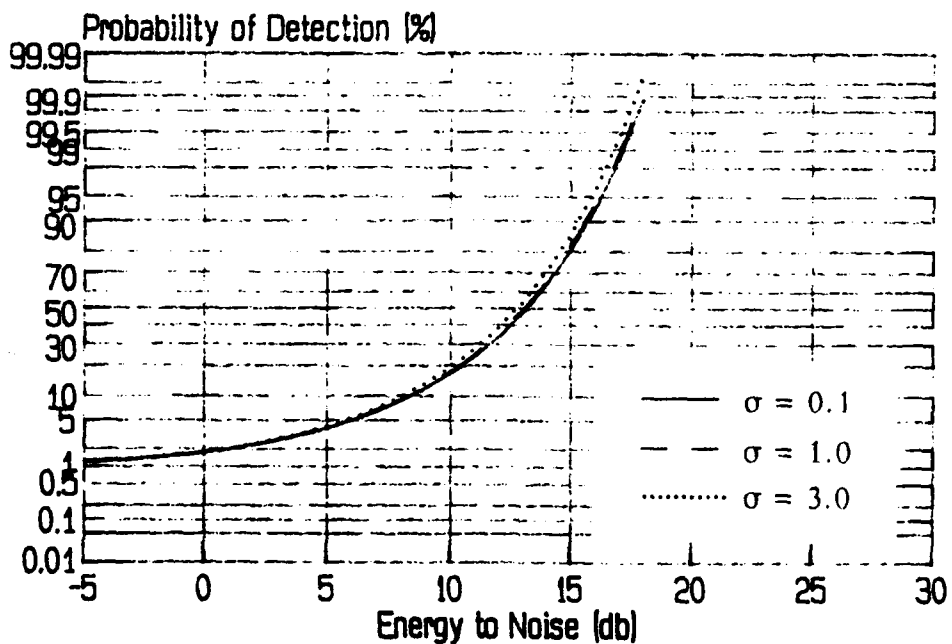


Figure 2.1c Comparison between Different Values of σ for Single-Pulse Constant Amplitude Scatterers when $N_l = 8$, $M = 10$, $\tilde{E} = 5$ and $P_{fa} = 1.E-2$

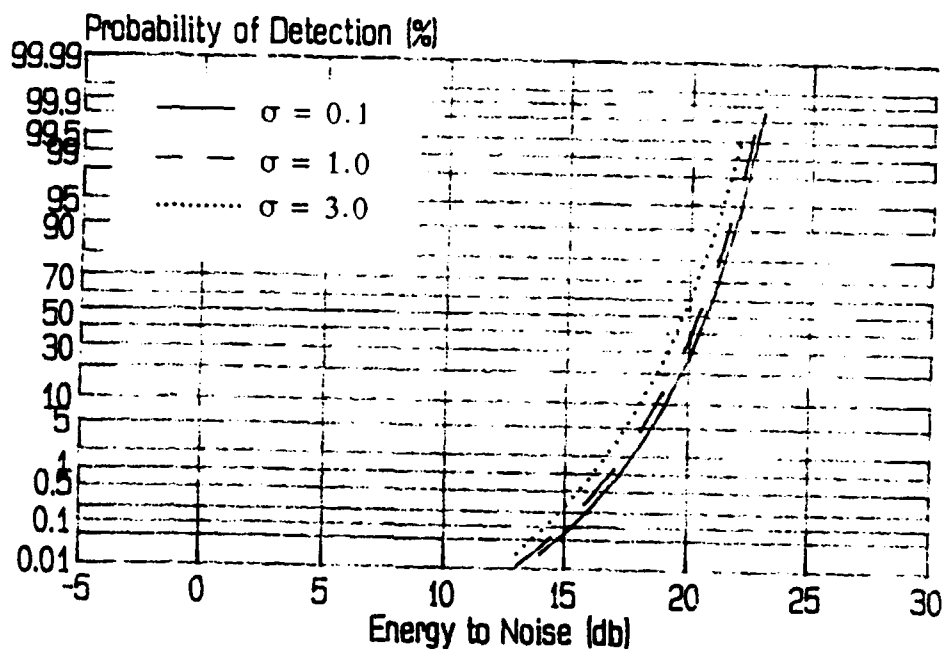


Figure 2.1d Comparison between Different Values of σ for Single-Pulse Constant Amplitude Scatterers when $N_I = 8$, $M = 10$, $\bar{E} = 5$ and $P_{fa} = 1.E-8$

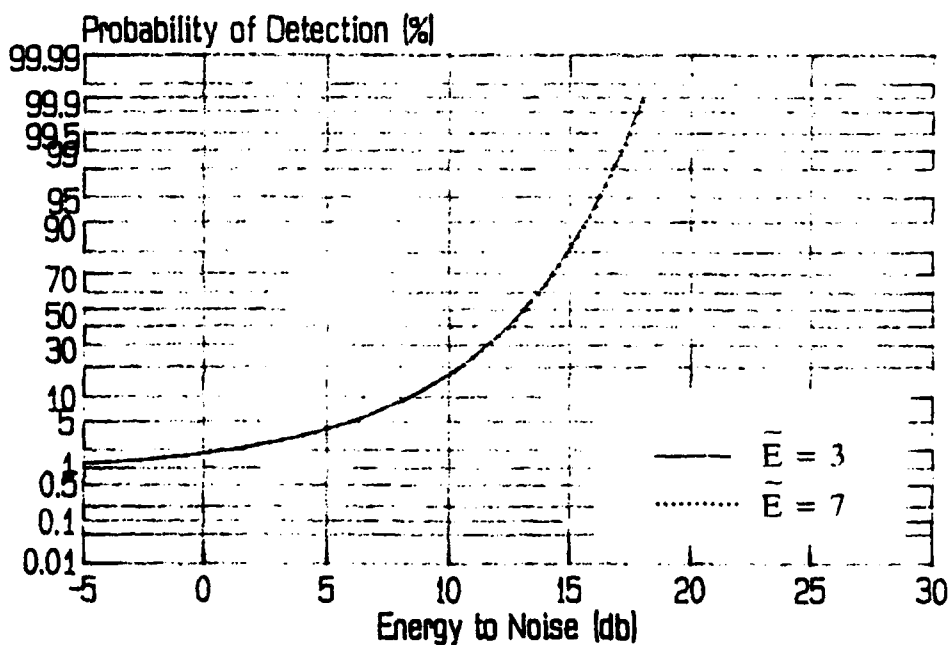


Figure 2.1e Comparison between Different Values of \bar{E} for Single-Pulse Constant Amplitude Scatterers when $N_I = 8$, $M = 10$, $\sigma = 0.5$ and $P_{fa} = 1.E-2$

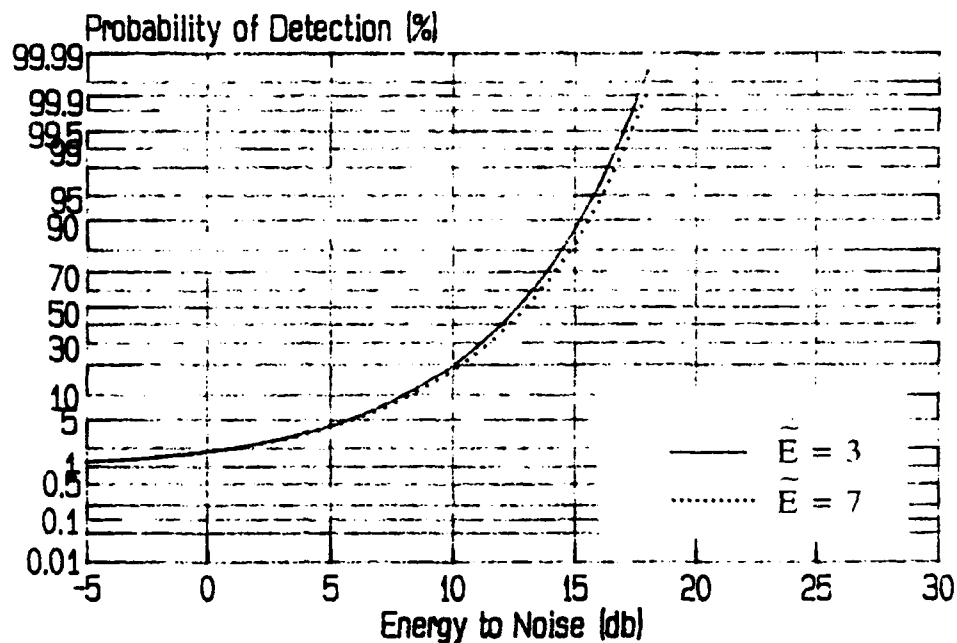


Figure 2.1f Comparison between Different Values of \tilde{E} for Single-Pulse Constant Amplitude Scatterers when $N_I = 8$, $M = 10$, $\sigma = 3.0$ and $P_{fa} = 1.E-2$

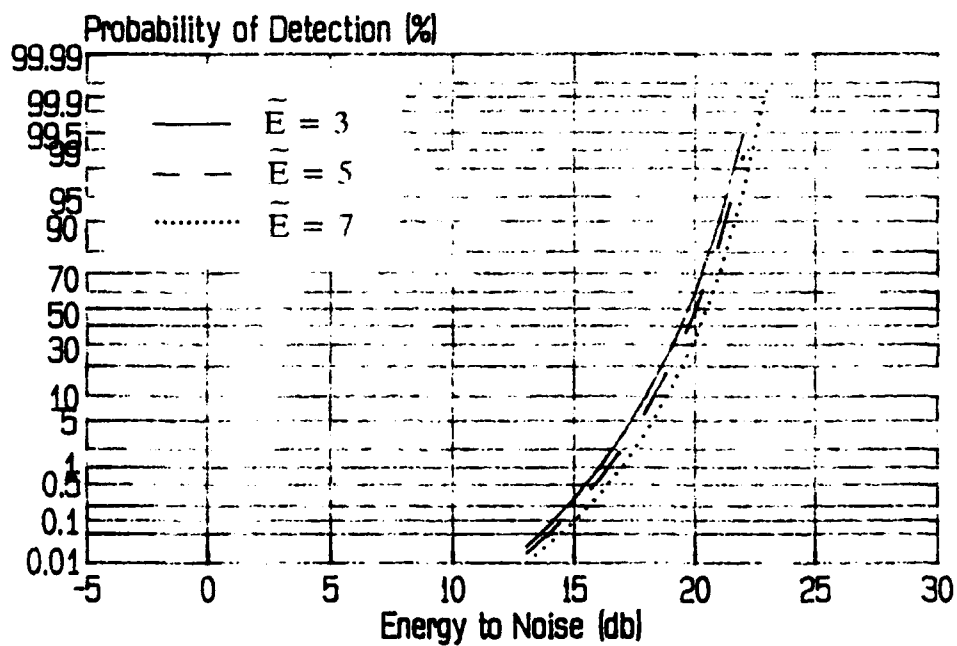


Figure 2.1g Comparison between Different Values of \tilde{E} for Single-Pulse Constant Amplitude Scatterers when $N_I = 8$, $M = 10$, $\sigma = 2.0$ and $P_{fa} = 1.E-8$

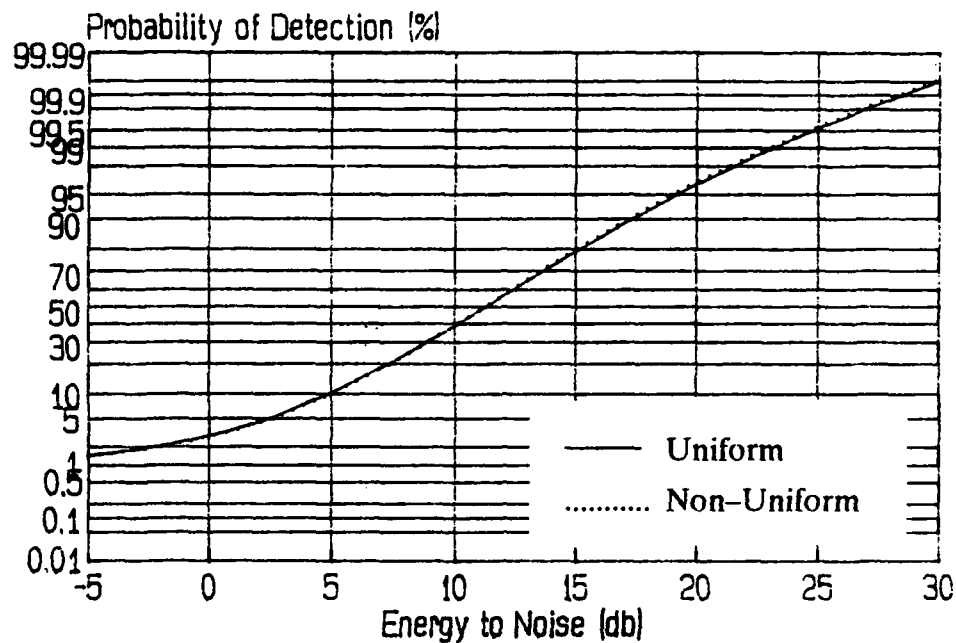


Figure 2.2a Comparison between Uniformly Distributed Energy and Non-Uniformly Distributed Energy for Single-Pulse Rayleigh Scatterers when $M = 2$ and $P_{fa} = 1.E-2$

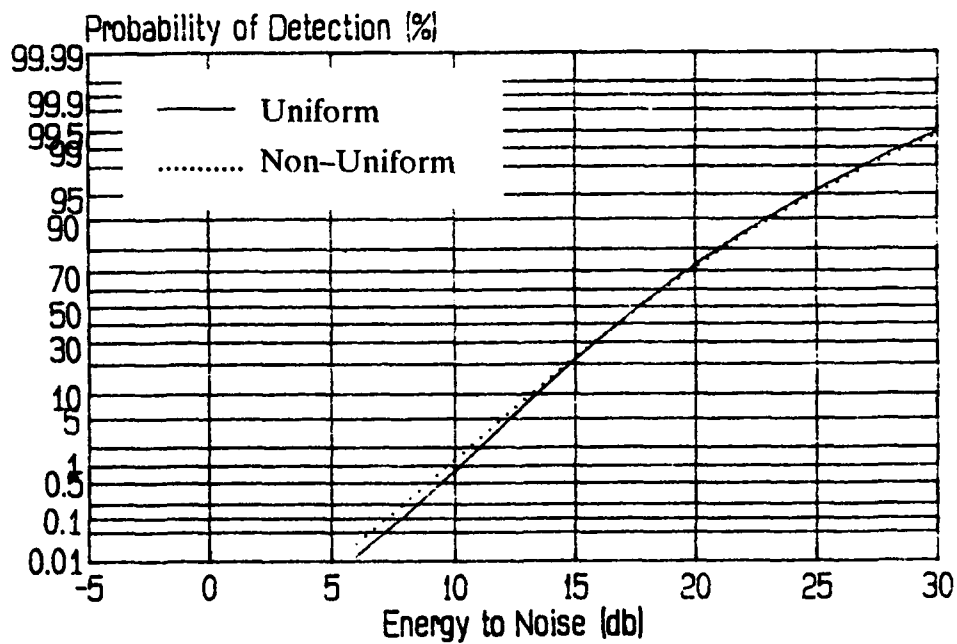


Figure 2.2b Comparison between Uniformly Distributed Energy and Non-Uniformly Distributed Energy for Single-Pulse Rayleigh Scatterers when $M = 2$ and $P_{fa} = 1.E-8$

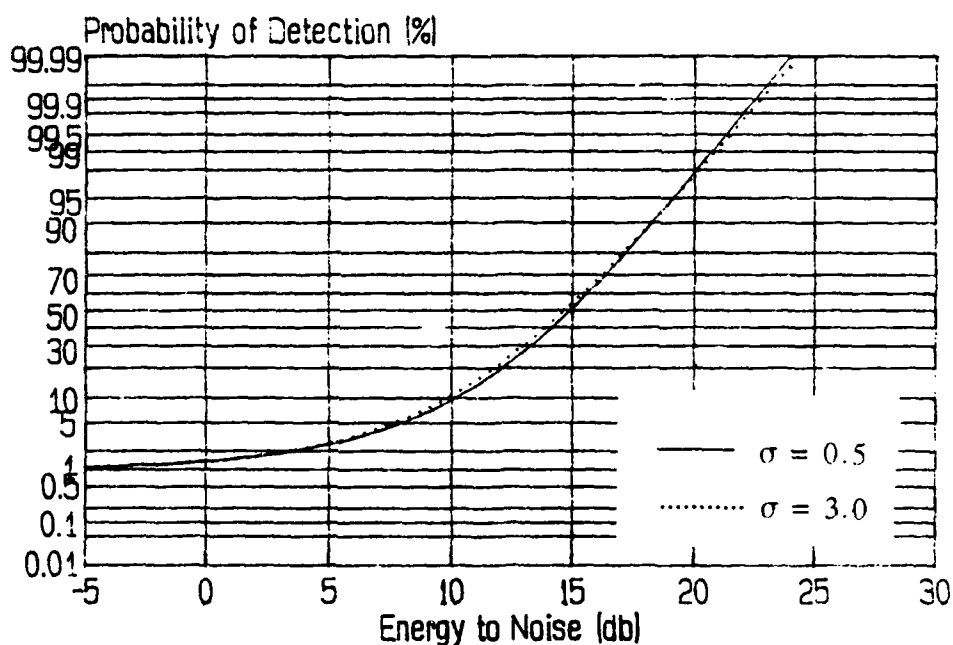


Figure 2.2c Comparison between Different Values of σ for Single-Pulse Rayleigh Scatterers when $N_f = 8$, $M = 10$, $\bar{E} = 5$ and $P_{fa} = 1.E-2$

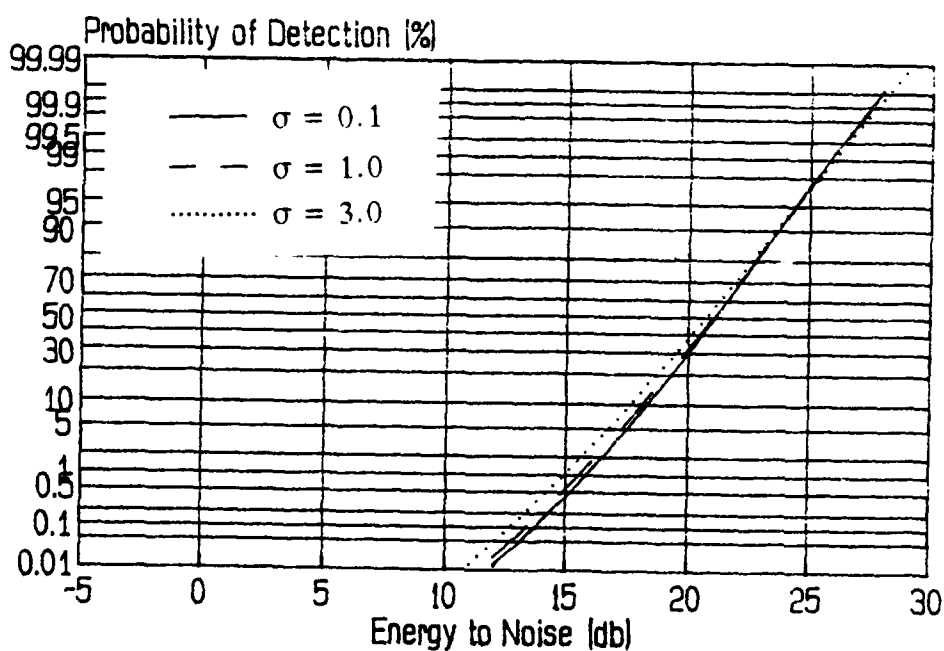


Figure 2.2d Comparison between Different Values of σ for Single-Pulse Rayleigh Scatterers when $N_f = 8$, $M = 10$, $\bar{E} = 5$ and $P_{fa} = 1.E-8$

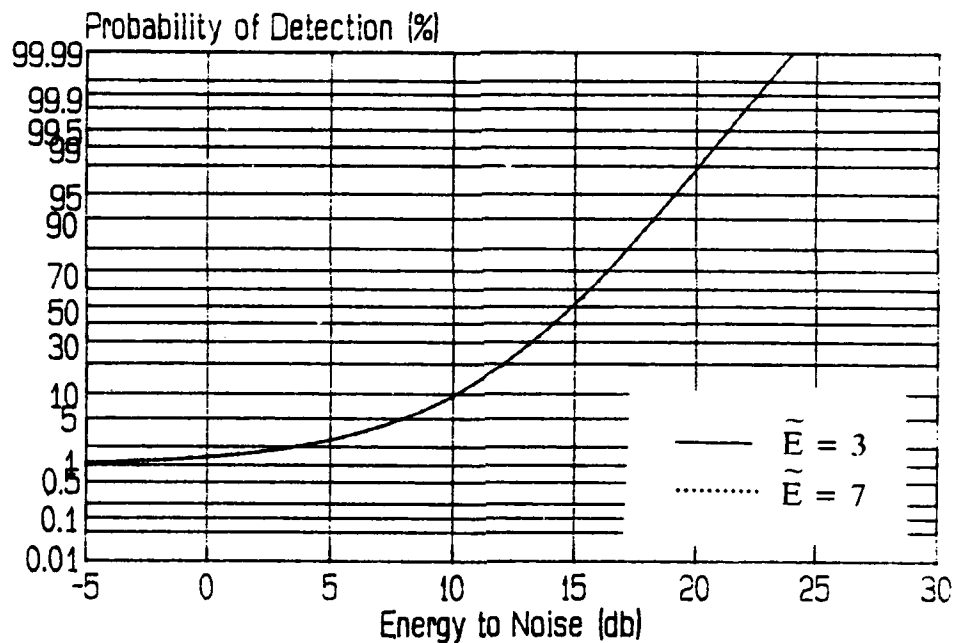


Figure 2.2e Comparison between Different Values of \tilde{E} for Single-Pulse Rayleigh Scatterers when $N_I = 8$, $M = 10$, $\sigma = 0.5$ and $P_{fa} = 1.E-2$

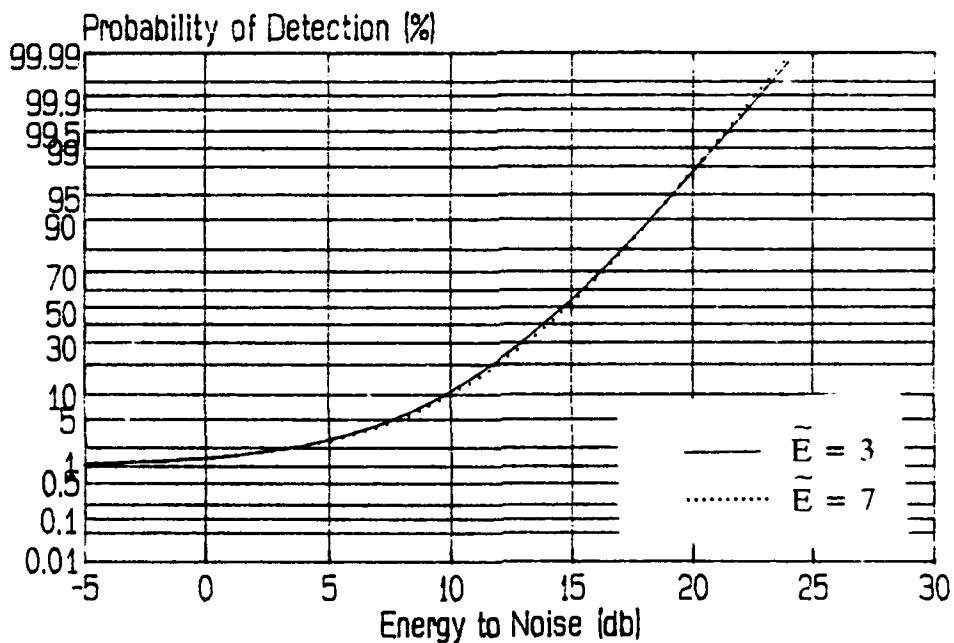


Figure 2.2f Comparison between Different Values of \tilde{E} for Single-Pulse Rayleigh Scatterers when $N_I = 8$, $M = 10$, $\sigma = 3.0$ and $P_{fa} = 1.E-2$

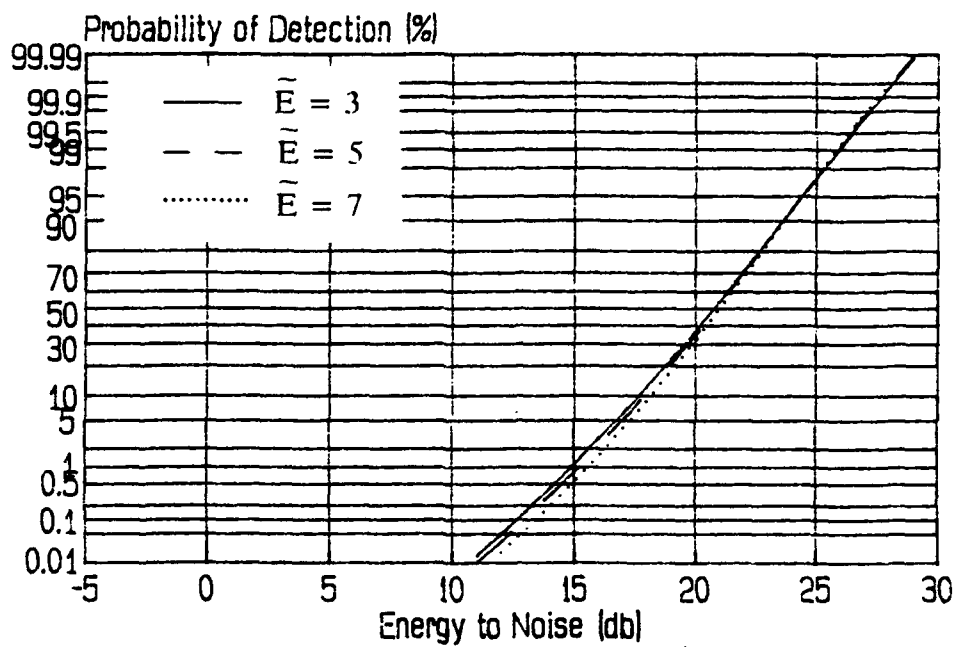


Figure 2.2g Comparison between Different Values of \tilde{E} for Single-Pulse Rayleigh Scatterers when $N_f = 8$, $M = 10$, $\sigma = 2.0$ and $P_{fa} = 1.E-8$

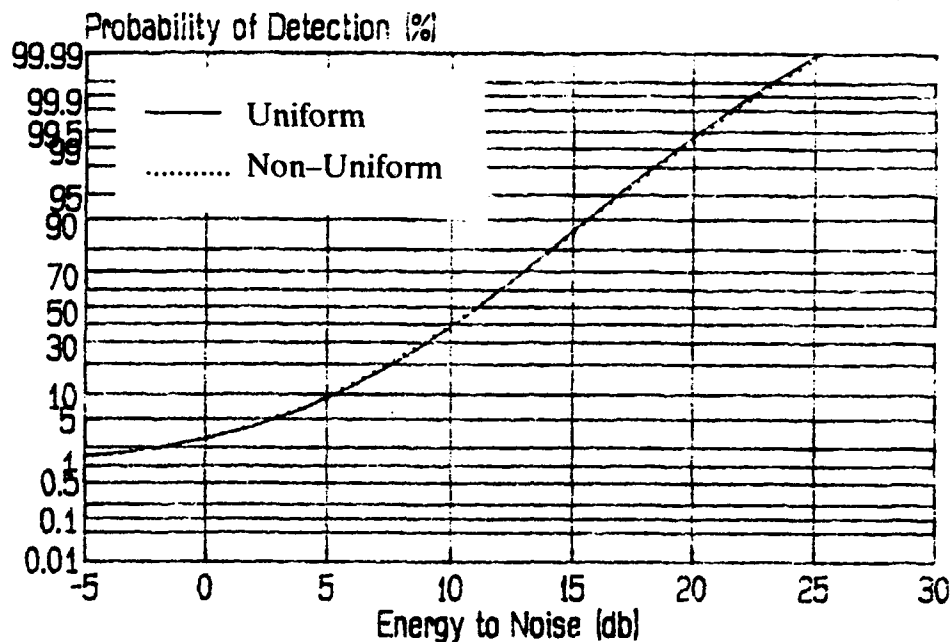


Figure 2.3a Comparison between Uniformly Distributed Energy and Non-Uniformly Distributed Energy for Single-Pulse Dominant plus Rayleigh Scatterers when $M = 2$ and $P_{fa} = 1.E-2$

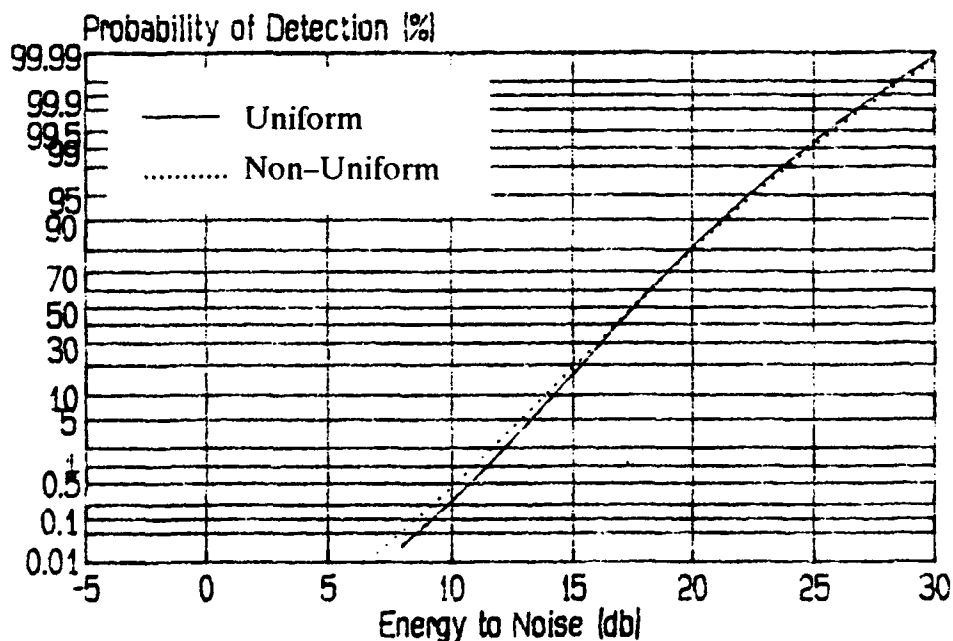


Figure 2.3b Comparison between Uniformly Distributed Energy and Non-Uniformly Distributed Energy for Single-Pulse Dominant plus Rayleigh Scatterers when $M = 2$ and $P_{fa} = 1.E-8$

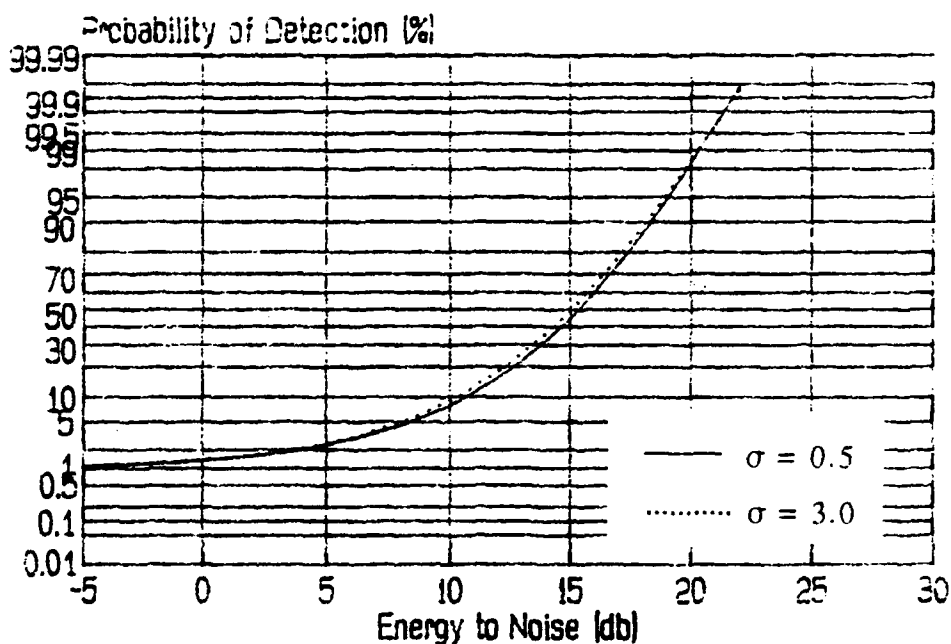


Figure 2.3c Comparison between Different Values of σ for Single-Pulse Dominant plus Rayleigh Scatterers when $N_f = 8$, $M = 10$, $\tilde{E} = 5$ and $P_{fa} = 1.E-2$

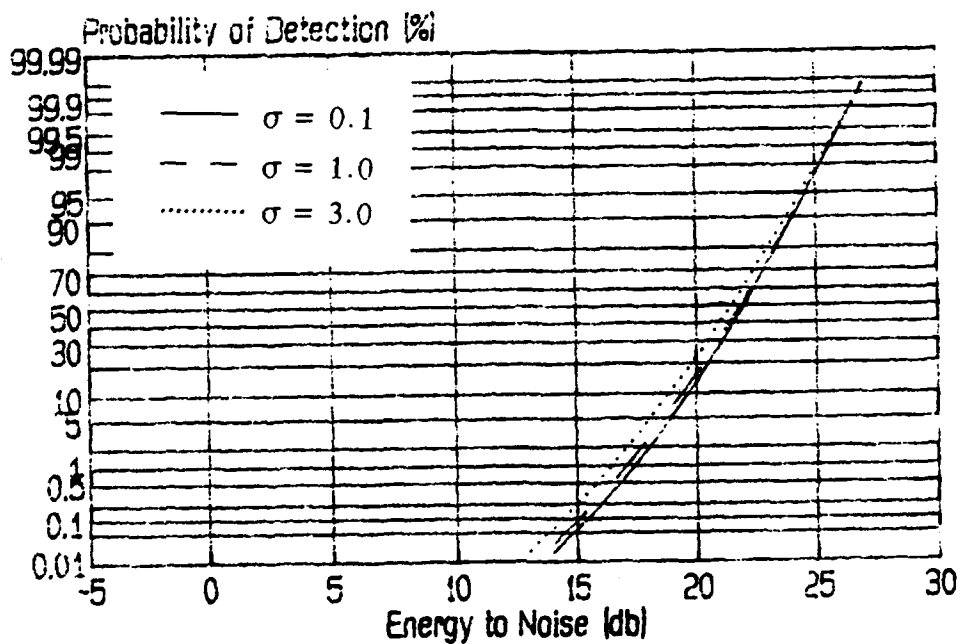


Figure 2.3d Comparison between Different Values of σ for Single-Pulse Dominant plus Rayleigh Scatterers when $N_f = 8$, $M = 10$, $\tilde{E} = 5$ and $P_{fa} = 1.E-8$

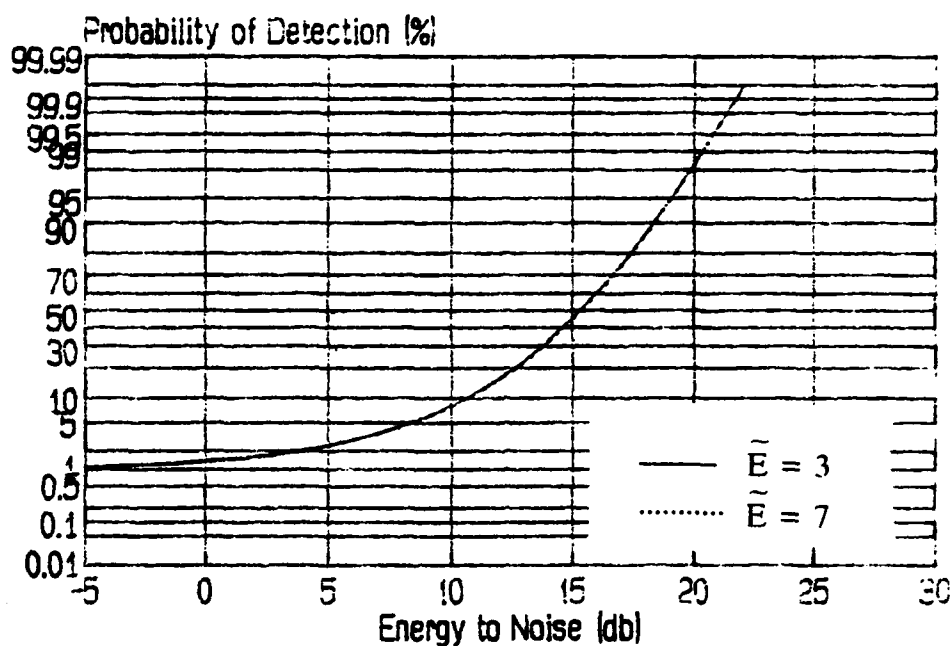


Figure 2.3e Comparison between Different Values of \tilde{E} for Single-Pulse Dominant plus Rayleigh Scatterers when $N_I = 8$, $M = 10$, $\sigma = 0.5$ and $P_{fa} = 1.E-2$

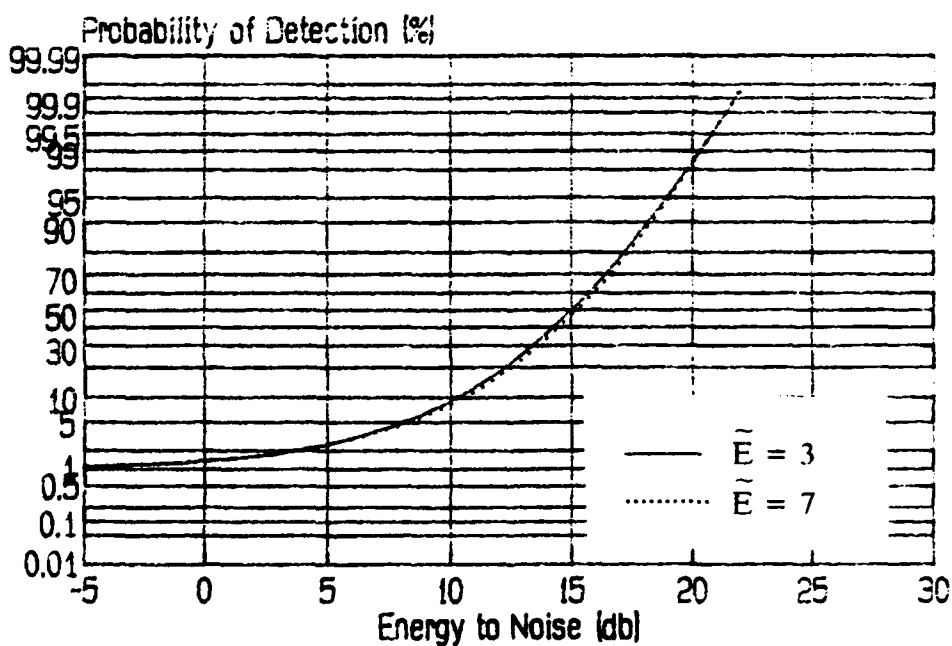


Figure 2.3f Comparison between Different Values of \tilde{E} for Single-Pulse Dominant plus Rayleigh Scatterers when $N_I = 8$, $M = 10$, $\sigma = 3.0$ and $P_{fa} = 1.E-2$

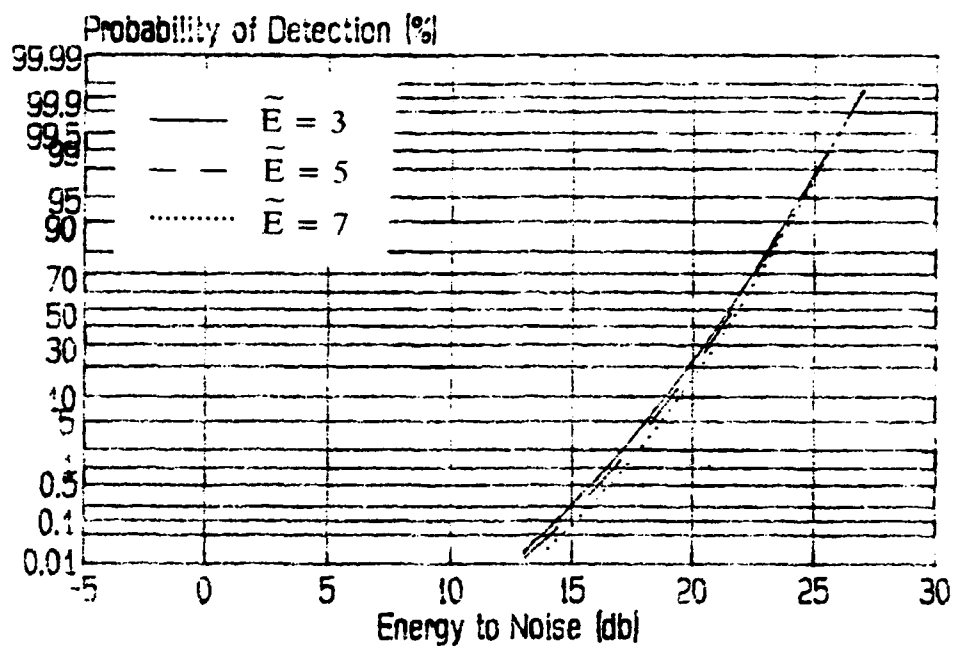


Figure 2.3g Comparison between Different Values of \tilde{E} for Single-Pulse Dominant plus Rayleigh Scatterers when $N_f = 8$, $M = 10$, $\sigma = 2.0$ and $P_{fa} = 1.E-8$

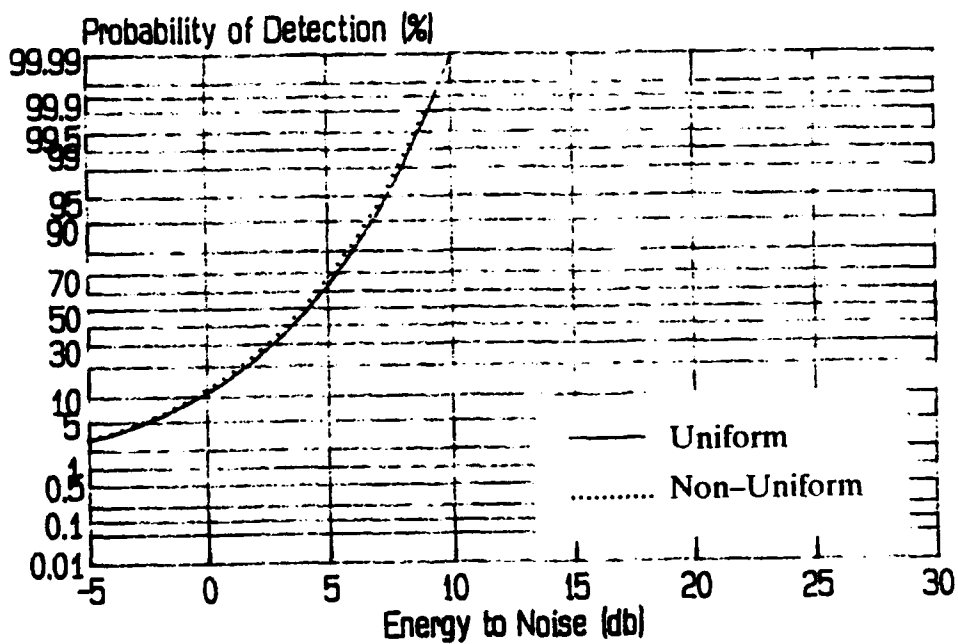


Figure 2.4a Comparison between Uniformly Distributed Energy and Non-Uniformly Distributed Energy for 4-Pulse Constant Amplitude Scatterers when $M = 2$ and $P_{fa} = 1.E-2$

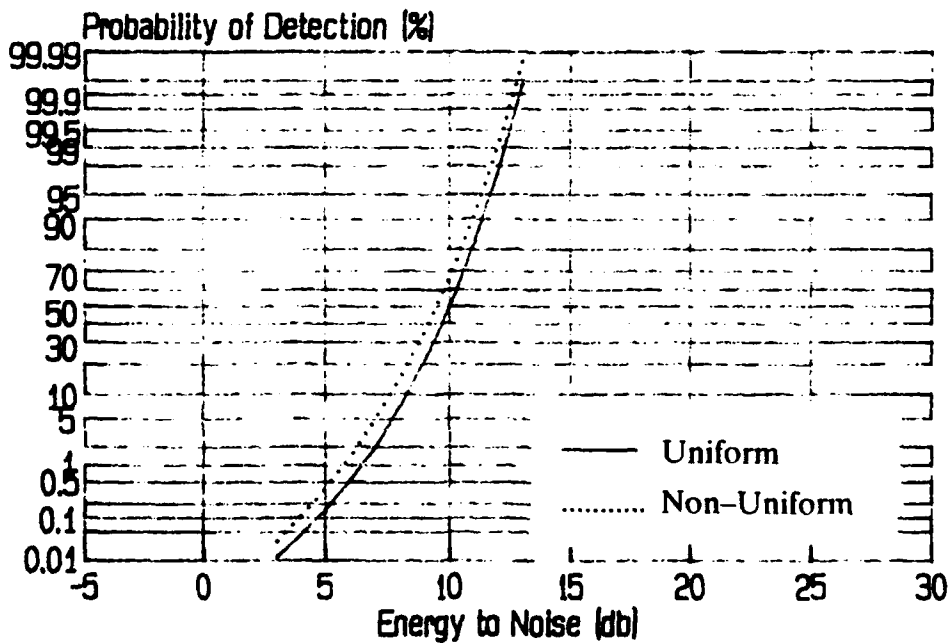


Figure 2.4b Comparison between Uniformly Distributed Energy and Non-Uniformly Distributed Energy for 4-Pulse Constant Amplitude Scatterers when $M = 2$ and $P_{fa} = 1.E-8$

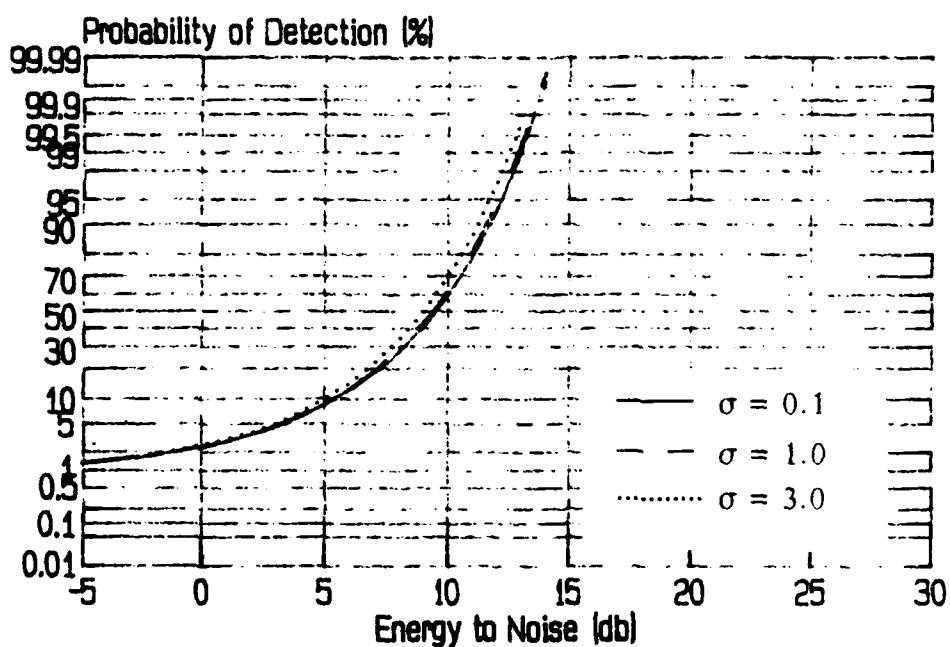


Figure 2.4c Comparison between Different Values of σ for 4-Pulse Constant Amplitude Scatterers when $N_f = 8$, $M = 10$, $\bar{E} = 5$ and $P_{fa} = 1.E-2$

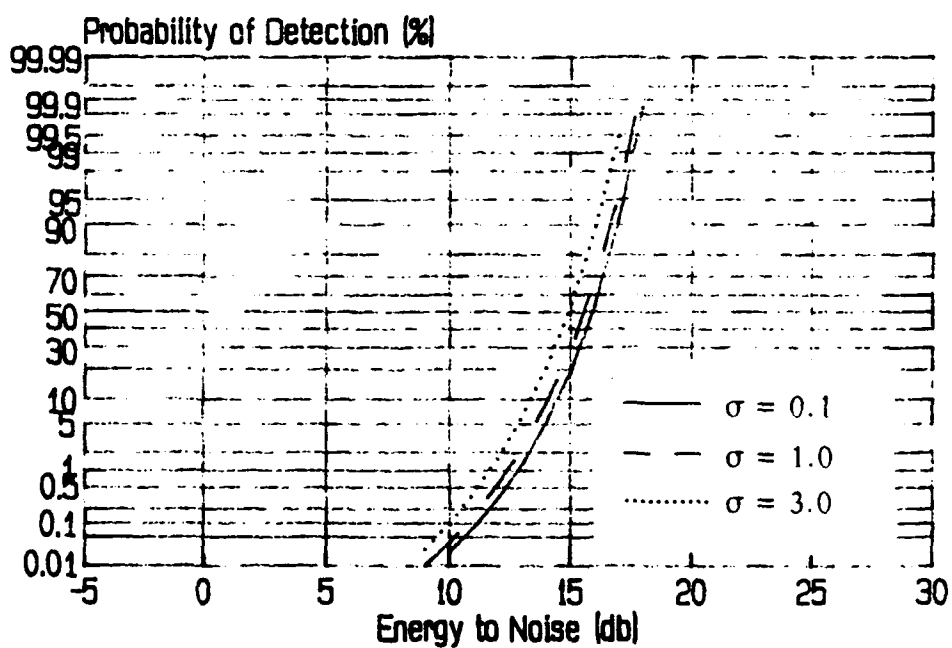


Figure 2.4d Comparison between Different Values of σ for 4-Pulse Constant Amplitude Scatterers when $N_f = 8$, $M = 10$, $\bar{E} = 5$ and $P_{fa} = 1.E-8$

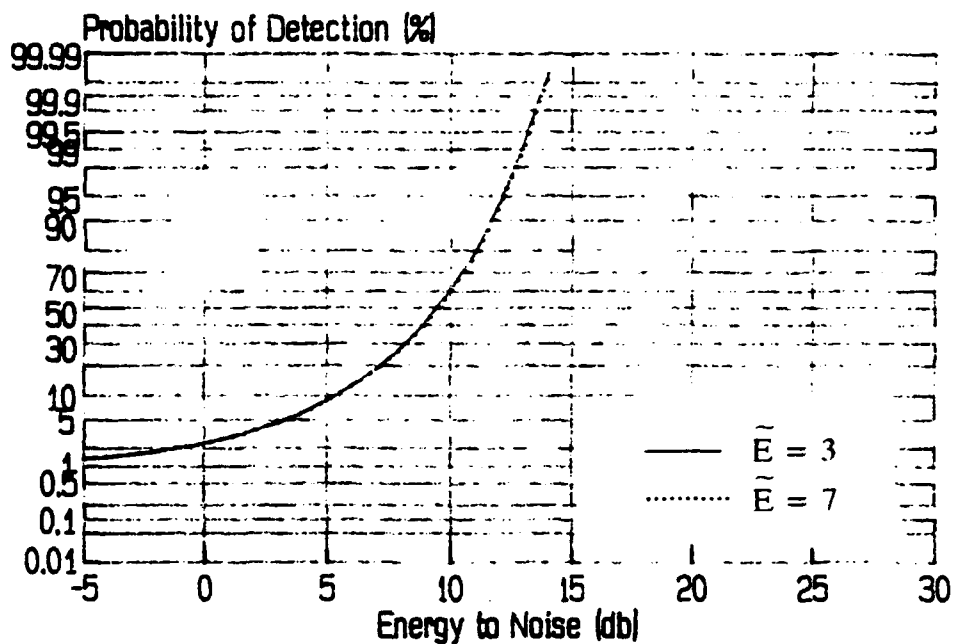


Figure 2.4e Comparison between Different Values of \tilde{E} for 4-Pulse Constant Amplitude Scatterers when $N_I = 8$, $M = 10$, $\sigma = 0.5$ and $P_{fa} = 1.E-2$

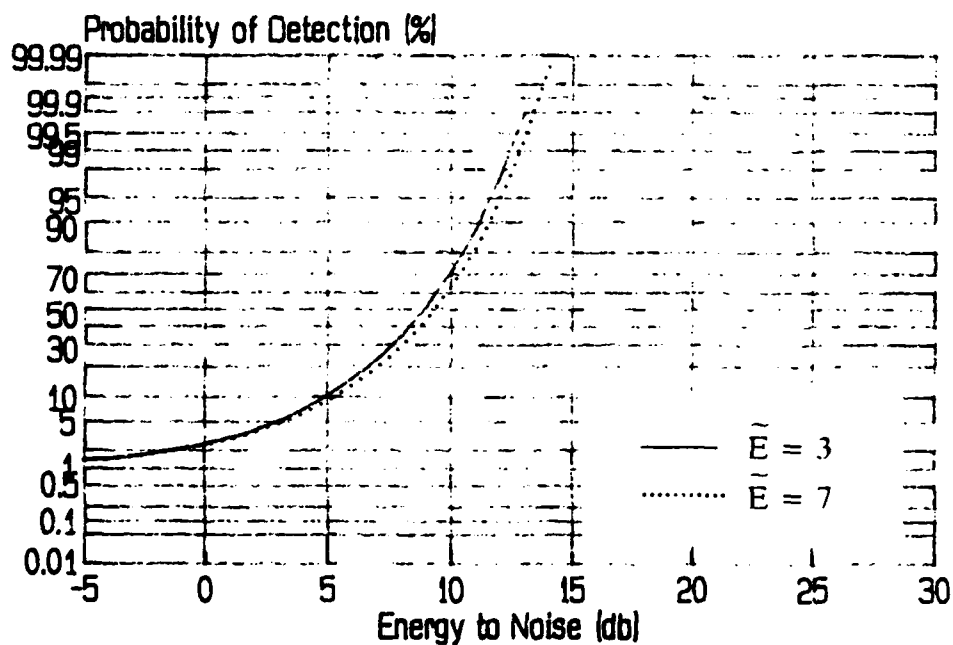


Figure 2.4f Comparison between Different Values of \tilde{E} for 4-Pulse Constant Amplitude Scatterers when $N_I = 8$, $M = 10$, $\sigma = 3.0$ and $P_{fa} = 1.E-2$

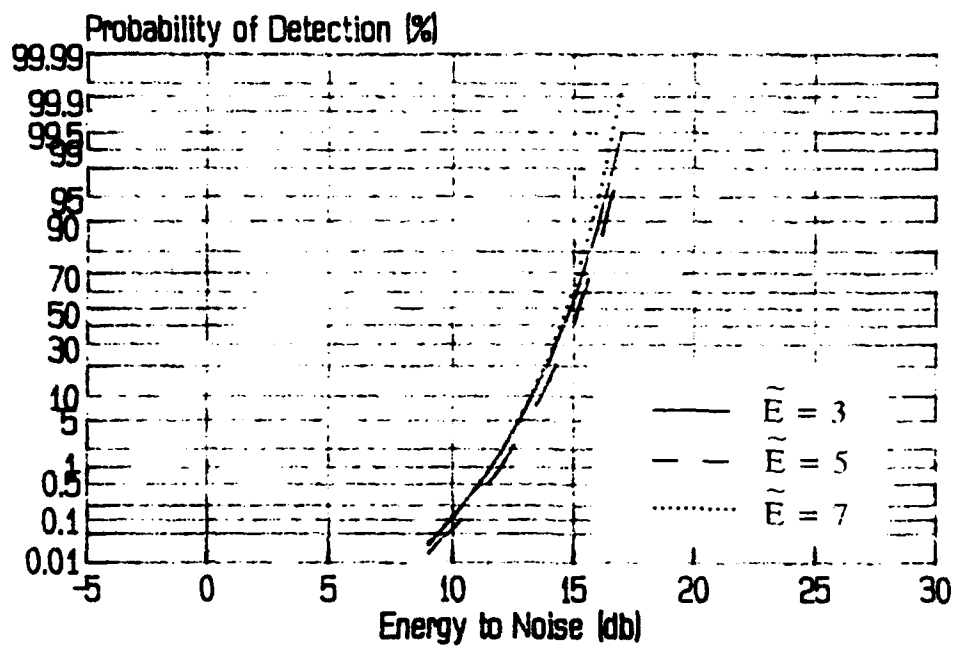


Figure 2.4g Comparison between Different Values of \tilde{E} for 4-Pulse Constant Amplitude Scatterers when $N_f = 8$, $M = 10$, $\sigma = 2.0$ and $P_{fa} = 1.E-8$

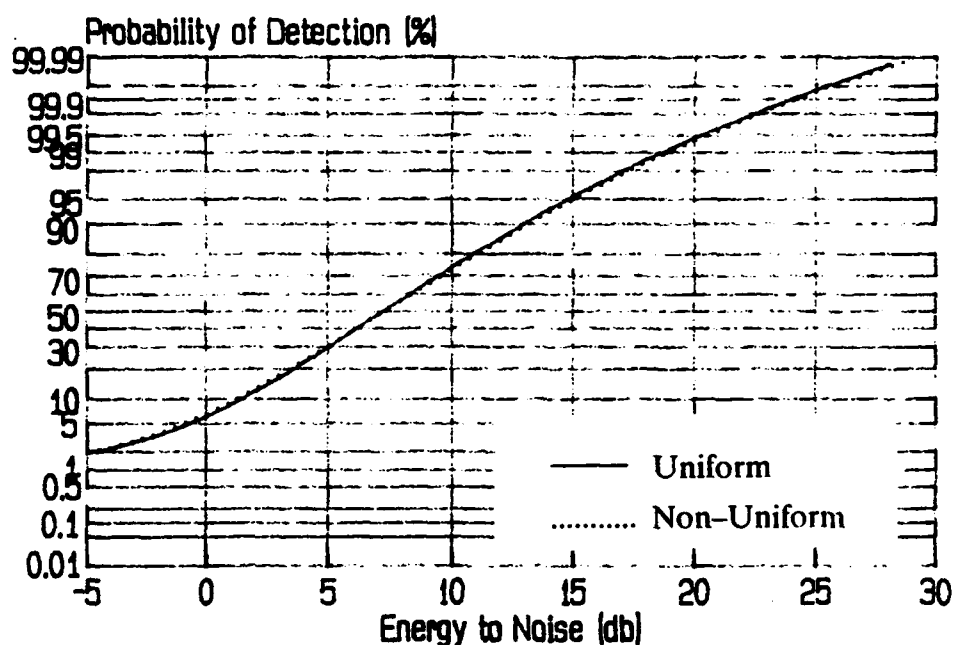


Figure 2.5a Comparison between Uniformly Distributed Energy and Non-Uniformly Distributed Energy for 4-Pulse Slow-Fluctuating Rayleigh Scatterers when $M = 2$ and $P_{fa} = 1.E-2$

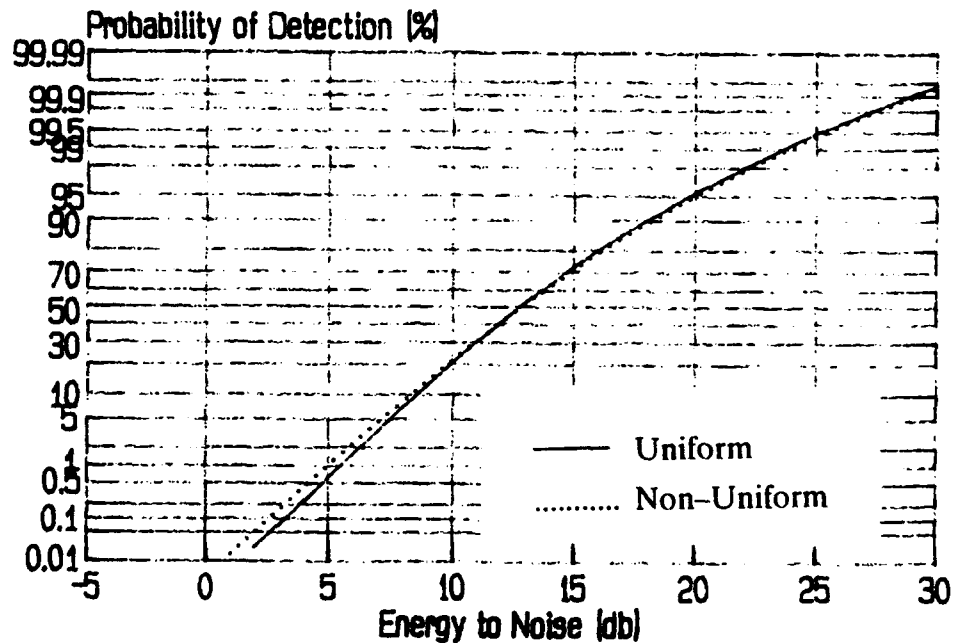


Figure 2.5b Comparison between Uniformly Distributed Energy and Non-Uniformly Distributed Energy for 4-Pulse Slow-Fluctuating Rayleigh Scatterers when $M = 2$ and $P_{fa} = 1.E-8$

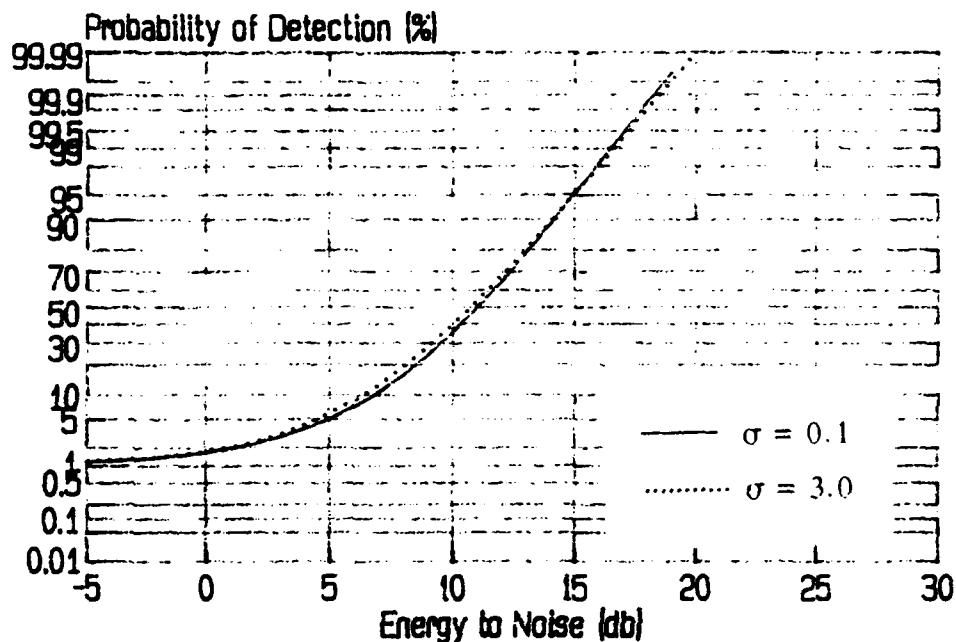


Figure 2.5c Comparison between Different Values of σ for 4-Pulse Slow-Fluctuating Rayleigh Scatterers when $N_I = 8$, $M = 10$, $\tilde{E} = 5$ and $P_{fa} = 1.E-2$

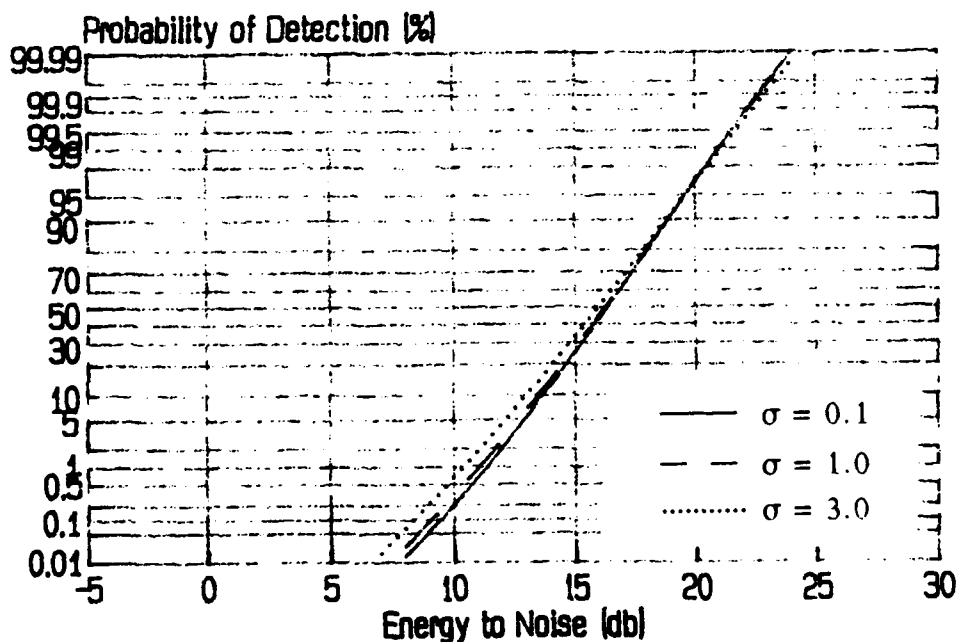


Figure 2.5d Comparison between Different Values of σ for 4-Pulse Slow-Fluctuating Rayleigh Scatterers when $N_I = 8$, $M = 10$, $\tilde{E} = 5$ and $P_{fa} = 1.E-8$

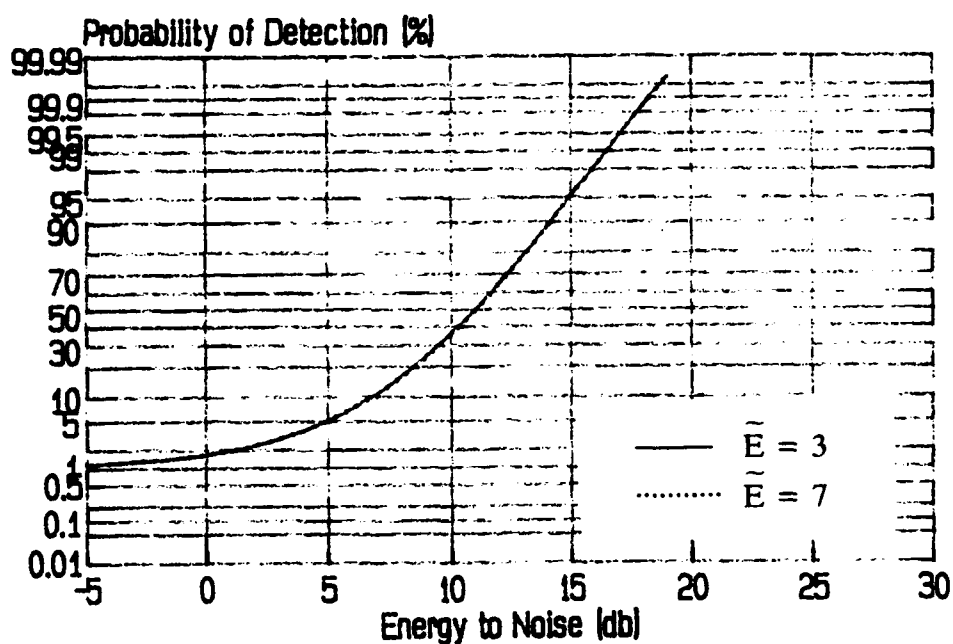


Figure 2.5e Comparison between Different Values of \tilde{E} for 4-Pulse Slow-Fluctuating Rayleigh Scatterers when $N_I = 8$, $M = 10$, $\sigma = 0.5$ and $P_{fa} = 1.E-2$

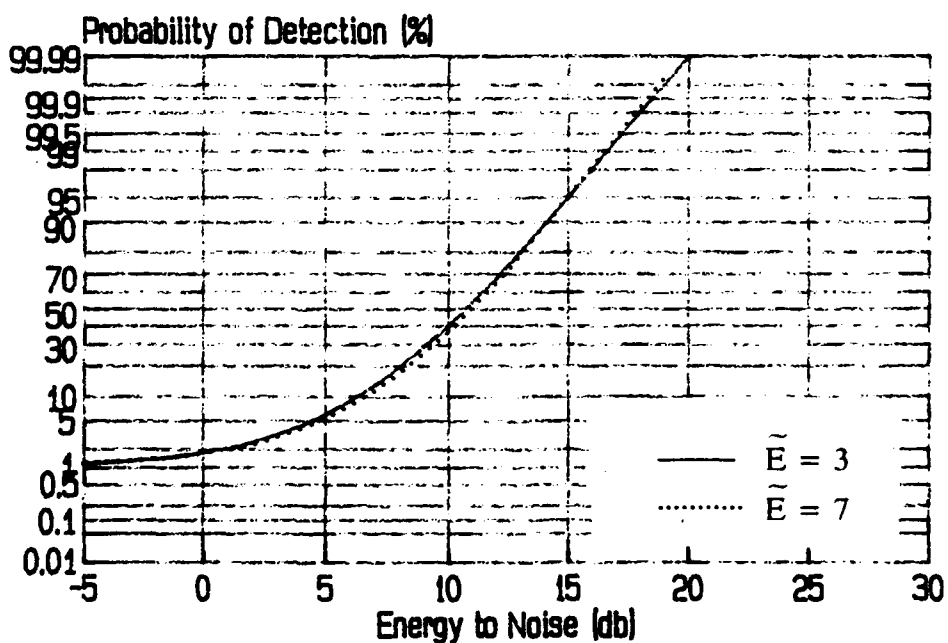


Figure 2.5f Comparison between Different Values of \tilde{E} for 4-Pulse Slow-Fluctuating Rayleigh Scatterers when $N_I = 8$, $M = 10$, $\sigma = 3.0$ and $P_{fa} = 1.E-2$

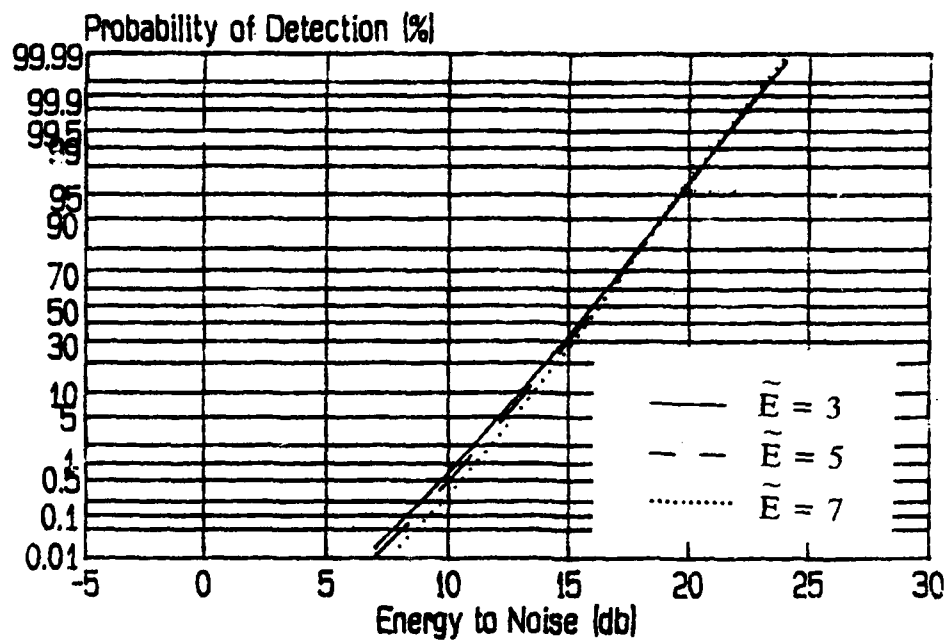


Figure 2.5g Comparison between Different Values of \tilde{E} for 4-Pulse Slow-Fluctuating Rayleigh Scatterers when $N_I = 8$, $M = 10$, $\sigma = 2.0$ and $P_{fa} = 1.E-8$

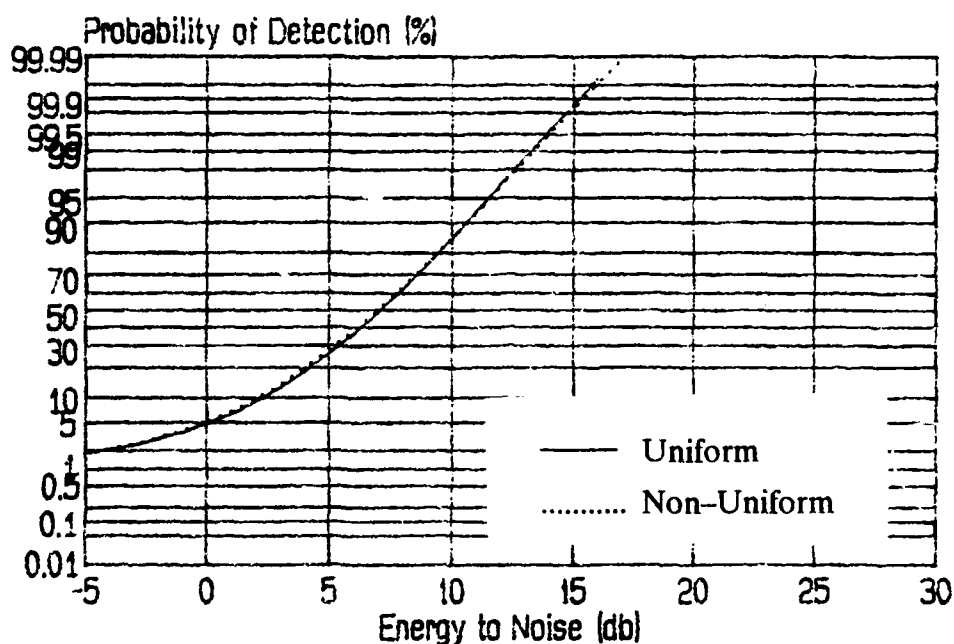


Figure 2.6a Comparison between Uniformly Distributed Energy and Non-Uniformly Distributed Energy for 4-Pulse Fast-Fluctuating Rayleigh Scatterers when $M = 2$ and $P_{fa} = 1.E-2$

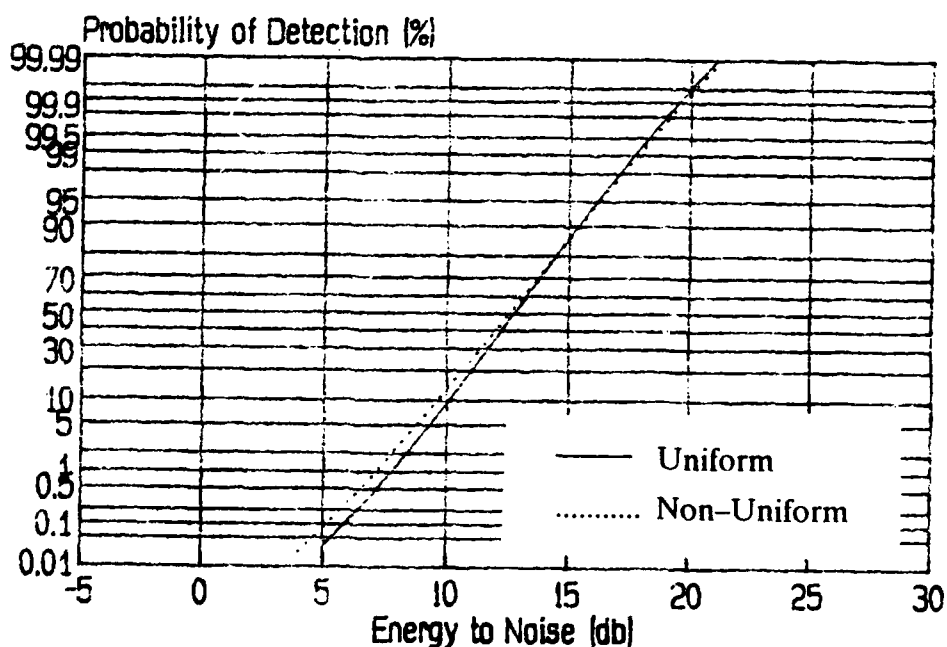


Figure 2.6b Comparison between Uniformly Distributed Energy and Non-Uniformly Distributed Energy for 4-Pulse Fast-Fluctuating Rayleigh Scatterers when $M = 2$ and $P_{fa} = 1.E-8$

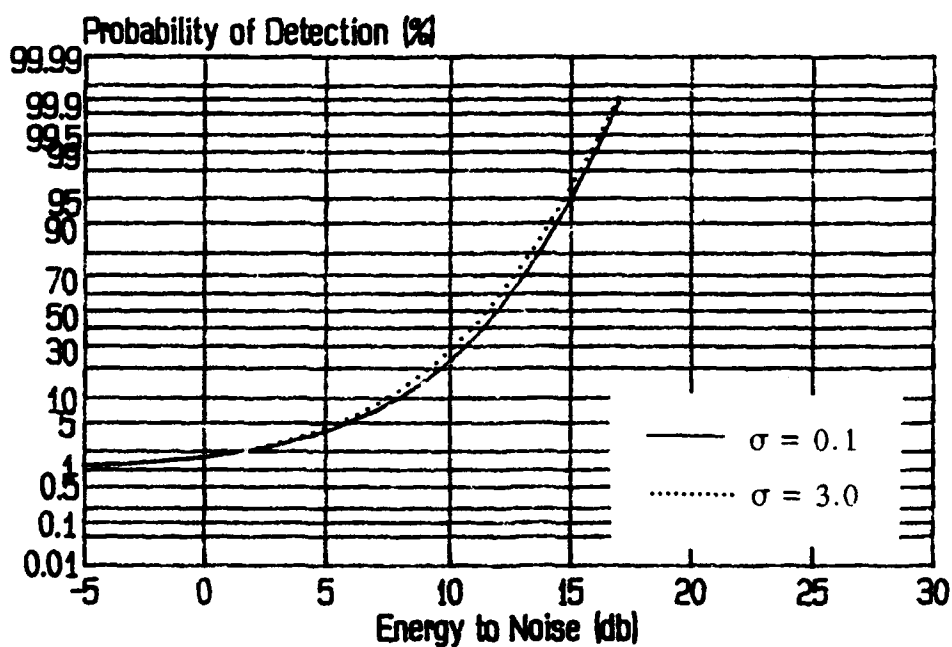


Figure 2.6c Comparison between Different Values of σ for 4-Pulse Fast-Fluctuating Rayleigh Scatterers when $N_f = 8$, $M = 10$, $\bar{E} = 5$ and $P_{fa} = 1.E-2$

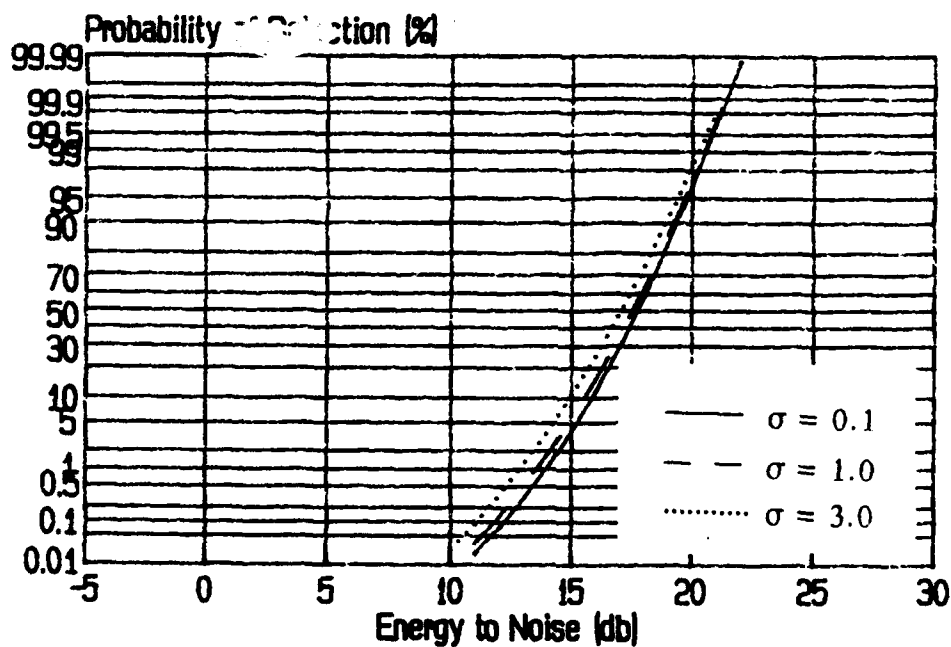


Figure 2.6d Comparison between Different Values of σ for 4-Pulse Fast-Fluctuating Rayleigh Scatterers when $N_f = 8$, $M = 10$, $\bar{E} = 5$ and $P_{fa} = 1.E-8$

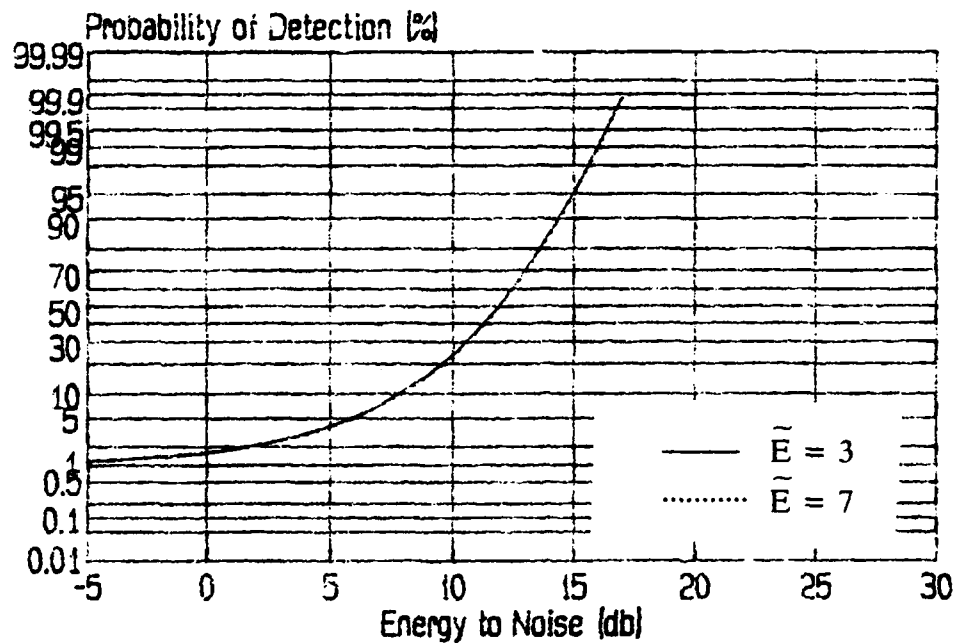


Figure 2.6e Comparison between Different Values of \tilde{E} for 4-Pulse Fast-Fluctuating Rayleigh Scatterers when $N_l = 8$, $M = 10$, $\sigma = 0.5$ and $P_{fa} = 1.E-2$

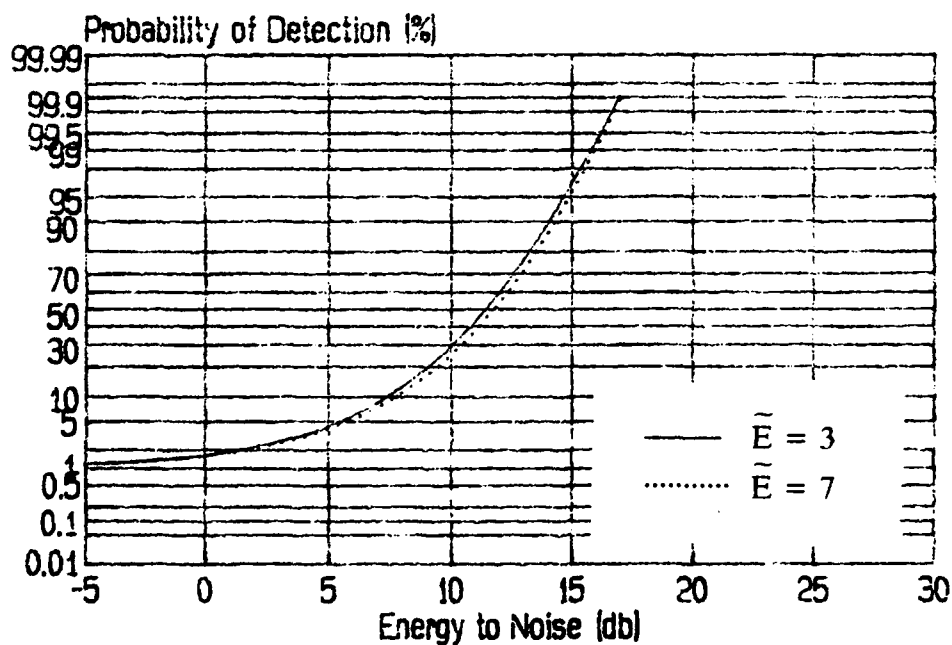


Figure 2.6f Comparison between Different Values of \tilde{E} for 4-Pulse Fast-Fluctuating Rayleigh Scatterers when $N_l = 8$, $M = 10$, $\sigma = 3.0$ and $P_{fa} = 1.E-2$

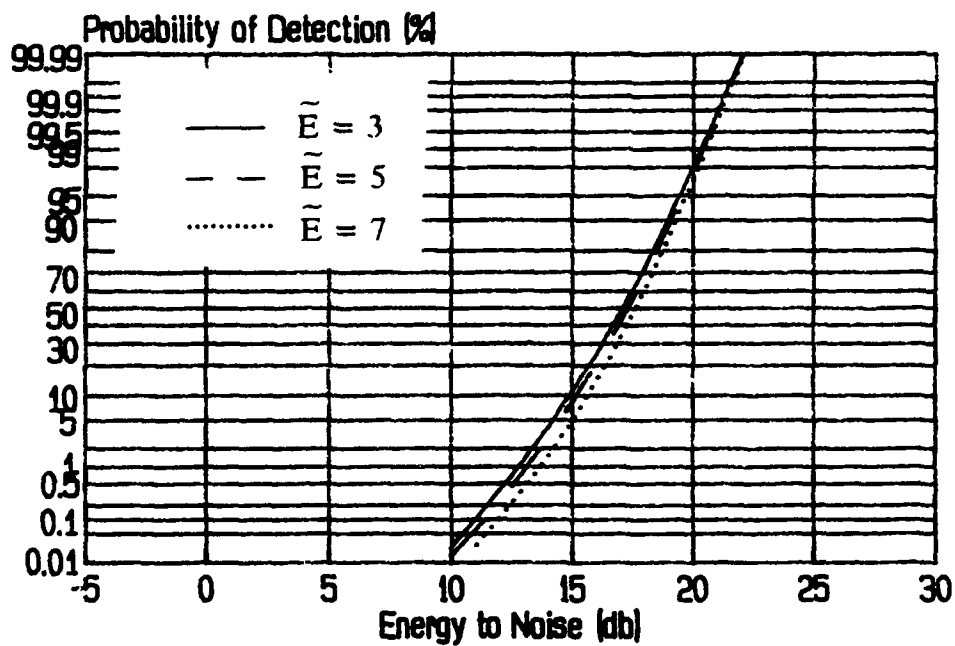


Figure 2.6g Comparison between Different Values of \tilde{E} for 4-Pulse Fast-Fluctuating Rayleigh Scatterers when $N_l = 8$, $M = 10$, $\sigma = 2.0$ and $P_{fa} = 1.E-8$

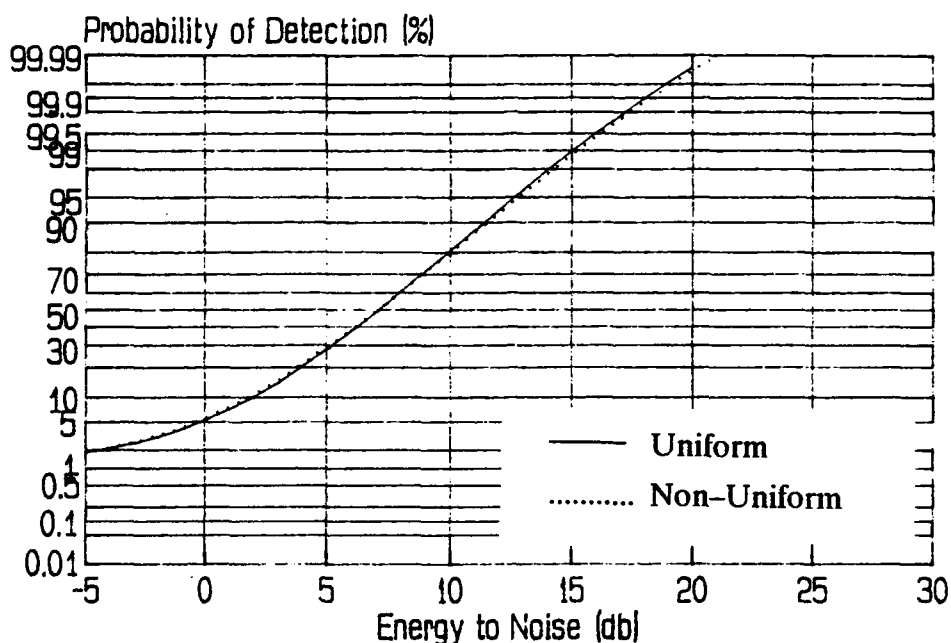


Figure 2.7a Comparison between Uniformly Distributed Energy and Non-Uniformly Distributed Energy for 4-Pulse Slow-Fluctuating Dominant plus Rayleigh Scatterers when $M = 2$ and $P_{fa} = 1.E-2$

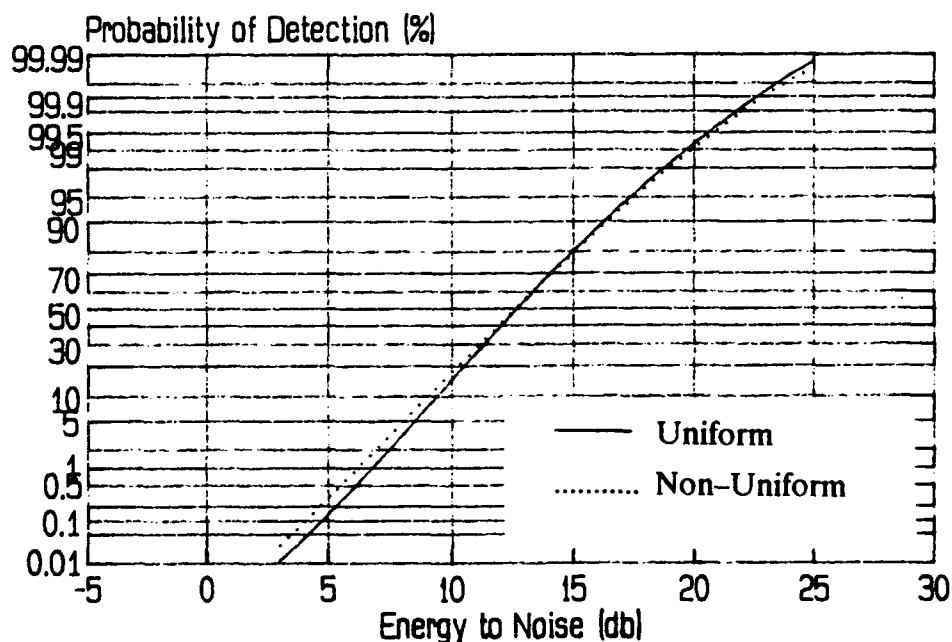


Figure 2.7b Comparison between Uniformly Distributed Energy and Non-Uniformly Distributed Energy for 4-Pulse Slow-Fluctuating Dominant plus Rayleigh Scatterers when $M = 2$ and $P_{fa} = 1.E-8$

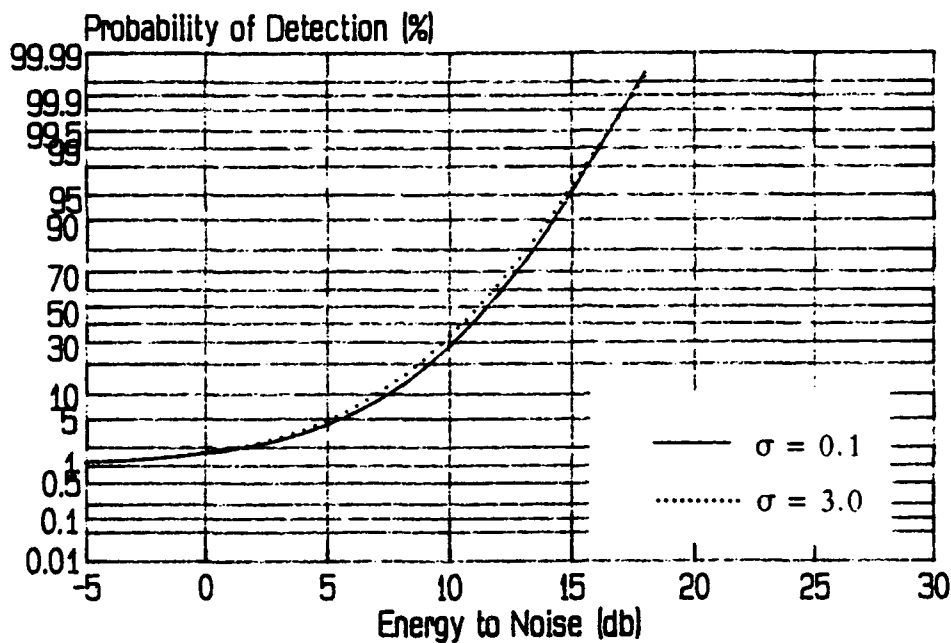


Figure 2.7c Comparison between Different Values of σ for 4-Pulse Slow-Fluctuating Dominant plus Rayleigh Scatterers when $N_I = 8$, $M = 10$, $\tilde{E} = 5$ and $P_{fa} = 1.E-2$

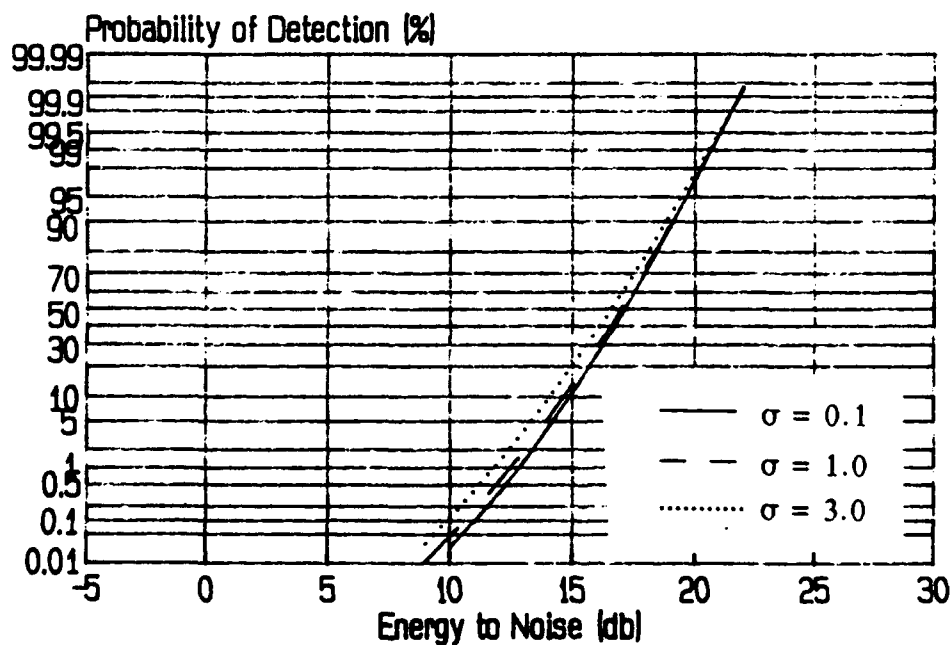


Figure 2.7d Comparison between Different Values of σ for 4-Pulse Slow-Fluctuating Dominant plus Rayleigh Scatterers when $N_I = 8$, $M = 10$, $\tilde{E} = 5$ and $P_{fa} = 1.E-8$

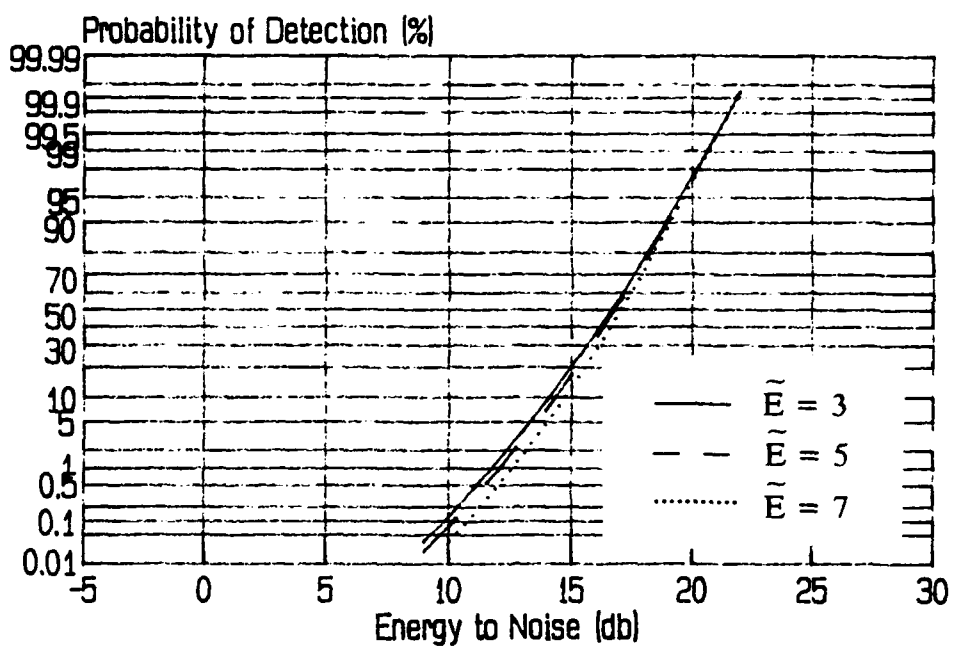


Figure 2.7g Comparison between Different Values of \tilde{E} for 4-Pulse Slow-Fluctuating Dominant plus Rayleigh Scatterers when $N_I = 8$, $M = 10$, $\sigma = 2.0$ and $P_{fa} = 1.E-8$

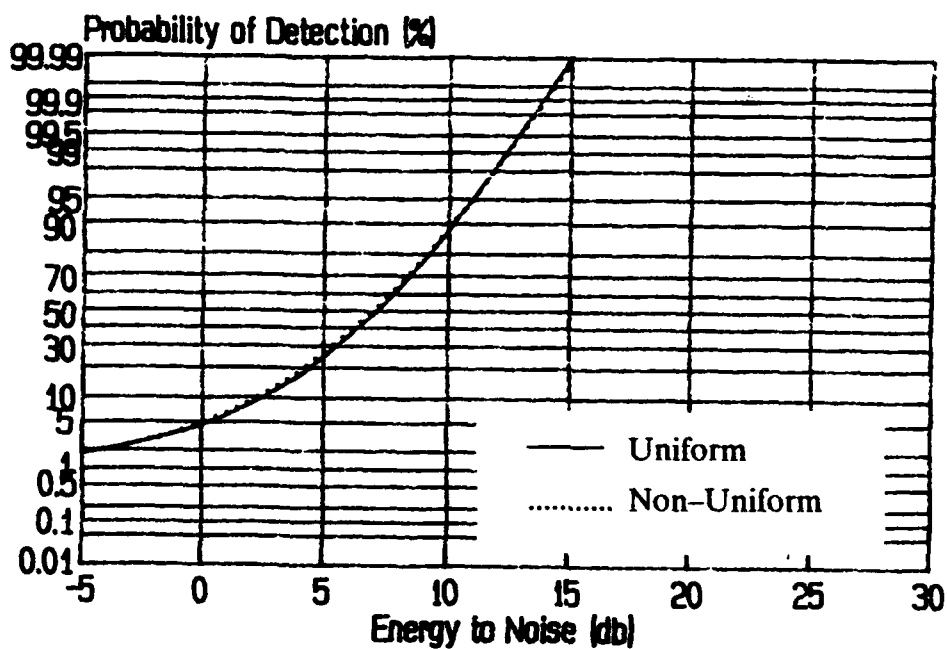


Figure 2.8a Comparison between Uniformly Distributed Energy and Non-Uniformly Distributed Energy for 4-Pulse Fast-Fluctuating Dominant plus Rayleigh Scatterers when $M = 2$ and $P_{fa} = 1.E-2$

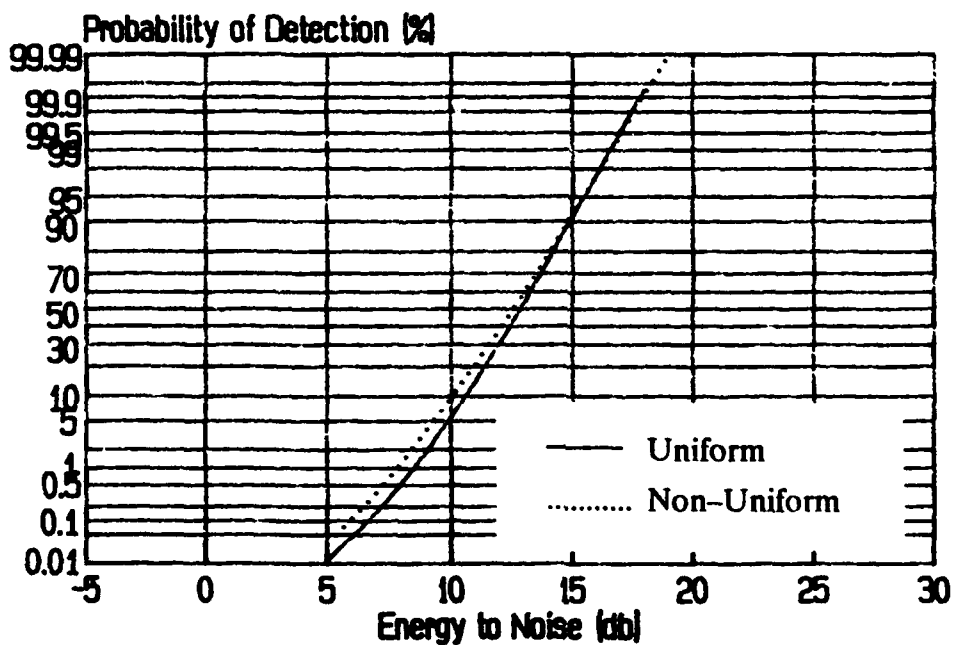


Figure 2.8b Comparison between Uniformly Distributed Energy and Non-Uniformly Distributed Energy for 4-Pulse Fast-Fluctuating Dominant plus Rayleigh Scatterers when $M = 2$ and $P_{fa} = 1.E-8$

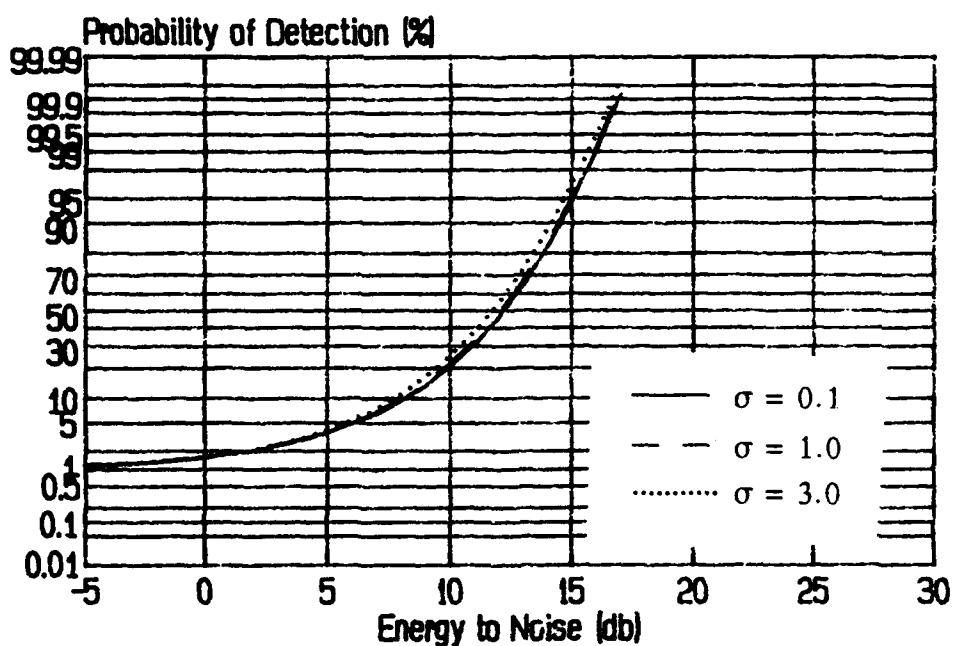


Figure 2.8c Comparison between Different Values of σ for 4-Pulse Fast-Fluctuating Dominant plus Rayleigh Scatterers when $N_f = 8$, $M = 10$, $\bar{E} = 5$ and $P_{fa} = 1.E-2$

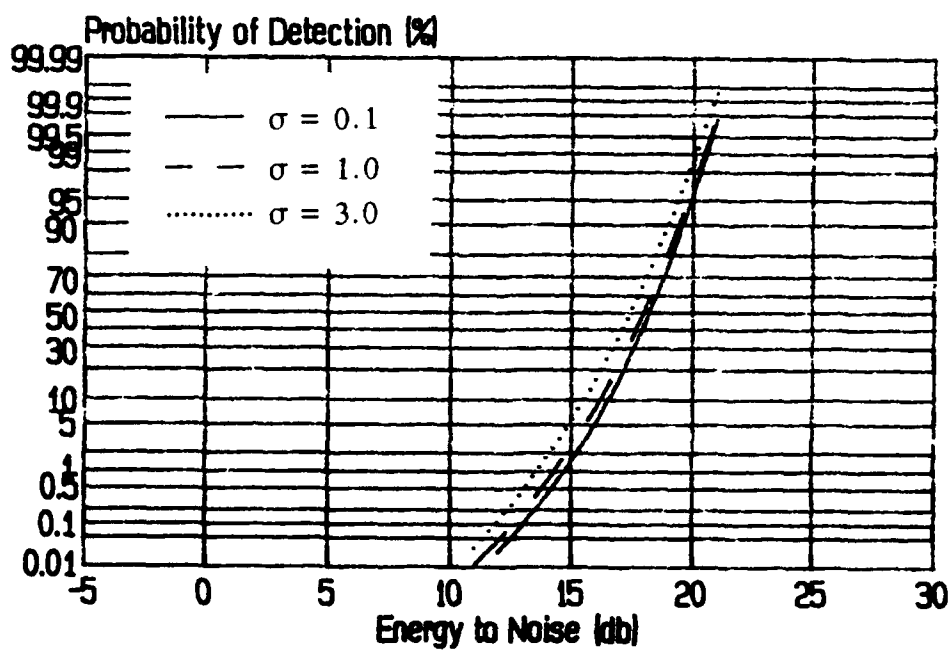


Figure 2.8d Comparison between Different Values of σ for 4-Pulse Fast-Fluctuating Dominant plus Rayleigh Scatterers when $N_f = 8$, $M = 10$, $\bar{E} = 5$ and $P_{fa} = 1.E-8$

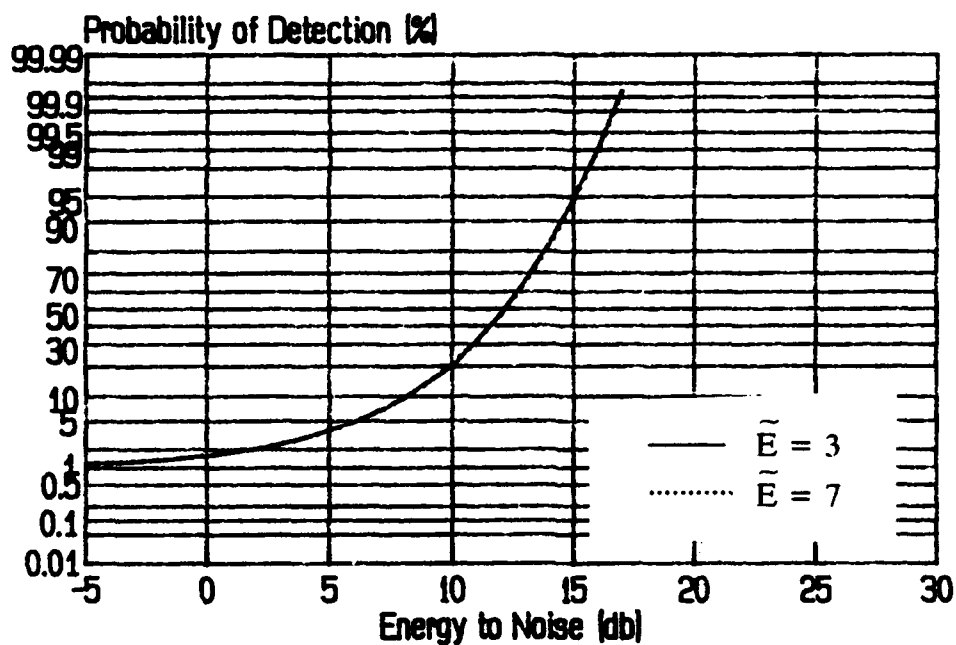


Figure 2.8e Comparison between Different Values of \tilde{E} for 4-Pulse Fast-Fluctuating Dominant plus Rayleigh Scatterers when $N_f = 8$, $M = 10$, $\sigma = 0.5$ and $P_{fa} = 1.E-2$

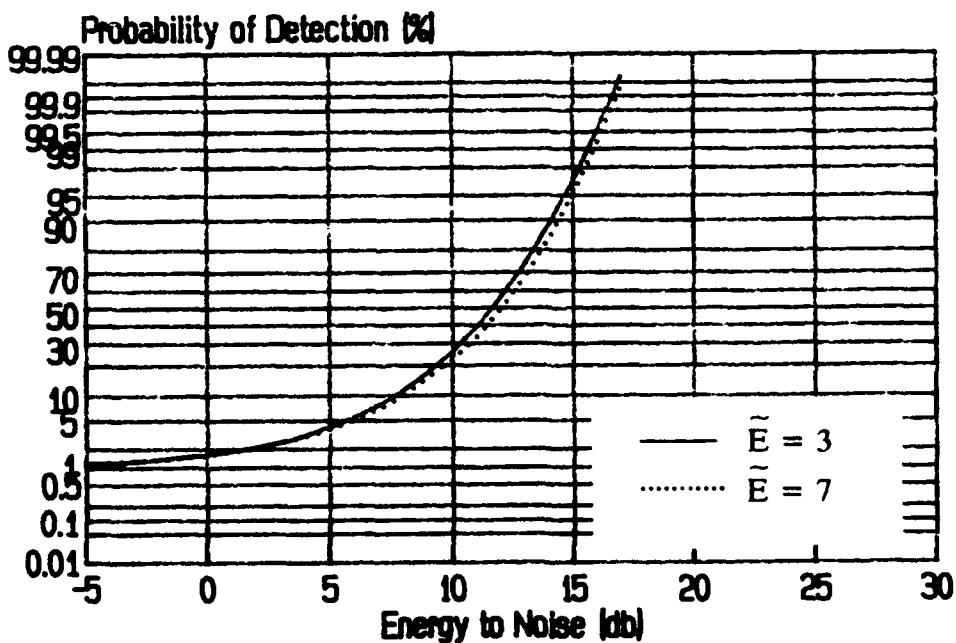


Figure 2.8f Comparison between Different Values of \tilde{E} for 4-Pulse Fast-Fluctuating Dominant plus Rayleigh Scatterers when $N_f = 8$, $M = 10$, $\sigma = 3.0$ and $P_{fa} = 1.E-2$

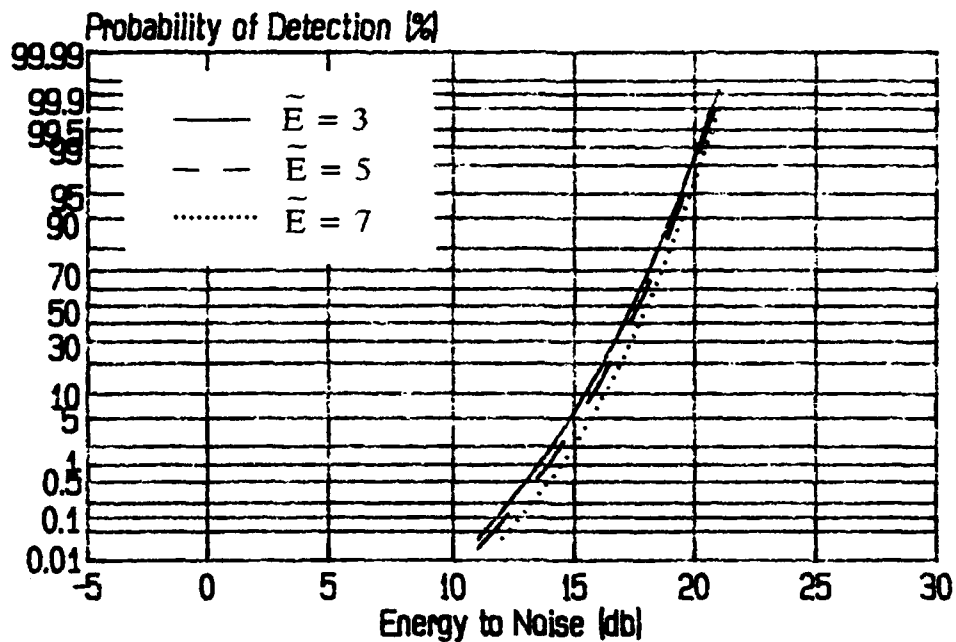


Figure 2.8g Comparison between Different Values of \tilde{E} for 4-Pulse Fast-Fluctuating Dominant plus Rayleigh Scatterers when $N_f = 8$, $M = 10$, $\sigma = 2.0$ and $P_{fa} = 1.E-8$

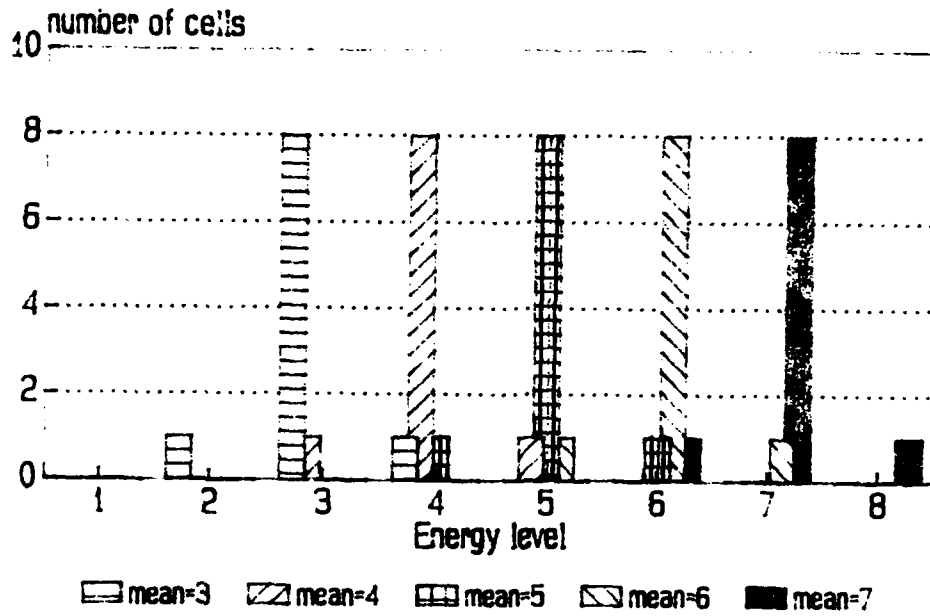


Figure 2.9 Distribution of 10 Cells over 8 Energy Levels for Different Values of \bar{E} when $\sigma=0.5$

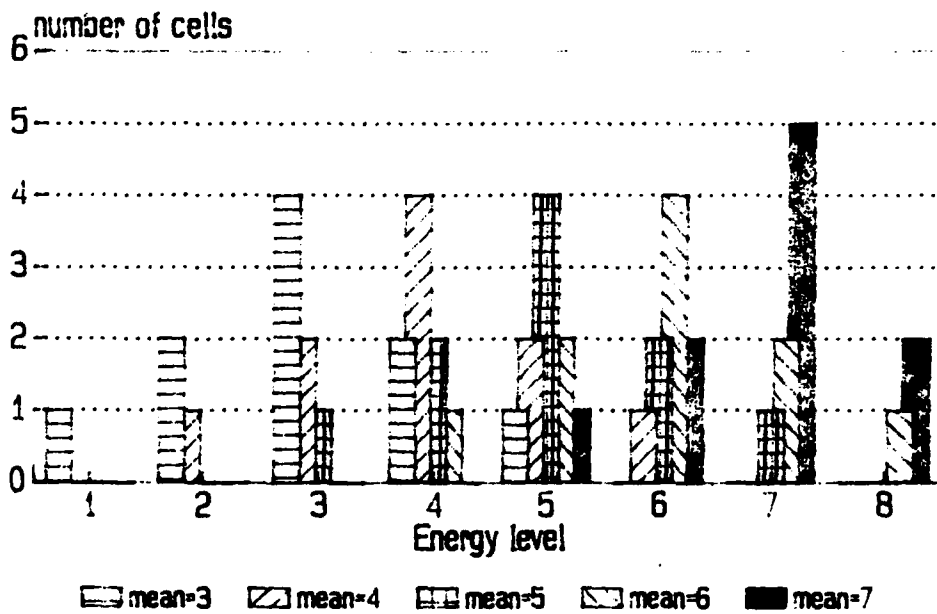


Figure 2.10 Distribution of 10 Cells over 8 Energy Levels for Different Values of \bar{E} when $\sigma=1.0$

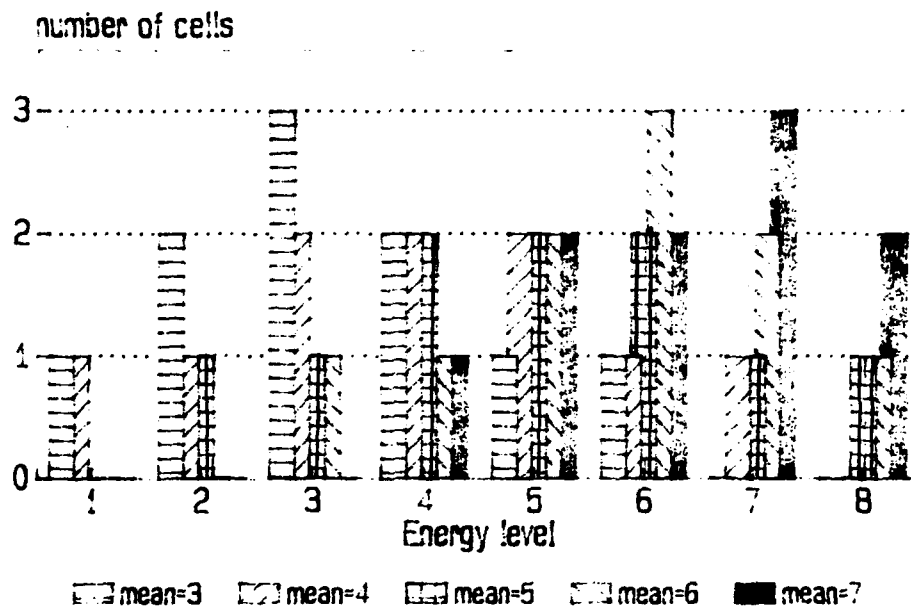


Figure 2.11 Distribution of 10 Cells over 8 Energy Levels for Different Values of \bar{E} when $\sigma=2.0$

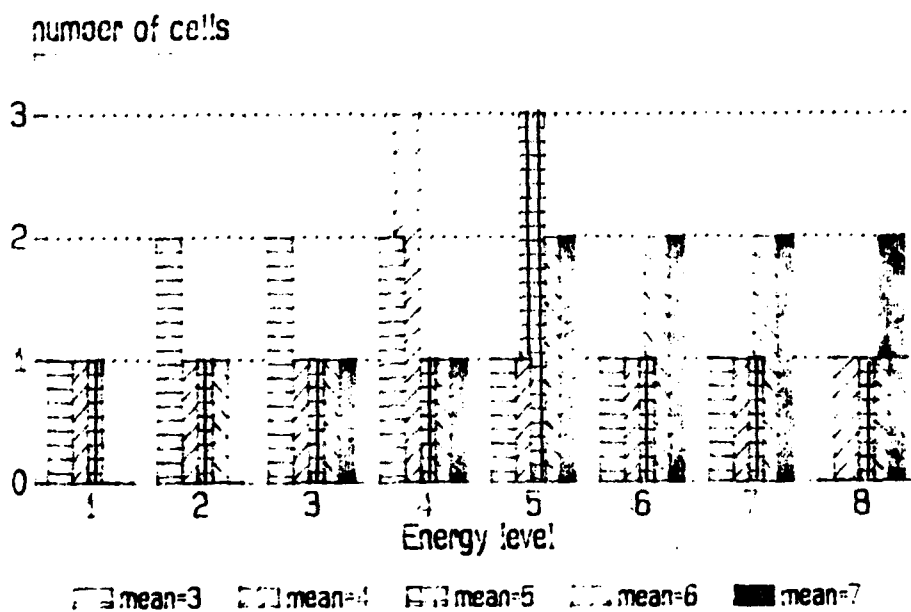


Figure 2.12 Distribution of 10 Cells over 8 Energy Levels for Different Values of \bar{E} when $\sigma=3.0$

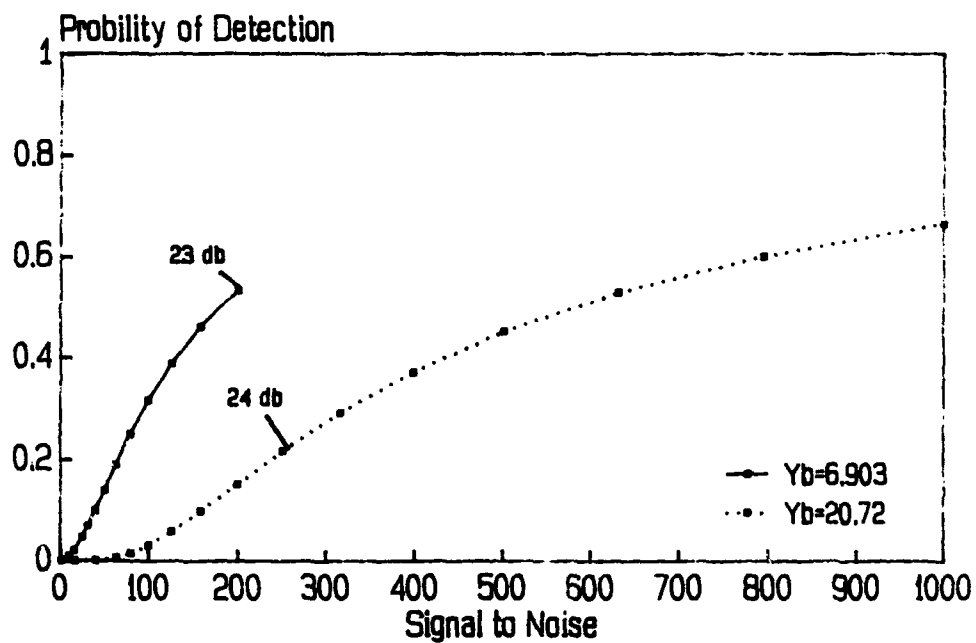


Figure 2.13 Cell Probability of Detection in Linear Scales for Single-Pulse Rayleigh Scatterers

REFERENCES

1. Vincent C. Vannicola and Kenneth G. Hillman, "Detection Performance for Over Resolved Targets," ROME AIR DEVELOPMENT CENTER, RADC-TR-84-61, In-House Report, Sep. 1984.
2. Woodward, P.M., *Probability and Information Theory with Applications to Radar*, McGraw-Hill, New York, 1953.
3. Swerling, P., "Probability of Detection for Fluctuating Targets," IRE Trans. on Info. Theory, Vol. IT-6, No. 2, pp. 269-308, 1960.
4. Marcum, J.I., "A Statistical Theory of Target Detection by Pulsed Radar," IRE Trans. Info. Theory, Vol. IT-6, No. 2, pp. 59-144, 1960.
5. DiFranco, J.V., and Rubin, W.L., *Radar Detection*, Prentice-Hall, Englewood Cliffs, New Jersey, 1968.
6. Nitzberg, R., "Effect of a Few Dominant Specular Reflectors Target Model upon Target Detection," IEEE Trans. Aerosp. and Electron. Sys., Vol. AES-14, No. 4, pp. 670-673, 1978.
7. Hughes II, P.K., "A High-Resolution Radar Detection Strategy," IEEE Trans. Aerosp. and Electron. Sys., Vol. AES-19, No. 5, pp. 663-667, 1983.
8. Skolnik, M.I., *Introduction to Radar Systems*, McGraw-Hill, 1980.
9. Swerling, P., "Recent Developments in Target Models for Radar Detection Analysis," Presented at AGARD Avionics Technical Symposium on Advanced Radar Systems, May 1970.